Notch Ligand Delta-like 4 (Dll4) Induces Epigenetic Mechanism in Regulatory T Cell Function During Pulmonary Viral Infection

by

Hung-An Ting

A dissertation submitted in partial fulfillment
of the requirements for the degree of
Doctor of Philosophy
(Molecular and Cellular Pathology)
in the University of Michigan
2018

Doctoral Committee:

Professor Nicholas W. Lukacs, Chair
Professor Yali Dou
Professor Gary B. Huffnagle
Associate Professor Ivan P. Maillard
Associate Professor Zaneta Nikolovska-Coleska

Hung-An Ting

tingha@umich.edu

ORCID iD: 0000-0001-9125-89944

Acknowledgements

To my PI Nick: I am so lucky to join Lukacs lab. Doing science with you is a lot of FUN. Your persistency, productivity, energy, open-mind, kindness and fairness to trainees stand as one example of the best mentor and best person! And you really cultivated an environment for graduate student to be collaborative and gradually independent. I hope to become a scientist with good personality and creativity like you one day.

To Steve: I decide to apply for PIBS program in the University of Michigan because of your talk in Acadmia Sinica back in 2011. You set up the landmark of good leadership. And I really appreciate all your help and advices in grants application

To committee members Ivan, Yali, Zaneta, and Gary: Thank you for your big supports and critical inputs during our annual meetings!

Thank you so much Matt for your advice and answers in our shared interest: Notch+ T cells+ epigenetics+ RNA-seq data analysis; thank you Denise for your initial navigation of Treg, teaching me the critical experimental techniques and lay the groundwork to become my thesis project; thank you Catherine for answering all of my weird questions; thanks Wendy for ILC2 knowledge and setting up collaboration; thank you Sami for all your advice and good vibes when I was down; thanks Andrew and Sue for your help at the end-point day; thank you Carrie for DC culture. Last but not least, thank you so much Judith for manuscript editing and consulting.

Outside our lab, thank you Peter for our collaboration of SMYD3 in cancer immunology. Also, I would like to thank my PIBS friends Jing-Ping, Justine, Shayna, Dysha for their support. I will not forget my tea group friends, my band, and Pathology students for doing outdoor fun things together.

To my loving and supportive family. This journey can't be more fruitful and fulfilling without all of you. Thank you Mom and Dad for the support of changing my career direction from bedside to bench. My husband Raymond, thanks for your company, encouragement and trust.

Table of Contents

List of Tables

List of Figures

Abstract

Respiratory Syncytial Virus (RSV) infects more than 90% of children under two years of age. It is the number one leading cause of hospitalizations for infants and young children. Inpatients suffer from RSV-induced moderate to severe bronchiolitis of the lower respiratory tract. RSV pathology that includes mucus hypersecretion, airway obstruction, bronchiolitis, eosinophilia is driven by pathogenic immune responses. Activated CD4 T cells include T helper cells type 1 (Th1), Th2, Th17, and Treg. Th2 and Th17 responses are pathogenic in that they trigger peribronchioalveolar lymphocytic aggregates, augment mucus production and reduce viral clearance. Regulatory T cells (Treg)—defined as Foxp3+ CD4 T cells—can be further induced by infection to mitigate RSV immunopathology including pathogenic Th2 responses. Understanding how Treg cells are regulated may reveal potential targets to therapeutically alleviate RSV-induced immunopathology. A recent study demonstrated that Notch ligand—Delta-like 4 (Dll4) was up-regulated to attenuate RSV pathology, and intracellular Notch signaling perturbs Treg cell stability in autoimmune disease. But the role of Notch ligand Dll4 in Treg cells in pulmonary infection is still elusive. In this dissertation, we will demonstrate **1)** The role of Dll4 in Treg and **2)** How Dll4 regulates Treg during RSV infection.

The current dissertation demonstrates that Dll4 was up-regulated by RSV infection especially on CD11b+ pulmonary dendritic cells (DC). Using systemic Dll4 neutralization and a Dll4 knockdown DC transfer model, we found that Dll4 enhanced Foxp3 expression and reduced RSV immunopathology. Dll4 promoted peripheral Treg cell differentiation, harnessed T_{reg} cell effector function, and stabilized Treg from Th17-like identities *in vitro and in vivo* during RSV infection.

Using an epigenetic enzyme PCR array, we found that Dll4 and Notch signaling enhanced the expression of a novel histone methyltransferase—SET and MYND domain containing protein 3 (SMYD3) *in vitro* and *in vivo* during RSV infection. SMYD3 catalyzed Dll4-facilitated histone 3 lysine 4 tri-methylation (H3K4me3) around the Foxp3 loci in induced Treg cells, and SMYD3 differentially regulated Dll4-stimulated genes discovered by RNA-seq. Consistent with Dll4 activation, SMYD3 sustained Treg cells promoted anti-inflammatory IL-10 expression and prevented IL-17A production from T cells to mitigate pathogenic cytokines and mucus production.

Collectively, the studies in this dissertation suggest that Notch and its ligand Dll4 augment immunomodulatory Treg cell programs to ameliorate RSV immunopathology in part through an epigenetic mechanism—SMYD3. The results presented herein lay the foundation for future therapeutics targeting pulmonary and other mucosal inflammatory diseases.

Chapter 1 Introduction

1.1 Respiratory syncytial virus (RSV) infection

Viral respiratory tract infections accounted for approximately 1 in 5 hospital admission among infants in the United States. Common viruses are influenza, parainfluenza, rhinovirus (RV), and respiratory syncytial virus (RSV)[1,2]. RSV is the most ubiquitous infectious virus as it infects more than 90% of infants by age 2, and it's the number one leading cause of infantile bronchiolitis worldwide. RSV is a single-stranded RNA virus that belongs to the *Paramyxoviridae* family and has a 10-gene genome. Humans are the only known host for RSV. The viral envelope contains three proteins: attachment glycoprotein (G), fusion glycoprotein (F) and small hydrophobic (SH) protein. RSV-F and RSV-G proteins are the main virulence factors that mediate airway epithelial cells penetrations[3]. The clinical feature of RSV infection—multinucleated epithelial cells, or syncytia—is the result of RSV-F protein that enables cell-to-cell fusion[4].

RSV mainly causes lower respiratory tract infections in children. A recent report from CDC showed that RSV induced on average 57,527 hospitalizations annually among children younger than 5 year-old in the US[5]. A retrospective review showed that RSV induced mortality for all ages combined has been approximately 30/100,000 humans from 1990-2000, with an annual average mortality of over 170,000 worldwide[6]. While RSV is detrimental in infants and young children, it is also dangerous for the elderly, adults with compromised immune systems and adults with chronic heart or lung diseases, including pneumonia, asthma, chronic obstructive pulmonary disease, and congestive heart failure to causes more than a hundred thousand of hospitalizations

annually in the United States in adults older than 65[7]. The common symptoms of RSV infections are: runny nose, a decrease in appetite, and sneezing, and the acute phase of infection usually leads to symptoms such as a wheezing cough that can be diagnosed as asthma but is non-responsive to typical atopic asthma treatments[7]. Clinical manifestations such as airway obstruction are driven by pathogenic immune responses but not by viral replication or virus cytotoxicity[7]. Moreover, there is no effective vaccine available. Hence, understanding the immune responses to protect us from RSV infection are critical for designing effective therapies.

The innate immune response during RSV infection was investigated using murine mouse models. After RSV entry into the airways, airway epithelial cells secrete pro-inflammatory mediators (e.g. TNF-α, type 1 interferon, CCL5, Thymic stromal lymphopoietin TSLP). The lung resident alveolar macrophages also secrete type 1 interferons to initiate antiviral responses within the first 2 days post infection (dpi). These cytokines further recruit NK cells, type 2 innate lymphoid cells (ILC2)[8], polymorphoneuclear leukocytes (PMN) and eosinophils to produce more inflammatory cytokines including IFNγ, IL-5, IL-13 and IL-4. Innate lymphoid cells (ILC2) is the major producer of IL-13 that initiates mucin production from the airway epithelial cells during RSV infection[8]. Pulmonary DC, especially CD11b+ conventional DC (CD11b+ cDC), display a massive influx into the lung after RSV infection[9]. Pulmonary DCs (Both CD11b+ cDC and CD103+ DC) are able to sample RSV and migrate to draining lymph node to present RSV antigen to T cells[9]. DCs then prime adaptive immunity to become long-term effectors during later phase (6dpi~12dpi) of infection and post RSV infection.

RSV re-infection occurs often throughout life, suggesting that it failed to initiate effective adaptive immunity including B cell and T cell memory responses[10,11]. In a mouse model, T cells enhanced disease since primary signs of RSV pathology were reduced after CD4 and CD8 T cells

depletion[12]. CD4 T cells appears to trigger peribronchioalveolar lymphocytic aggregates and augment disease while decreasing viral load; while CD8 T cells cause RSV clearance and reduce eiosinophilia and bronchiolitis severity[13–15]. Intriguingly, while total depletion of CD4 T cells (mostly CD4 T helper cells) suggested that CD4 T cells drive RSV disease, recent work identifies that a small subset of CD4 T cells—namely, T regulatory (Treg) cells—could instead mitigate RSV immunopathology. The CD4 T cell subsets will be introduced in the next section.

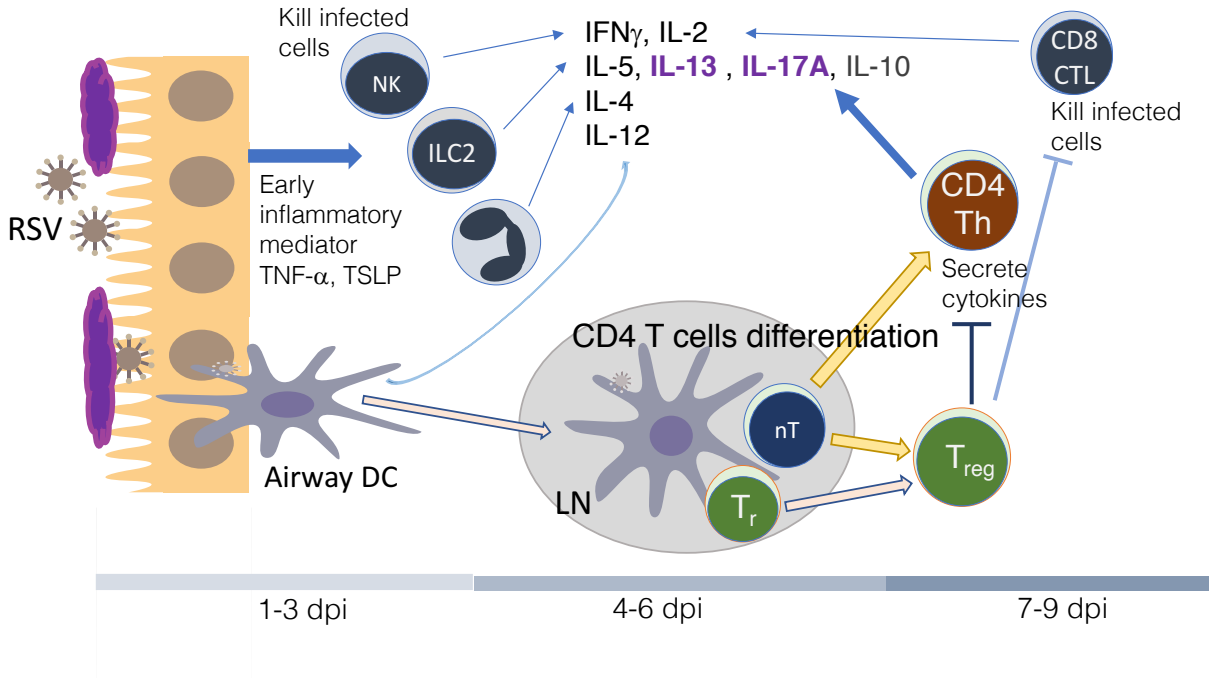

Figure 1.1 RSV-initiated innate and adaptive immune responses[1]

[1] This figure was created by Hung-An (Anna) Ting

1.2 CD4 T helper cells and the pathogenesis of RSV infection

The CD4 T helper (Th) cells combat pathogens after antigen recognition by mounting an effective and precise immune response. A successful immune response requires a coordinated effort by discrete subtypes of Th cells, each group characterized by their cytokine profile. Th cells type 1 (Th1) are characterized by Interferon-gamma (IFN-γ) production that helps to combat intracellular pathogens. Th type 2 (Th2) cells are characterized by Interleukin(IL)-4 (IL-4), IL-5 and IL-13 secretion to respond to parasitic infections and allergic responses. Th17 cells secrete IL-17A and IL-17F to combat extracellular pathogens. Th9 is a recently identified subset that secrete IL-9 in response to allergic reactions. The pro-inflammatory actions of these Th subsets can be tempered by CD4+ Treg cells. There are two types of Treg cells: nTreg cells are developed in the thymus; while iTreg cells are adaptively induced from matured CD4+ naïve T cells (nT). iTreg and different Th subsets are derived from naïve CD4 T cells (nT) by the biological process called CD4 T cells differentiation.

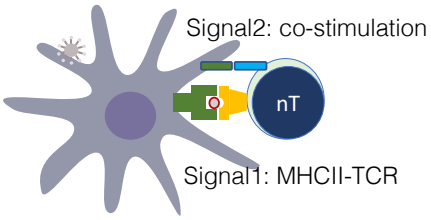

Signal 3: cytokine mileau	Transcription factor	Th	Featured cytokine	Immune responses
IL-12	T-bet	Th1	IFNγ, IL-10	Anti-viral immunity Anti-intracellular bacteria
IL-4	GATA3	Th2	IL-4, IL-5, IL-13	Anti-parasitic allergy
TGF-β+IL-6+(IL-23+IL-1β)	RORγt	Th17	IL-17A, IL-21, IL -22	Anti-bacterial (esp. extracellular)
TGF-β+IL-4	Being debated	Th9	IL-9	Allergy
TGF-β+IL-2	Foxp3	Treg	IL-10, TGF-β	Tolerance to inert antigens Reduce immunopathology
IL-27+(TGF-β)	Being debated	T_R1	IL-10	Reduce immunopathology

Figure 1.2 CD4 T cells differentiation [2]

[2] This figure was created by Hung-An (Anna) Ting

Naïve CD4 T cells could be primed by antigen presenting cells (APC). APC presents antigen-bearing MHC class II and B7.1/B7.2 to bind to TCR/CD3 complex and CD28, respectively. MHCII-TCR and B7.1/CD28 are signals 1 and 2 to induce full activation of CD4 T cells. In addition to signals 1 and 2, the environmental cytokine mileau skews naïve T cells toward different Th subtypes. These Th cells acquire discrete molecular signatures (transcription factors) and effector functions (cytokine secretion). The role of CD4 Th cells and their effector cytokines in RSV immunopathogenesis had been well studied. We will discuss these findings in the following paragraphs.

1.2.1 Th2 and type 2 cytokines: IL-4, IL-5, IL-13

In humans, RSV infection induces mucus production, eosinophilia, elevated IgE levels and airway hyperreactivity[16–18], symptoms associated with Th2-mediated immune responses. Clinical data point out that an imbalanced cytokine production skewed towards an increased ratio of IL-4 over IFNγ, correlates with RSV immunopathogenesis in human infants[19]. Infants are more predisposed to Th2 responses than Th1 responses since they express higher levels of IL-4 receptor on their CD4 T cells following RSV stimulation when compared to adult[20], while neonatal CD4 cells produces less IFNγ[21]. RSV infection elicits both Th1 and Th2 responses by distinct surface glycoproteins. Sensitization of mice with recombinant vaccinia viruses expressing RSV-G mount Th2-dominated responses, while vaccinia viruses expressing RSV-F mount Th1[22].

In a murine pre-clinical model, blockage of IL-4 and IL-5 mitigates the development of eosinophilia and airway hypersensitivity in primary RSV infection[23], although the role of IL-4 is more questionable than that of IL-5 since IL-4 deficiency doesn't affect eosinophilia in RSV-G bearing vaccinia virus infection[24]. IL-13 not only contributes to eosinophilia but also induces mucus hypersecretion to exacerbate RSV immunopathogenesis[3,25,26]. It is worth noting that type 2

cytokines are secreted from immune cells other than Th2, for example IL-4 from basophils[27] and IL-13 from ILC2 cells during RSV infection[8]. Therefore, pathogenic type 2 responses are contributed not only from Th2 but other innate cells.

The magnitude of type 2 cytokines responses following RSV infection in mice appears to be dependent on the viral strain. The Line 19 and 2–20 strains of RSV induce significantly greater amounts of IL-13 in the lung than the A2 and Long strains, resulting in increased mucus production and airway hyperreactivity[25,28]. The present thesis consistently used Line 19.

1.2.2 Th17 and IL-17 family

Clinical data showed that IL-17A is increased in the tracheal aspirates but not in nasal washes of RSV-infected infants[29,30], indicating that IL-17A may play a more significant role in the lower respiratory tract rather than in the upper airways. Using experimental models of RSV infection, IL-17A is mostly produced from CD4 Th17 cells but not double negative T or γδ T cells[30]. Unlike type 2 cytokines that start to be abundant in the lung from 4 to 6 dpi, IL-17A production peaked at 8 dpi[30]. There are multiple reports investigating how IL-17A is regulated. Efficient lymph node priming[31], IL-27 receptor signaling[32], IL-13 and STAT1[33] impede IL-17A production from CD4 T cells. The function of IL-17A in RSV infection is to diminish CD8+ T cell responses, and it also increases mucus hypersecretion in both murine models and human primary airway epithelial cells [30,34,35].

1.2.3 Th9 and IL-9

As a newly identified subset, recent studies find that IL-9 is increased in both human tracheal samples and mice bronchial alveolar lavage (BAL) fluid and lung during RSV infection[36,37]. Furthermore, human *IL9* gene polymorphisms are associated with increased RSV disease severity[38]. Thus, the function of IL-9 in RSV infection need to be carefully elucidated.

1.2.4 Treg, IL-10 and TGF-β

Opposite to the pathogenic role of CD4 Th cells, an increasing body of literature demonstrates that a subset of CD4 T cells, namely Treg cells, ameliorate RSV immunopathogenesis. Treg was identified as Forkhead box p3 (Foxp3)+ CD4 T cells, and they were enriched and expanded in lung and BAL during RSV infection[39,40]. Deletion of Treg cells during or before RSV infection using Diphtheria toxin (DT) treatment in Foxp3-DTR mice or anti-CD25 antibody, resulted in an increased influx of NK, eosinophil, Th2, and CD8 T cells[39–42]. Also, the systemic depletion of Treg cells creates a pro-inflammatory environment that results in weight loss and mucus hypersecretion in the depleted mice. Thus, Treg is required to limit pulmonary inflammation and pathogenic Th2 responses during RSV infection[39,41,42]. The Treg inhibitory molecules: Cytotoxic T lymphocyte antigen 4(CTLA-4)[39] and GranzymeB (GzmB)[42] are responsible to mitigate RSV immunopathology. But the pathway for Treg differentiation, the function of other inhibitory Treg markers, and the cytokine profile in Treg post RSV infection are still elusive.

IL-10 polymorphisms are associated with susceptibility to severe disease in infants[43,44], although severe RSV-infected infants have variable IL-10 levels that correlate with post-bronchiolitis wheeze[45–47]. In murine models, IL-10 is produced by the adaptive immune system[48,49], mostly by CD4 T cells following RSV infection[50]. It is intriguing to note that IL-10 is not only produced by Foxp3+ Treg but also by Foxp3⁻⁻IFN-γ+ Th1 cells during RSV infection. Accumulated evidences using IL-10 knockout, IL-10 neutralizing antibody and IL-10 receptor blockade all confirm that lack of IL-10 drives weight loss, airway hypersensitivity, more CD4 and CD8 effector cells, increased IL-17A+ Th17 cells and IFN-γ+ Th1 cells, and decreased Treg cells compared to cells expressing IL-10 [48,50,51]. However, IL-10 depletion and Treg depletion don't significantly affect RSV viral clearance[40,48].

TGF-β, an anti-inflammatory cytokine, is expressed more in human neonatal DC than in adult DC. Following RSV infection in human cells, TGF-β suppresses IFN-γ, IL-2, and IL-12p70 production and elevates RSV viral titer cells[52]. Unlike IL-10 that is mainly produced by CD4 T cells, TGF-β is mainly produced by human epithelial cells that is induced by RSV non-structural protein NS1 [53]. The role of TGF-β on CD4 T cells and the mechanism in RSV pathogenesis is lacking in both murine models and humans.

1.3 Notch signaling in CD4 T cells differentiation

1.3.1 Canonical and non-canonical Notch signaling pathway activation

Notch is a highly conserved signaling pathway throughout the metazoan family. It was first discovered in *Drosophila* [54] where there was one Notch receptor and two ligands--Delta and Serrate[55]. In mammalian animals, there are 4 Notch receptors (Notch1, Notch2, Notch3, Notch4) and 5 different ligands (Delta-like ligand 1(Dll1), Dll3, Dll4, Jagged1(Jag1), Jag2). Notch receptors are present on the cell surface as heterodimeric transmembrane proteins. The functionality of Notch receptor-ligand binding is context-dependent in many developmental processes.

Notch receptor-ligand binding enables the matrix metalloproteases of the ADAM family access to the Notch receptor 'S2' cleavage site. The 'S2' cleavage enables further cleavage of Notch receptor at its intramembrane 'S3' site by the γ-secretase complex. The γ-secretase complex cleavage is the critical step for Notch signaling activation. Cleavage of Notch by the γ-secretase complex results in the release of Notch intracellular domain (NICD). NICD can translocate into nucleus and interact with Recombining binding protein suppressor of hairless (RBP-Jκ), co-activator Mastermind-like family (MAML1-3), and another co-activator, p300, to initiate Notch target genes transcription (eg Hes, Hey, Deltex). This is called the "non-canonical" Notch signaling described in *Drosophila*[56,57]. See Figure 1.3.

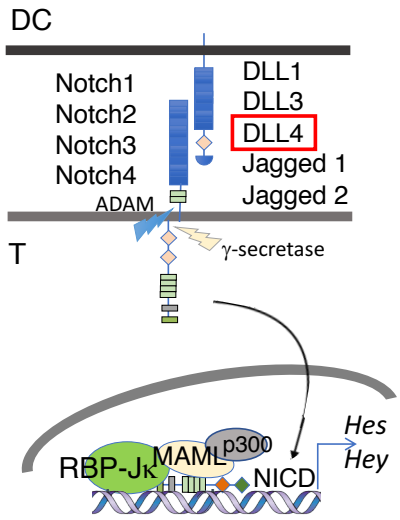

Figure 1.3 Canonical Notch signaling primes CD4 T cells[3]

In mammals there is another canonical Notch activation pathway that is reported to cooperatively initiate signaling with other pathways, including NF-κB and TGF-β/Smad3 pathways. In CD4 T cells, Dll1 and Dll4 prefer to activate Notch1 or Notch2 signaling to drive

[3] This figure was created by Hung-An (Anna) Ting

NICD translocation and association with the NF-κB gene to affect *Ifng* expression that is RBP-Jκ-independent[58,59]; the crosstalk and cooperation between the TGF-β pathway and Notch are mainly demonstrated during epithelial-to-mesenchymal transition (EMT) in epithelial cells and during myogenic differentiation. *In vitro* and *in vivo* pull-down assay shows that overexpressed NICD directly associates with Smad3 to drive the Notch target genes--Hey1 and Jagged1 expression for EMT[60] and Hes1 for myogenesis[61]. Recent reports reveal the cross-talk may happen in primary CD4 T cells also, as Notch DNA-binding protein RBP-Jκ cooperatively activates *Il9* and *Foxp3* with Smad3 in Th9[62] and iTreg differentiation[63], respectively.

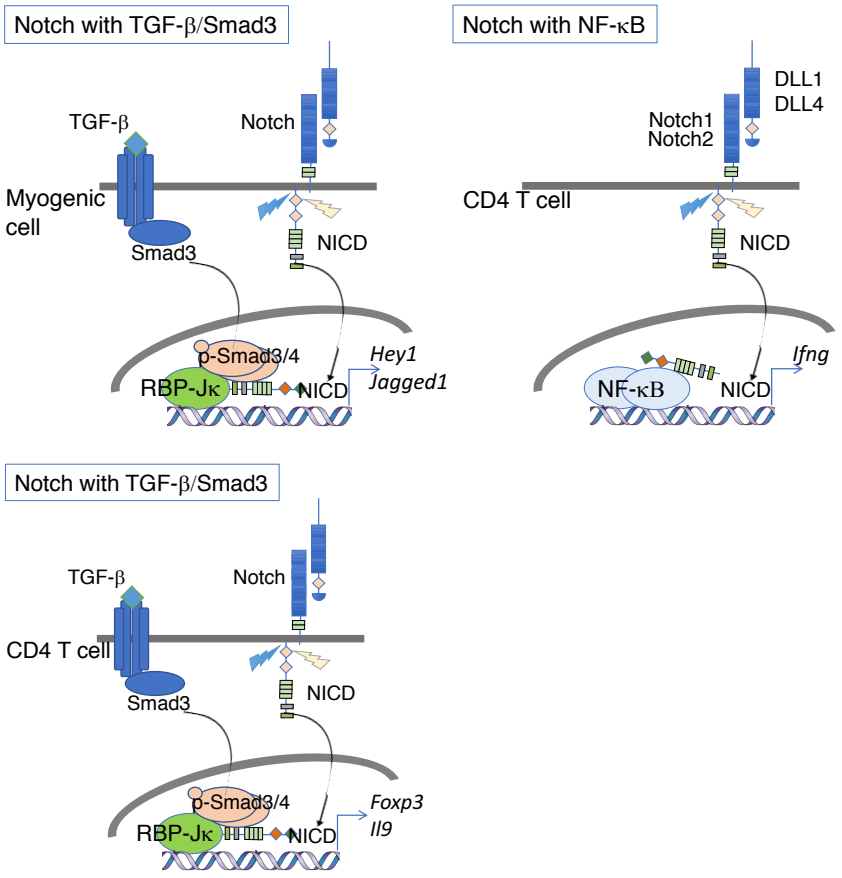

Figure 1.4 Pathways that cooperative with Notch signaling [4]

[4] This figure was created by Hung-An (Anna) Ting

1.3.2 Notch signaling in mature T cell differentiation and function

Notch signaling is emerging as a regulator of CD8 T cell differentiation and effector function, despite the fact that the role of Notch in CD8 T cells differentiation is less known than it is in CD4 T cell activation and differentiation. Relatedly, Notch 1 directly regulates master transcription factor Eomesodermin (Eomes)[64]that is critical in IFN-γ production and cytolytic effector functional molecule (Perforin and Granzyme B) expression[65,66]. Other studies further identify that Notch 2 and its ligand Dll1 support granzyme B and IFN-γ expression [67,68].

Notch appears to be a key regulator and amplifier in CD4 T cell differentiation. In peripheral organs, naive CD4 T cells express Notch1 and Notch2 but little Notch3 and Notch4[69], as is also true in Treg cells[70]. Notch signaling regulates various stages of T cells lineage development and differentiation, including early stages of thymocyte development, as well as CD4 Th differentiation[69,71]. In the priming stage of Th cell differentiation, Notch1 contributes to CD4 T cell activation by promoting CD25 expression, early activation marker CD69, IL-2 production, and Akt-GSK3β downstream of co-stimulatory molecule CD28 *in vitro*[72,73]. More recent work further substantiates that Notch ligand Dll4 on DC sensitizes antigen responses and augmented T cells activation by facilitating co-stimulation and glucose metabolism[74].

The role of Notch signaling in Th1 and Th2 differentiation has been suggested to have a binary paradigm. Notch ligand DLL4 promotes Th1 differentiation while inhibiting Th2 differentiation whereas the Jag1 ligand promotes Th2 differentiation [69,75]. However, a recent study questions the paradigm that Notch can regulate multiple subsets of Th[76]. In Th1, Dll4 and Notch not only promote Th1 effector IFNγ and transcription factor T-bet expression *in vitro*[69,76,77], but also Th1 responses *in vivo*. Intracellular Notch signaling and Notch3 inactivation prevents Th1 mediated experimental autoimmune encephalomyelitis (EAE)[77,78]. Redundant Notch1 and Notch2

are required to promote IFN-γ secretion in *Leishmania major* infection[59]. Thus, Notch facilitate Th1 differentiation and effector functions.

During Th2 cell differentiation, Jag1 and Notch promote *Gata3* and *Il4* expressionn by direct binding of RBP-Jκ onto *Il4* and *Gata3* promoters[32–34], while Dll4 has been reported to suppress *Il4, Il5, and Il13* gene expression [67,73]. Dll4 inhibition exacerbates Th2 cell and type 2 cytokine secretion in cockroach antigen-induced allergic asthma[83] and primary RSV infection[82] *in vivo*. But in chronic allergic disease, DLL4 but not Jag1 supports Th2 memory cell expansion in *Schistosoma mansoni* (*S. mansoni*) infection[84], and Dll4 also supports Th2 cytokine expression in a STAT5-dependent manner in RSV-exacerbated allergic asthma[85]. These conflicting data suggest that Notch regulates Th2 differentiation and effector function in context-dependent manner.

Notch was reported to promote Th9 differentiation by the interaction between Smad3 and RBP-Jk to bind to the *Il9* promoter[86]. But compared to their role in Th9 cell differentiation, the role of Notch in Th17 and IL-17A differentiation have been more extensively investigated. Our lab and other scientists show that RBP-Jκ bind to the *Il17a* and *Rorc* promoters to directly affect the Th17 program in murine Th17[87] and human Th17 cells[88]. Dll4 intracellular Notch activation both promote pathogenic Th17 cells to exacerbate EAE pathogenesis[88,89] and pneumonitis post bone marrow transplantation[90].

A new paradigm was proposed recently that Notch can serve as an amplifier for multiple Th lineages. Notch supports persistent Th1, Th2 and Th17 cell responses simultaneously *in vitro* and *in vivo* during *Trichuris muris* infection [76]. Another independent study suggests that both Th1 and Th2 responses are dampened by intracellular Notch inactivation in CD4 cells to *Cryptococcus neoformans* infection[91]. These new results indicate that Notch signaling may not be skewing

signals but rather enhance co-activation of multiple Th differentiation pathways to serve as a Th differentiation amplifier.

The role of DLL4 and Notch signaling in Treg cells remains enigmatic. Jagged2 and specific receptors, Notch1 and Notch3, promote the Treg cell master transcription factor, *Foxp3* expression and Treg cell survival [92–96], and RBP-Jκ is reported to directly bind the *Foxp3* promoter and cooperatively facilitate Foxp3 transcription with TGF-β/Smad3[96]. In contrast, inactivating Notch signaling after Foxp3 expression enhanced Treg cell numbers and promoted tolerance [70]. Blockage of Notch receptors and Notch ligands expanded Foxp3+ T cell populations *in vivo* in experimental autoimmune encephalomyelitis (EAE), graft-versus-host disease (GvHD), and Type 1 diabetes (T1D) [97–100]. Therefore, the role of Notch as supportive or inhibitory in Treg differentiation is still debatable. Also, the expression of Notch ligands and their role in Treg functions and in Treg cells resistance to inflammation during infection have not been well-defined.

1.4 Regulatory T cells (Treg) differentiation, stability, and plasticity

1.4.1 History of regulatory T cells discovery

The concept that CD4 T cells contains a subset of "suppressor T cells" was prevalent in the 1970s [101]but came out of favor in the 1980s because the proposed soluble suppressor molecules were not found[102]. The re-emergence of this concept started in 1997 when scurfy mice that had X-chromosome linked autoimmunity (ruffled skin, reddened eyes, enlargement of spleen and lymph nodes, and premature death) was characterized and the scurfy mutation was mapped to a gene named Forkhead box p3 (Foxp3)[103]. A seminal study showed that CD4+CD25+ T cells suppressed CD25- T cells activation resulting in tolerance to self-antigen[104], and this subpopulation expresses Foxp3[104,105]. CD4+CD25+Foxp3+ cells were re-named as "regulatory T

cells". Foxp3 is essential for Treg lineage[106,107] and lineage-specific master transcription factor[108]. Foxp3 is not only crucial for systemic tolerance in mice (especially in male mice) but also in humans. Patients with immune-dysregulation, polyendocrinopathy, enteropathy and X-linked (IPEX) syndrome have a mutation in their FOXP3 gene, and induction of FOXP3 gene in human CD4 cells also exhibit a suppressor function [109,110].

1.4.2 Regulatory T cells differentiation and nomenclatures

Treg cells are heterogeneous. To better define their function, there are at least two taxonomies proposed. The first strategy is based on their developmental origin. One subpopulation of Treg cells is derived from CD4+CD8+ double positive or CD4 single positive T cells (CD4SP) in the thymus, is self-antigen reactive, and are called thymus-derived Treg (tTreg) cells. These were also called natural-occurring Treg (nTreg) cells. Another Treg cell population is derived from CD4SP cells in the periphery to be a mix of non-self- and self-antigen reactive cells, called periphery-derived Treg (pTreg) cells. Importantly, the pTreg consist of the original tTreg cells that migrated out of the thymus and the inducible iTreg cells that differentiated from Foxp3- naïve CD4 T cells (see section I.3 above about CD4 T helper cells differentiation). The old name of pTreg cells was adaptive Treg or inducible Treg (iTreg) cells before the nomenclature simplification[111]. There are several studies suggesting biomarkers that differentiate tTreg from pTreg, including Helios[112,113] and Neuropilin-1 (Nrp1) [114,115]. But their reliability and the conclusiveness of their relative functional contribution to maintaining peripheral tolerance are unclear so a second classification evolved based on their homeostatic status. $CD62L^{hi}CD44^{lo}Foxp3^{+}$ cells are called central Treg (cTreg) cells and are relatively quiescent with respect to proliferation, express high levels of Bcl-2 and Mcl-1, reside in lymphoid organs because of the CCR7+ signature, and have high CD25 (IL2 alpha chain receptor) expression to entrap exogenous IL-2. In contrast,

$CD44^{hi}CD62L^{lo}Foxp3^{+}$ effector Treg (eTreg) cells are more proliferative and are abundant in non-lymphoid tissue (e.g. lung, gut, adipose tissue)[116,117]. There were some reports suggesting that cTreg and eTreg cells can be selectively regulated by different signals[117–120], but the relation between Treg homeostatic status and their function status remains unclear.

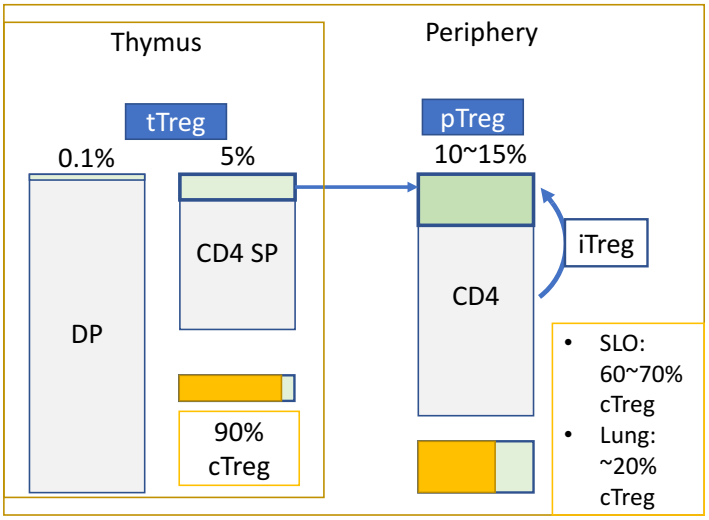

Figure 1.5 Treg subsets and subphenotypes[5]

tTreg cells are derived from CD4+CD8+ double positive or CD4+ single positive cells. pTreg cells consist of Treg cells that migrated from the thymus and inducible iTreg cells derived from naïve T cells. As the thymus is a primary lymphoid organ, most of the Treg cells express $CD62L^{hi}CD44^{lo}$ and are cTreg cells. cTreg cells acquired effector status in secondary lymphoid organ (SLO) and non-lymphoid tissue (such as lung) after encountering antigens and stimulating cytokines.

Regulatory T cells can also be defined by their function. For example, IL-10-producing CD4 T cells are called type 1 regulatory T cells (Treg1)[121]. We will introduce Treg function in the next section.

[5] This figure was created by Hung-An (Anna) Ting

1.4.3 Regulatory T cells function

Treg cells are 'a jack of all trades'. Over decades of study, we now know that Treg cells not only prevent autoimmunity as originally defined but also drive tolerance in multiple diseases and physiological states (e.g pathogen-induced pathology, allergy, oral tolerance, fetal tolerance…etc). This versatility represents the diversity of Treg cell function and as we shall see, the heterogeneity of its suppression mechanisms.

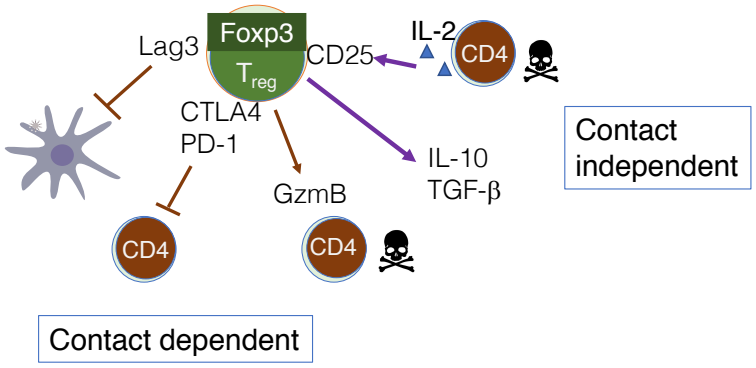

Figure 1.6 Treg function[6]

Of the two classifications of suppression mechanisms one is contact-dependent and the second is contact-independent. In the contact-dependent suppression there are two different mechanisms. In the first suppression mechanism, Treg cells in SLO inhibit effector T cells indirectly through the modulation of DC function *in vivo*. After interacting with Treg cells, these DCs are unable to present antigens to Foxp3- conventional T (Tconv) cells [122–124]. Also, Treg cells compete with Tconv cells for TCR/co-stimulation activation to suppress Tconv proliferation through functional molecule. These 'functional molecules' have been proposed based on the transcriptome and surface marker comparison between Foxp3+Treg and Foxp3- Tconv cells. These include CTLA-4, Lag3, PD-1, ICOS, OX40. For example, CTLA-4 competes with CD28 for co-stimulation activation, and Lag3 competes with CD4 to form the TCR-CD3-CD4 activation complex. Not all

[6] This figure was created by Hung-An (Anna) Ting

functional markers are TCR-co-stimulation dependent. Treg PD-1 receptors have their own ligands on DC that after receptor ligand binding renders the Tconv proliferation. One caveat is that several of these functional markers are not Treg cell specific. PD-1 is also expressed on exhausted CD8 T cells, ICOS and OX40 are also expressed on activated Tconv cells, and Lag3 is on Foxp3$^-$ IL-10 producing T regulatory 1 cells (Treg1). Thus, since many of these functional markers are not exclusive to Treg cells, other functional assays are required to define Treg cells.

The second, contact-dependent Treg cellular suppression mechanism is through cytotoxicity. Similar to effector CD8 T cells, Treg cells can secrete both Granzyme B (GzmB) and perforin to directly kill the effector T cells[42,125]. This mechanism is more prevalent in non-lymphoid tissues since GzmB is activated after T cell activation when it is found to be abundant in eTreg but not cTreg cells.

As mentioned above, Treg cells can also suppress effector T cells in a contact-independent manner. Treg cells are prone to secrete anti-inflammatory cytokines including IL-10 and TGF-β in non-lymphoid tissues such as gut[126,127]. IL-10 was originally identified as one of the Th2 cytokines[128], but numerous studies now suggest that it can be secreted by Treg and other CD4 T cells (ex Treg1, iTreg, Th1, Th17)[121,129–131]. IL-10 from Treg cells is required to impede mucosal inflammation in the gut[132]. IL-10$^+$Foxp3$^+$ Treg cells only exist in the gut in steady state but not in other SLOs or non-lymphoid tissue because IL-10 secretion by Treg cells depends on TGF-β *in vivo* [133,134].

TGF-β is required for iTreg induction and differentiation (see section 1.4.4 below), and the idea that the secretion of TGF-β from Treg cells is part of the suppression function is plausible. Although TGF-β knockout Treg cells are as functional as wild type Treg cells in the *in vitro* suppression assay[135], *in vivo* experiments show that TGF-β receptor knockout Treg cells fail to

suppress Tconv[136]. TGF-β production by Treg cells inhibits colitis and Th1 differentiation[137,138]. These recent findings suggest an extrinsic role for TGF-β secreted from Treg cells to suppress Tconv cells , supporting the older hypothesis that TGF-β is essential for Treg cell survival[137].

Treg cells have high expression levels of IL2Ra (CD25) to bind IL-2, an interaction needed for their own survival[139]. Since IL-2 is also essential for Tconv cell survival, Treg cells could outcompete the Tconv cells for this cytokine and thus control the viable number of Tconv cells, as suggested in the *in vitro* suppression assay[105].

1.4.4 Foxp3 induction: outside-in signals and cis-regulatory elements

Foxp3 is the most indispensable factor in Treg cell fate specification, while it's still debatable if Foxp3 is the 'sole requisite' to define Treg (See Section 1.4.2 above).

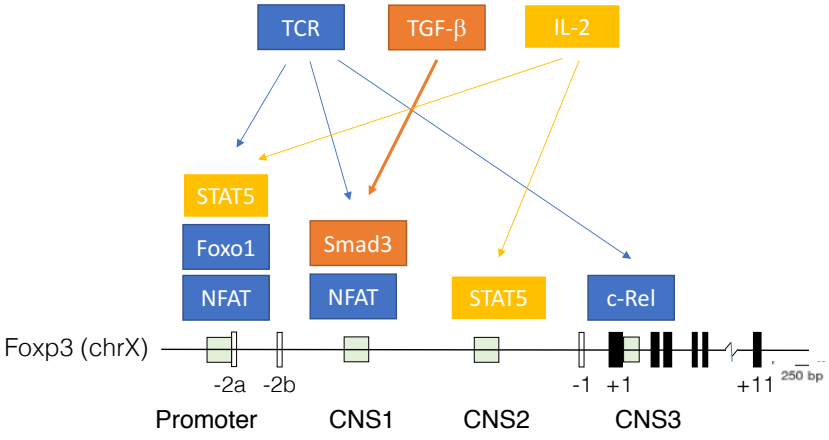

Figure 1.7 Foxp3 induction is regulated by multiple signals and cis-regulatory elements

There are three consensus non-coding sequence (CNS) –CNS1, CNS2, and CNS3—that are well-conserved through out mammals and function as enhancers[140]. Foxp3+ Tregs cells are subject

to higher order regulation by epigenetic modifications of the conserved non-coding sequences (CNS) in the Foxp3 locus[141–143], adding to the complexity in the canonical Foxp3-centric scheme of Treg differentiation

A body of work has identified the out-side-in regulator of Foxp3. TCR activation, TGF-β, and IL-2 have all been shown to contribute to Foxp3 regulation. TCR appears to be the primary determinant of Treg cell differentiation, and the Treg cells' TCRs mostly recognize self-antigens with high-affinity [144–146]. TCR activation is also required for peripheral pTreg differentiation. The TCR activation pathway could induce CD4 tolerance to non-self antigens (e.g. pathogenic pathogens as well as commensal bacteria). Activation of TCR stimulates downstream signals that are required for Foxp3 expression: namely nuclear factor of activated T cells (NFAT), nuclear factor-kB (NF-κB), and Protein kinase B (Akt)--Forkhead box O 1 (Foxo1)[147–149]. NFAT and Foxo1 directly bind to the Foxp3 promoter, and NF-κB is on conserved non-coding sequence 3 (CNS3) (**Figure 1.6**).

TGF-β facilitates Foxp3 expression *in vitro*[150], and TGF-β signaling is required for Foxp3+ Treg cell differentiation *in vivo*, especially pTreg cells during mucosal homeostasis and inflammation[151–153]. TGF-βRII knockout in T cells have decreased numbers of pTreg cells as well as multi-organ autoimmunity. TGF-β could activate the Smad2/Smad3 complex for binding to Foxp3 CNS1 element, which is also the Foxp3 5' enhancer. CNS1 supports extrathymic iTreg cells and impedes Th2-type mucosal inflammation. Deletion of CNS1 did not lead to unprovoked multi-organ autoimmunity or Th1 and Th17 inflammation[154].

Although the requirement of IL-2 and IL-2Ra (CD25) in Treg cell early development and function was plausible[139], currently the consensus is that IL-2Rβ and STAT5 activation are required for stability and functionally developed Foxp3+ Treg cells *in vivo*[155–157]. Moreover, this

regulation required CNS2. CNS2 is the 3' enhancer that is required to maintain Foxp3 stability and inheritance *in vivo*[158,159]. CNS2 contains CpG island for another layer of regulation—epigenetics. We will discuss Treg epigenetics in section I.6.2.

1.4.5 Regulatory T cells stability and plasticity

Treg cell stability means Treg could retain their Foxp3+ feature in different eviromental stimuli. Currently, Treg stability remains controversial *in vivo*. Bluestone and colleagues first provided evidence to suggest Treg cell instability by using lineage-tracing Foxp3-GFP-Cre X Rosa-STOP-YFP. Their evidence showed that Foxp3 Treg cells are unstable and lost their Foxp3 expression in inflammatory microenvironment (for example Type 1 diabetes) to become GFP-YFP+ 'ex-Treg' and pathogenic effector T cells[160]. But Rudensky and colleague later using Foxp3-GFP-CreERT2 that was inserted in the endogenous Foxp3 locus to show that ex-Treg was not changed in lymphopenic conditions and Th1 infection[161]. This conflict was later reconciled by Hori and colleagues when they inserted Foxp3-GFP-Cre in the endogenous locus. They found GFP-YFP+ eTreg cells that produced cytokines, but these ex-Treg cells consisted of only 5% of the Treg cells derived from Foxp3- Tconv cells [162]. Together, these studies demonstrate that: 1) most of Treg cells are stable *in vivo;* 2) unstable Treg cells are mostly iTreg cells and demonstrate the adaptability of Treg in different microenvironments, while this versatility may challenge the concept of iTreg cells as a therapeutic agent.

Besides stability, the emerging paradigm of paired differentiation between Treg and effector T cells demonstrates that Treg cells possess plasticity in that they co-express the transcriptional program of specific effector T cells[163]. For example, Foxp3+ Treg cells acquire T-bet+ to become Th1-like Treg cells and then they accumulate at sites of type 1 inflammation (e.g. *Mycobacterium tuberculosis* infection)[164]. Also, the expression of IRF4+ in Treg cells is able to control type 2

inflammation since Treg-specific deletion of IRF4 exhibited increased IL-4, IL-5, and IgE antibodies[165]. Interestingly, the master transcription factor of Th2—GATA3—is also expressed in Treg and it is required for Foxp3 expression and function[166]. Further, STAT3 expression in Treg cells skews it to a Th17-like Treg cell phenotype to prevent spontaneous intestinal Th17 inflammation[167]. Also, there are IL-17A producing and RORγt+ Treg cells in the small intestine. The function of RORγt+ Treg cells are still unknown. In earlier reports, in Th17-like Treg cells, Foxp3 antagonized RORγt function and inhibited IL-17A, suggesting that loss of Foxp3 expression allowed Treg cells greater Th17 plasticity with pathogenic effector function [168,169], e.g, allergic airway inflammation[170]. However, another study suggested that RORγt+Foxp3+ Th17-like Treg cells are suppressive in a colitis model[171]. Another example of plasticity is Th2-like Treg. While Th2-like Treg cells are pathogenic in a food allergy model[172], another report suggests that it's still have the suppression function in a worm infection model[166]. All these results are still being studied, and further knowledge about Treg plasticity will contribute to the more precise manipulation of Treg cells resulting in better therapeutics.

1.5 Epigenetics and its role in regulatory T cells

1.5.1 Epigenetic mechanisms in the development and maintenance of Treg

Treg cell biology is complex because Foxp3 expression *per se* might not be stable and sufficient for maintaining Treg phenotypes and functions. For example, CD4 T cells from human peripheral blood are FOXP3+, not suppressive and produce inflammatory cytokines[173]. In a murine model, $Foxp3^{gfp}$ mice that disrupt Foxp3 expression after Foxp3 promoter is activated by the GFP label shows that there are GFP+ but $Foxp3^{-}$ populations that still can express Treg functional

markers including CTLA-4[174]. Moreover, overexpression of Foxp3 in Tconv cells doesn't reconstitute many Treg cell signatures and functional markers[175]. Together, the inconsistent expression of Foxp3 and Treg cell functional markers suggests that Treg cell development is not simple. Foxp3 expression itself may not be sufficient to define the Treg fate and function. Other layers of regulation are to be expected and explored.

Post-translational modifications that alter gene expression without changing the DNA sequence, are called "epigenetic modifications". Epigenetic alterations, including histone modifications, DNA methylation, chromatin remodeling, and microRNAs, play indispensable roles in cell differentiation[176,177] and many other normal and malignant cellular functions. There exists a heritability aspect of epigenetic modifications that is relevant here as a layer of regulation that may provide mechanistic answers to T cell fate phenotypes[177,178].

DNA methylation plays a critical role in Treg cell fate phenotype. Recent genome-wide analyses revealed that tTreg and *in-vivo* derived pTreg are hypomethylated around *Foxp3* CNS2, while Foxp3- Tconv cells and Foxp3+ iTreg cells have more CpG island methylation[179,180]. The methylation status correlates with Foxp3 stability since iTreg cells are less stable than tTreg cells (see section I.5.5), and demethylated CNS regions becomes accessible to transcription factors including Ets-1 and STAT5[181]. There are several DNA demethylases that are also responsible for Foxp3 stability and Treg cell maintenance *in vivo*, including TET1/2[182–184].

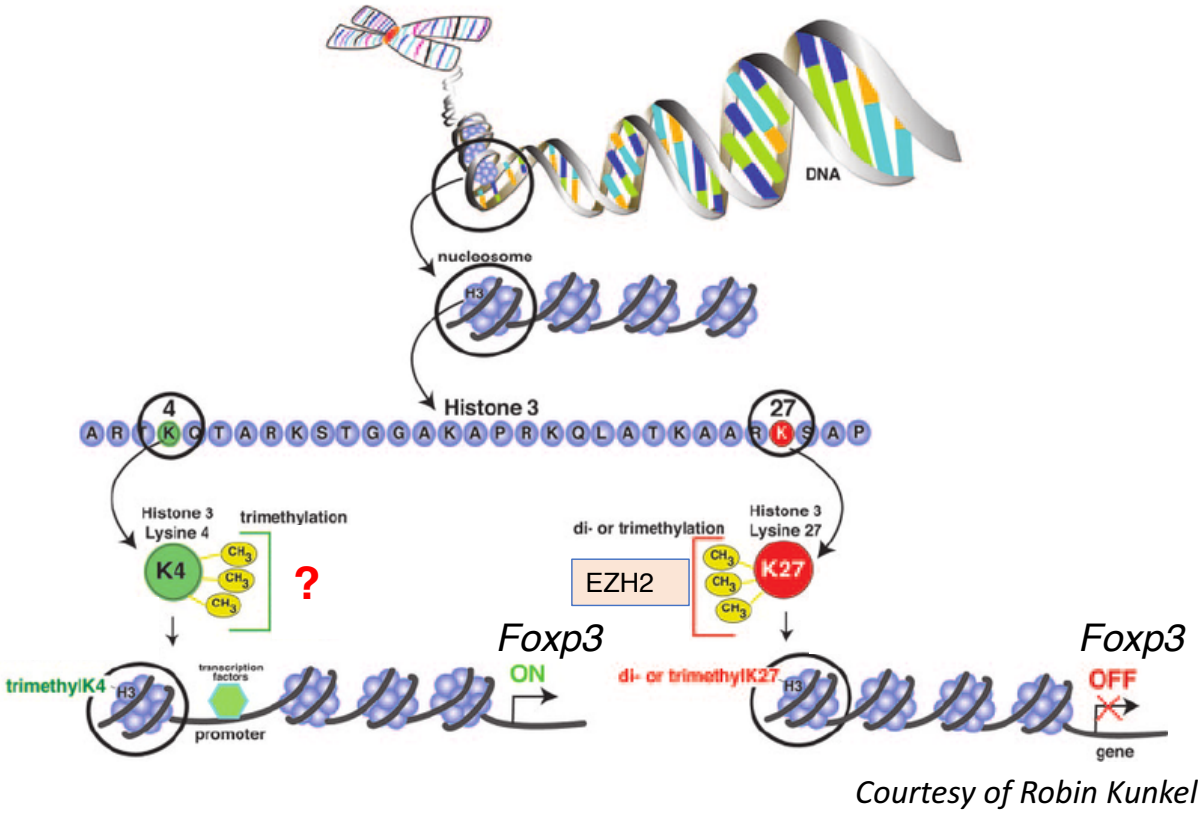

Figure 1.8 Histone 3 lysine modifications in Foxp3 regulation

Histone modifications are also critical in Treg differentiation. The histone 3 lysine 4 tri-methylation (H3K4me3) and histone 3 lysine 27 tri-methylation correlate with gene expression or gene repression of Foxp3 reciprocally in Treg cells[185] (**Figure 1.8**). The permissive epigenetic marks, histone 3 lysine 4 tri-methylation (H3K4me3), is mostly enriched around the Foxp3 CNS1 segment and the Foxp3 promoter but not as significantly around CNS2 and CNS3[140] . The suppressive mark, H3K27me3, was removed from the Foxp3 promoter and the CNSs elements compared to these regions in uncommitted naïve CD4 T cells[185].

There is H3K27 demethylases reported to be involved in Treg cell development *in vivo*. EZH2 demethylase removes H3K27me3 around Foxp3-bound genes to stabilize Treg cell phenotype[186]

and enhance the suppressive function in response to inflammation[187]. On the other hand, MLL4 adds the H3K4me1 mark for early tTreg survival but not for pTreg cell function[188], but the role of an H3K4 tri-methylase in Treg differentiation is relatively unexplored. Our lab first identified that SMYD3, which is a protein methylase and H3K4 di- and tri-methyltransferase[189], is induced by TGF-β and supports pTreg cell differentiation to decrease immunopathogenesis in pulmonary RSV infections[190]. These studies demonstrate that epigenetic mechanisms are vital to Treg cell differentiation and stability. New two-step model that both Foxp3 expression and epigenome signature are required for a stable Treg lineage specification is prevalent in the field.

1.5.2 SET and MYND domain containing protein 3 (SMYD3)

SET and MYND domain containing protein 3 (SMYD3) is also known as lysine methyltransferase 3E (KMT3E). It functions as protein methyltransferase. Smyd3 has been reported to be histone 3 lysine 4 di- (H3K4me2) and tri- (H3K4me3) methyltransferase[189]. Recently, SMYD3 are also reported to be histone 4 (H4) K20 methylase and protein methylase to have broad impact on gene regulations[191,192].

Smyd3 is over-expressed in multiple cancers and correlates with poor prognosis in cancer patients. [193–198]. It promotes cell growth and inhibits apoptosis in cancer cells and thus is a cancer potentiator [193,194,199]. Smyd3 turns on multiple oncogenic pathways including RAS-, estrogen receptor-, and E-caderin-driven tumorogenesis to facilitate the initiation of transcription [192,199,200]. But the role of Smyd3 in non-cancerous models is unknown.

Our laboratory first showed a novel role for Smyd3 in CD4 T cells. Agreeing with other reports, Smyd3 is TGF-β-dependent and regulates TGF-β family genes[201–203]. Moreover, Smyd3 perturbed iTreg cell formation while allowing dysregulated IL-17A to worsen the immunopathology during RSV infection[201]. However, the upstream signals that regulate Smyd3

and their role in maintaining tolerance to infection at mucosal surface are still unclear. The studies in this thesis have further elucidated that Dll4/Notch activation is a primary mediator of inducing Smyd3 that further stabilizes the Treg phenotype and promotes Treg function. These changes include a regulatory T cell program in both Foxp3+ and Foxp3- T cells.

Chapter 2 Materials and Methods

2.1 Mice

6-8 week old female BALB/cJ and C57BL/6J mice were purchased from Jackson Laboratory. Female CD45.1 (B6-Ly5.1/Cr) mice were purchased from Charles River. Foxp3^{EGFP} mice (B6.Cg-*Foxp3*^{tm2Tch}/J, stock number 006772) were bought from Jackson Laboratory and bred in house. *Cd4*-specific DNMAML mice (Cd4-Cre x R26^{DNMAMLf}) and *Cd4*-specific Rbpj knockout mice (Cd4-Cre x Rbpj$^{f/f}$) are the gift of Dr. Maillard's lab generated as described[58,204,205]. *Cd4*-specific Smyd3 knockout mice was generated in our lab as described[190]. SMYD3$^{tm1a\ (KOMP)\ Wtsi}$ mice in a C57BL/6 background were derived from KOMP Repository at UC Davis (Davis, CA). The allele contains loxP and FRT sites, thus Cre and FLP deletion were used to create a SMYD3 conditional knockout resulting in a null allele in CD4 cells (SMYD3$^{fl/fl}$CD4^{Cre}.). Cd4-specific Smyd3 knockout mice were backcrossed with Foxp3^{eGFP} to create Foxp3-GFP labeled Smyd3 conditional knockout mice (Foxp3-GFP X SMYD3 KO). All mice were housed in the University Laboratory Animal Facility under animal protocols approved by the Animal Use Committee in University of Michigan.

2.2 Respiratory syncytial virus (RSV) infection

RSV Line 19 was a clinical isolate originally from a sick infant in University of Michigan Health System, which has shown in animal models to mimic human infection with increased mucus production, more airway hypersensitivity, and exacerbated IL-13 production[25,28]. BALB/c mice or B6 mice were anesthetized and infected intratracheally (IT) with $1*10^5$ PFU of Line 19 RSV, as previously described[82].

2.3 In vivo neutralization of Dll4

For Dll4 blockade *in vivo*, 2.5 mg of purified polyclonal anti-Dll4 antibody or control IgG were injected intraperitonialy two hours before RSV infection at day 0 as described[85]. The same dose of control or anti-Dll4 antibody were given on day 2, 4, and 6.

2.4 Histopathology

Left lobe of the lung was fixed with 4% formaldehyde and embedded in paraffin, and 5 μm sections were stained with Periodic acid-Schiff (PAS) stain to detect mucus.

2.5 RNA isolation and quantitative PCR

RNA were extracted with TRIzol (Invitrogen) by following the manufacturers protocol, and one μg of total RNA was reverse transcribed to cDNA to determine gene expression using Taqman gene expression primer/probe sets. *Dll1, Dll4, Jag1,* and *Jag2* were detected by SYBR as described[69]. Delta4 primers: 5'-AGGTGCCACTTCGGTTACACAG-3' and 5'-CAATCACACACTCGTTCCTCTCTTC-3' were used as described[69]**.** *Muc5ac* and *Gob5* expression were assessed by custom primers as described [206]. Detection was performed in ABI 7500 Real-time PCR system. Gene expression was calculated using the ΔΔCt method as $2^{-\Delta\Delta Ct}$ when ΔΔCt= experimental Ct−input Ct)-(control Ct−input Ct) and normalized with *Gapdh* as input control.

2.6 Murine lung cells isolation

Mice lungs were chopped then lungs and mediastinal lymph nodes were enzymatically digested using 1 mg/mL Collagenase A (Roche) and 25 U/ml DNaseI (Sigma-Aldrich) in RPMI 1640 with 10% fetal calf serum for 45 min at 37°C. Tissue were further dispersed through an 18 gauge needle/10 mL syringe, and filtered through 100-μm nylon mesh twice.

2.7 Murine intestine lamina propria lymphocyte/leukocyte (LPL) isolation

Intestinal and colon feces were flushed out by holding the intestine with forceps and flushing with a syringe filled with DPBS. Residual mesenteric fat tissue and Peyer's Patches were resected. After placing feces removed, longitudinally opened small intestine lamona propria (SI-LP) and colon lamina propria (C-LP) in ice-cold 1X DPBS without Ca or Mg, the colon or intestine were cut into 0.5 cm pieces. The pieces of intestine were incubated in 20 mL of predigestion solution (1X DPBS (-Ca -Mg)+2mM EDTA+5% FBS) for 20 min at 37^{o}C with rotation (200rpm) in a thermal incubator in a 50 ml tube. The remaining pieces were passed through a 100 μm cell strainer. The pieces were added together into fresh predigestion solution for 20 min at 37^{o}C under 200rpm rotation in a 50 ml tube. The flow-through contains colonic content with epithelial cells and can be decanted or stored for the isolation of intraepithelial lymphocytes (IEL). The pieces were again passed through a 100 μm cell strainer the remaining EDTA was washed away with 1X DPBS. The tissue was collected into 50 ml tubes containing 10 mL of pre-warmed digestion solution—same as lung digestion (RPMI+10% FBS+1 mg/mL Collagenase A+ 40 μg/mL of DNase I). The pieces were digested by incubation at 37°C for 30 min under 200 rpm rotation. (Colon digestion takes more time than small intestine). After incubation, the cell solution was rigorously vortexed for 20 s and passed through a 40 μm cell strainer set over a 50 mL tube. The digestion was repeated 2 times. Ideally, all gut pieces should be digested to invisible small pieces. (Colon digestion may take more time than small intestine). Combine the supernatants from all digestion steps in a fresh 50 ml tube and centrifuge for 10 min at 500 xg at 20°C Discard the supernatant. Wash the pellet in RPMI only medium and centrifuge the cells again at 500g for 10 min at 20°C. Enriched lymphocyte/leukocyte are obtained by Ficoll filtration. In brief, using a Pasteur pipette, carefully overlay the cell suspension on top of 3 mL of the Ficoll solution in a 15 mL tube. Centrifuge the

Ficoll gradient for 30 min at 500 xg at 20°C without brakes (0 deceleration). Following centrifugation, obtain the ring of lymphocyte/leukocyte cells (@ between 2.5~3.5 mL). Wash with 1% FBS in DPBS buffer (FACS buffer), 500xg, 5'.

2.8 Extracellular and Intracellular flow cytometry analysis

Mice lungs mediastinal lymph nodes were enzymatically digested as described above. The single-cell suspension of lung and lymph nodes were stimulated with with 100 ng/mL Phorbol-12-myristate 13-acetate (PMA), 750 ng/mL Ionomycin, 0.5 µL/mL GolgiStop (BD), 0.5 µL/mL GolgiPlug (BD) for 5 hours. After excluding dead cells with LIVE/DEAD Fixable Yellow stain (Invitrogen), cells were pre-incubated with anti-FcγR III/II (Biolegend) for 15 minutes and labeled with the following antibodies from Biolegend (or otherwise specified):

Antigen	Clone	Conjugates	Dilution	Isotype
CD3	145-2C11 or 17A2	PE or Pacific Blue	1:200	Rat IgG 2b
CD4	GK1.5	APC/Cy7	1:200	Rat IgG 2b
CD8α	53-6.7	PerCP/Cy5.5	1:200	Rat IgG1
CD25	PC61	Pacific Blue or PE	1:200	Rat IgG1
CD44	IM7	FITC or PE	1:200	Rat IgG2b
CD62L	MEL-14	PE/Cy7	1:200	Rat IgG2a
CD69	H1.2F3	PE/Cy7	1:200	Hamster IgG
I-A/I-E (MHC II)	M5/114.15.2	Pacific Blue or Alexa700	1:200	Rat IgG2b
CD11b	M1/70	PE/Cy7	1:200	Rat IgG2b
CD11c	N418	APC/Cy7	1:200	Hamster IgG
CD103	2E7	APC	1:200	Hamster IgG
Dll4	HMD4-1	PE or APC	1:200	Hamster IgG
ICOS	C398.4A	PE/Cy7	1:200	Hamster IgG
PD-1	J43, eBioscience	PE	1:200	Hamster IgG
Neuropilin-1	Polyclonal. R&D	PE	1:200	
CCR7	4B12	PE	1:200	Rat IgG2a
Lag3	eBioC9B7W	PE/Cy7	1:200	Rat IgG1

Table 2.1 Antibodies for entracellular staining

For intracellular staining, cells were fixed and permeabilized with transcription factor staining buffer set (eBioscience). After 3 washes, cells were labeled with antibody from eBioscience:

Antigen	Clone	Conjugates	Dilution	Isotype
Foxp3	FJK-16s	APC	1:50~1:75	Rat IgG2a
IL-17A	eBio17B7	PE/Cy7	1:100 (Ex vivo) 1:200 (In vitro culture)	Rat IgG2a
IL-13	eBio13A	PE	1:100	Rat IgG1
GATA3	TWAJ	PE	1:100	Rat IgG2b
RORγt	AFKJS-9	PE	1:100	Rat IgG2a
CTLA-4	UC10-4B9	PE	1:100	Hamster IgG
Granzyme B	NGZB	PE	1:100	Rat IgG2a
H3K4me3	Polyclonal (Millipore)	FITC anti-rabbit Ab	1^0: 1:200 2^0:1:200	

Table 2.2 Antibodies for intracellular staining

Antibodies were incubated with cells for 30 min at room temperature. After 3 times washing, flow cytometry data were acquired from a LSR II (BD) or a Novocyte (ACEA) flow cytometer and were analyzed with FlowJo software (TreeStar).

2.9 Cell sorting and suppression assay

Single cell sorting was performed on FACSAria II (BD). For RNA analysis, viable CD4 and CD8 T cells were directly sorted into TRIZoL reagent; for suppression assays, $DAPI^{-}CD4^{+}eGFP^{+}$ viable Treg cells were sorted with more than 93% efficiency. Suppression assays were performed as described with small modification [207]. In brief, naïve T cells isolated from CD45.1 mice were labeled with Cell Trace Violet (CTV) (Invitrogen). 2.5 X 10^4 of CTV-labeled CD45.1+ naïve T cells were co-cultured with serial-diluted $EGFP^{+}$ Treg cells in a 96 well round bottom plate. 0.625

μL of Dynabeads® mouse T activator CD3/CD28 (Invitrogen) were added to 0.2 mL of culture. After 72 hours, cells were harvested, and $CD45.1^+$ responder cell proliferation was accessed by CTV dilution.

2.10 Lymph node re-stimulation and cytokine production assay

$5X10^5$ cells from mediastinal lymph nodes were plated in 96-well plates and re-stimulated with 10^5 RSV for 48 hours. IFNγ IL-4, IL-5, IL-13, IL-17A, IL-10, IL-9 levels in the supernatant were measured using a Bio-plex cytokine assay (Bio-Rad).

2.11 Naïve CD4 T cell isolation and stimulation

$CD4+CD25-CD62L^{hi}CD44^{lo}$ naïve T cells were enriched from wild type B6 spleen using the naïve CD4 T cells isolation kit (Miltenyi Biotec) to more than 92% purity. Naïve T cells were then plated and cultured in round-bottom 96-well plates (for luminex analysis) or 24-well plates (for CD4 T cells skewing). $2X10^5$/ml to 10^6/ml of naïve T cells were stimulated with plate-bound anti-CD3 (2.5 μg/ml; eBioscience), soluble anti-CD28 (3 μg/ml; eBioscience), and plate-bound recombinant Dll4 (1.65 μg/mL or the dose mentioned; R&D); to skew toward *in vitro*-induced Treg cells (iTreg), human TGF-β (2 ng/ml; R&D System) and mouse IL-2 (10 ng/ml; R&D System) were added at the same time; to skew toward Th17 cells (Th17), mouse IL-6 (10 ng/ml; R&D System), human TGF-β (2 ng/ml; R&D System), anti-IFNγ neutralizing antibody (10 μg/mL; eBioscience), anti-IL-4 neutralizing antibody (10 μg/mL; eBioscience), and anti-IL-12/23 p40 neutralizing antibody (10 μg/mL; eBioscience) were added at the same time.

2.12 Chromatin Immunoprecipitation (ChIP)

ChIP was performed based on manufacturer's instruction (Upstate Biotechnology) as described[208]. In brief, $2*10^6$ stimulated T cells were cross-linked with 1% paraformaldehyde for 10 min in room

temperature. Cross-linking was stopped with 1X glycine, then cells were frozen. After lysing the cell pellet in 200 uL SDS lysis buffer, the resulting lysate was sonicated using a Branson Sonifier 450 (VWR, West Chester) under the following condition: 3 times for periods of 11 seconds each. After centrifuging, the supernatant was diluted and 2% were saved for Input. Other diluted supernatant underwent immunoprecipitation at 4°C overnight with the following antibodies:

Antigen	Brand; Clone or concentration	Ab/Dilution V	Results
IgG control	Millipore; 1 mg/mL	2uL/500uL	O
H3K4me3	Millipore/Abcam; 1 mg/mL	2uL/500uL	O/O
H3Ac	Millipore; 1 mg/mL	2uL/1000uL	O
RBP-Jk	Abcam; 1 mg/mL	2.5 uL/500uL	O
N1ICD	Cell signaling;D3B8	2.5 uL/500uL	X
SMAD3	Cell signaling;C67H9	5 uL/500uL	X
H3K79me3	Millipore; 0.7 ug/mL	3 uL/500uL	O

Table 2.3 Antibodies for chromatin immunoprecipitation

or rabbit IgG as a control (Millipore). The precipitated complex was pulled down by protein A beads and cross-linking was reversed by high salt in 5 hours under 65°C. DNA was purified by standard phenol/chloroform and ethanol precipitation and was subjected to real-time PCR. ChIP-specific enrichment was calculated using the ΔCt method as $2^{-(\text{experimental Ct}-\text{input Ct})}$

Smyd3 promoter: 5'-ACAGGGCTTCTCTGTTGTATAGC -3' and 5'-GAGTTTAAAGCCAGCGTGGT -3'

2.13 Immunoblot analysis

Total cells lysates were prepared using 1X Cell Lysis Buffer (Cell Signaling). The same amount of total proteins (3~10 μg) were separated by Nu-PAGE(Invitrogen) and transferred onto a nitrocellulose membrane. The primary Ab was diluted in 5% BSA in 1X TBST and incubated overnight. The secondary Ab—anti-Rabbit-HRP (Cell signaling)—was diluted in 5% non-fat milk in 1X TBST for 1 hour. Protein bands were visualized and quantified with SuperSignal West Femto Masimun Sensitivity substrate.

Antigen	**Brand**	**Dilution**	Secondary
SMYD3	Abcam; ab16027 and ab187149	1:500	Rabbit
Notch 1 intracellular cleaved domain (N1ICD)	Cell Signaling; #4147	1:1000	Rabbit
H3K4me3	Abcam; ab8580	1 : 1000	Rabbit
H3	Cell Signaling : #9715	1: 1000	Rabbit

Table 2.4 Antibodies for Western blotting

2.14 RNA sequencing sample preparation

Naïve CD4 T cells ($CD4^{+}CD25^{-}CD62L^{hi}CD44^{lo}$) were enriched as described above from three 10~13 weeks old female Cre- control and three Cre+ Smyd3 conditional knockout mice. After 48 hours of iTreg differentiation, total RNA was extracted using TRIzol and cleaned with QUIAGEN RNA CleanUp kit. The cDNA library was converted from mRNA using the following condition: non strand specific, poly-A selection. Deep sequencing was performed on HiSeq-4000 platform

with 50 bp single strand sequencing. The fragment length is around 120nt with 30 to 40 million reads per sample.

2.15 RNA sequencing data analysis pipeline

FastQC—Trimmomatic—HISAT2—Samtool—HTSeq—DESeq2 pipeline were performed for RNA sequencing data analysis. After download the fastq.gz file from DNA sequencing core, FastQC were implemented. All of our 12 samples were pass the quality control by Fast QC. Second, Trimmomatic-0.36 was downloaded with binary model and coded using ~bash (Terminal in MacOS). Quality scores were at the highest (40) in every sample. Third, the reads were aligned to that of the reference genome using HISAT2 under bash. The reference genome is GRCm38 in Ensembl. After alignment, the .sam file was compressed with Samtool to become a .bam file. Fourth, we counted the reads in genes using HTSeq under Python. Raw counts and htseq.out file were the outputs. Finally, DESeq2 under R were implemented to normalize the reads and do differential analysis with Likelihood Ratio Test (LRT). Principle component analysis (PCA), Venn diagram, volcano plots, and heatmap were performed and drawn in R. Gene Ontology were performed using DAVID Bioinformatics resources 6.8, and treemap were drawn by REVIGO.

2.16 Statistical analysis

Data were analyzed by Prism6 (GraphPad). Data presented are mean values ± SEM. Comparison of two groups was performed in unpaired, two-tailed, Student's *t*-test. Comparison of three or more groups was analyzed by ANOVA with Tukey's post-tests. Significance was indicated at the level of *:$p<0.05$, **: $p<0.005$, ***: $p<0.0005$

Chapter 3 Notch Ligand Dll4 Reduces RSV Immunopathology and Sustains Treg Identities

3.1 Abstract

Treg cells establish tolerance, prevent inflammation at mucosal surfaces, and regulate immunopathology during infectious responses. Recent studies have shown that Delta-like ligand 4 (Dll4) was up-regulated on antigen presenting cells after RSV infection and its inhibition lead to exaggerated immunopathology. The present studies outline the role of Dll4 in Treg cell differentiation, stability and function in RSV infection. Here we found that Dll4 was expressed on $CD11b^+$ pulmonary DC in the lung and draining lymph nodes in wild type BALB/c mice after RSV infection. Dll4 neutralization exacerbated RSV-induced disease pathology, mucus production, group 2 innate lymphoid cells (ILC2) infiltration, IL-5 and IL-13 production, as well as IL-17A+ CD4 T cell infiltration. Dll4 inhibition decreased the abundance of $CD62L^{hi}CD44^{lo}Foxp3^+$ central Treg cells (cTreg) in draining lymph nodes. The RSV-induced disease was accompanied by an increase in Th17-like effector phenotype in $Foxp3^+$ Treg cells and a decrease in Granzyme B expression after Dll4 blockade. Finally, Dll4-exposed induced iTreg cells maintained a $CD62L^{hi}CD44^{lo}$ cT_R cell phenotype, had increased Foxp3 expression, became more suppressive, and were resistant to Th17 skewing *in vitro*. These results suggest that Dll4 activation during differentiation sustained Treg cell phenotype and function to control RSV infection.

3.2 Introduction

Notch is a highly conserved signaling pathway that contributes to cell differentiation and function. Engagement of Notch receptors (Notch 1-4) and Notch ligands (Delta-like ligand 1, 3, 4, Jagged 1, 2) initiates cleavage of the Notch intracellular domain (NICD). NICD binds to recombination binding protein-J (RBP-Jκ) and activates the transcription of Notch target genes in association with a co-activator of the Mastermind like family (MAML 1-3). Notch signaling regulates various stages of T cells lineage development and differentiation, including early stages of thymocyte development, as well as CD4 T helper (Th) differentiation[69,71]. In the priming stage of Th cell differentiation, Notch ligand Dll4 sensitized antigen responses and augmented T cells activation [74], while separate studies demonstrated that Dll4 and Notch could activate production of IFNγ and the Th1 transcription factor T-bet [76,77,79]. During Th2 differentiation, Jagged1 and intracellular Notch promoted *Gata3* and *Il4* expression [79–81], while Dll4 suppressed *Il4, Il5, and Il13* [75,82]. Furthermore, Dll4 and Notch was reported to promote Th17 and Th9 differentiation by enhancing *Il17a*, *Rorc* and *Il9 expression* [86,209]. Together, Notch can serve as an amplifier for persistent Th1, Th2, and Th17 cell differentiation [76], suggesting that it is not a skewing signal, but rather enhances co-activation. However the role of Dll4 and Notch signaling in Treg cells remains unresolved. Jagged2 and specific receptors, Notch1 and Notch3, promoted the Treg cell master transcription factor—*Foxp3* expression and Treg cell survival [92–96], and RBP-Jκ was reported to directly bind the *Foxp3* promoter and regulate Foxp3 transcription [96]. In contrast, inactivating Notch signaling after Foxp3 is first expressed enhanced T_{reg} cell numbers and promoted tolerance [70]. Blockade of Notch receptors and Notch ligands expanded Foxp3+ T cell populations *in vivo* in experimental autoimmune encephalomyelitis (EAE), Graft-versus-host disease (GvHD), and Type 1 diabetes

(T1D) [97–100]. However, the role of Notch ligands in subsets of Treg cells and in their resistance to inflammation during infection have not been well-defined.

Notch ligands can be induced on antigen presenting cells by pathogen-associated molecular patterns (PAMPs) [79,80]. Pathogens themselves can also induce Notch ligands. Studies showed that RSV induced Dll4 expression on DC *in vitro* [82,210], and Dll4 blockade exacerbated RSV-induced Th2 airway pathogenesis [82]. Since Treg cells are required to limit pulmonary inflammation and pathogenic Th2 responses during RSV infections [39,41,42], we hypothesized that the initial exposure of Dll4 may modulate peripherally-induced iTreg cell differentiation, homeostasis and stability to control the intensity of the immune response and lung pathology during RSV infection. In the present study, we report that Dll4 sustained $CD62L^{hi}CD44^{lo}$ central Treg cells and solidified iTreg identity during infection. This study defined novel roles of Dll4 in iTreg cell subset regulation and iTreg cell stability.

3.3 Results

3.3.1 Up-regulation of Dll4 during RSV infection on $CD11b^{+}$ pulmonary DC

Previously published data have shown that Dll4 expression was up-regulated on DC post RSV infection *in vitro* [82,210]. To further characterize the expression of Dll4 during RSV infection *in vivo*, BALB/cJ mice were intratracheally (i.t.) infected with 1 X 10^5 pfu of RSV before harvesting of lung tissues at 2 and 6 days post infection (dpi). *Dll4* transcripts were up-regulated significantly at 6 dpi, while transcripts for the other Notch ligands *Dll1, Jagged (Jag) 1* and *Jag2,* were not increased in the lung (**Figure 3.1**).

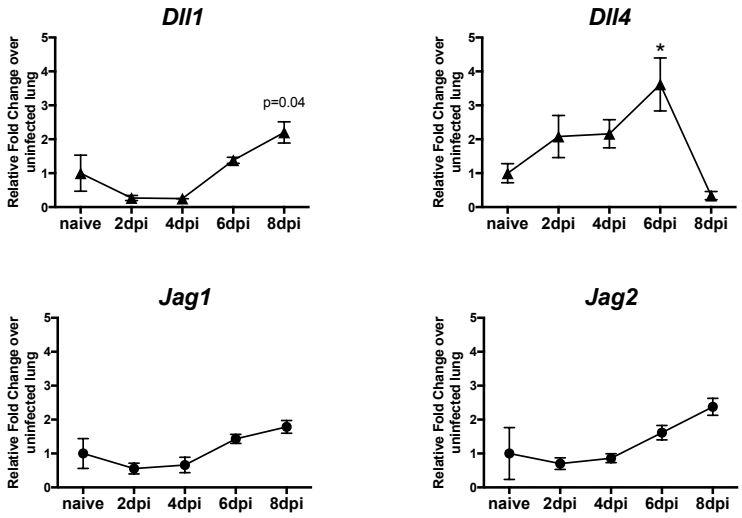

Figure 3.1 Notch ligand expression kinetics during RSV infection

Abundance of *Dll1, Dll4, Jag1, and Jag2* mRNA in RSV-infected lung at the indicated time points relative to uninfected naïve lung. *: $p<0.05$

After gating on MHC^{hi} $CD11c^{+}$ DC, Dll4 expression level consistently was increased on $MHCII^{hi}$ $CD11c^{+}$ DC after 6 dpi (**Figure 3.2**).

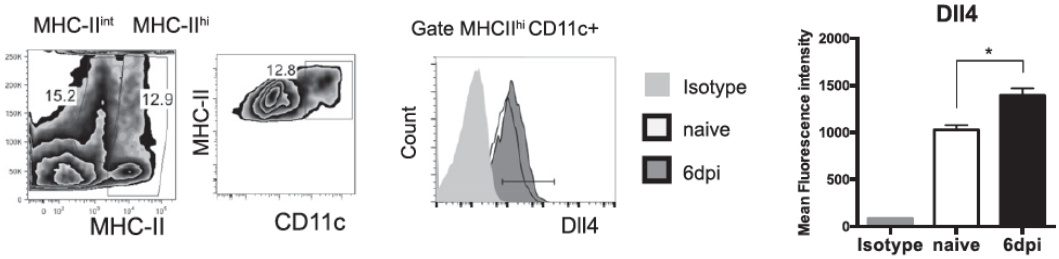

Figure 3.2 Notch ligand Delta-ligand 4 (Dll4) is up-regulated on $MHCII^{hi}CD11c^{+}$ pulmonary DC post RSV infection

Lung cells from either uninfected naïve mice or RSV-infected Balb/c mice were immunostained with MHC-II, CD11c, and Dll4. $MHCII^{hi}CD11c^{+}$ pulmonary DC population were gated, and Dll4 expression were measured. *: $p<0.05$

To further understand which type of DC expressed Dll4 after RSV infection, two populations of pulmonary DC were identified as follows to determine Dll4 expression: $MHCII^{hi}$ $CD11c^{+}$

$CD11b^+$ $CD103^-$ DC and $MHCII^{hi}$ $CD11c^+$ $CD103^+$ $CD11b^-$ DC. $CD11b^+$ DC expressed Dll4, whereas few of the $CD103^+$ DC expressed Dll4 during RSV infection (**Figure 3.3**).

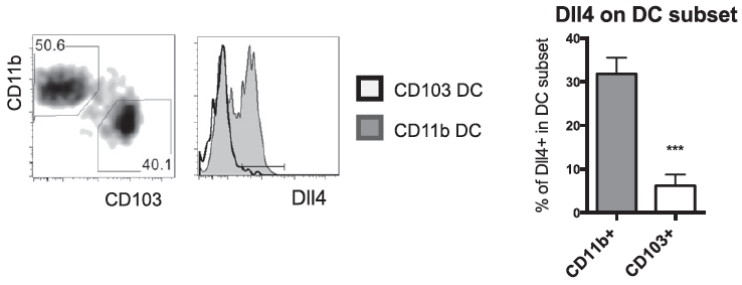

Figure 3.3 Dll4 is prevalent on $MHCII^{hi}CD11c^+$ $CD11b^+$ conventional DC but not much on $MHCII^{hi}CD11c^+$ $CD103^+$ DC post RSV infection

Lung cells from either uninfected naïve mice or RSV-infected Balb/c mice were immunostained with MHC-II, CD11c, CD11b, CD103, and Dll4. $MHCII^{hi}CD11c^+CD11b^+$ conventional DC and $MHCII^{hi}CD11c^+CD103^+$ DC were gated, and Dll4 expression were measured. ***: $p<0.0005$

When we examined the number of DC in lung and draining lymph node at 6 dpi, increasing numbers of $Dll4^+$ $CD11b^+$ DC in both lung and the draining LN--mediastinal lymph node (mLN) were detected as the infection progressed (**Figure 3.4**). In contrast, the number of $Dll4^+$ $CD103^+$ DC was significantly lower and variable in lung (left) or mLN (right) after infection (**Figure 3.4**).

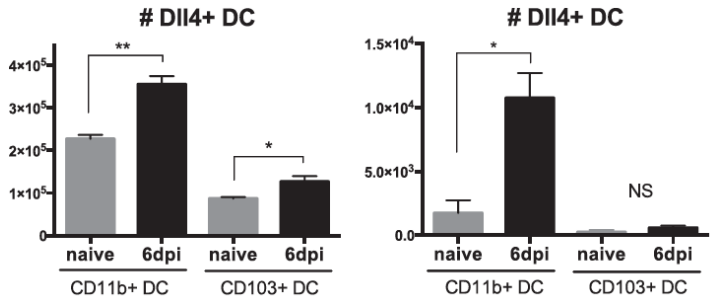

Figure 3.4 $Dll4^+CD11b^+$ DC is more enriched than $Dll4^+CD103^+$ DC post RSV infection

Lung cells from either uninfected naïve mice or RSV-infected Balb/c mice were immunostained with MHC-II, CD11c, CD11b, CD103, and Dll4. The numbers of $MHCII^{hi}CD11c^+CD11b^+Dll4+$ and $MHCII^{hi}CD11c^+CD103^+Dll4^+$ were counted. *: $p<0.05$, **: $p<0.005$

These data indicated that Dll4 was expressed on pulmonary DC, especially CD11b^{+} DC, after RSV infection *in vivo*.

3.3.2 Inhibition of Dll4 exacerbated RSV-induced immunopathology *in vivo*

Next, we explored the role of Dll4 in controlling RSV immunopathology by blocking Dll4 *in vivo* during RSV infection. We have previously demonstrated that our polyclonal anti-Dll4 antibody is specific for Dll4 and not other Notch ligands[82]. The polyclonal anti-Dll4 antibody decreased the abundance of Notch target gene *Hes1* transcripts in activated T cells (Th0) in co-culture with fixed Dll4-expressing stromal cells (**Figure 3.5**), indicating that anti-Dll4 antibody blocked Dll4-mediated Notch activation *in vitro*. We next aimed at blocking Dll4 *in vivo* by injecting 2.5 mg of purified anti-Dll4 antibody intraperitoneally (i.p). Mice were then infected i.t with RSV 2 hours after antibody injection at day 0, followed by i.p injection of anti-Dll4 every other day. After 8 days, the abundance of *Hey1*—Notch target gene transcripts was decreased in the lung and sorted CD4 T cells from mLN (**Figure 3.5**) of anti-Dll4-treated mice, suggesting that systemic administration of anti-Dll4 antibodies inhibited Notch signaling activation in CD4 T cells *in vivo*.

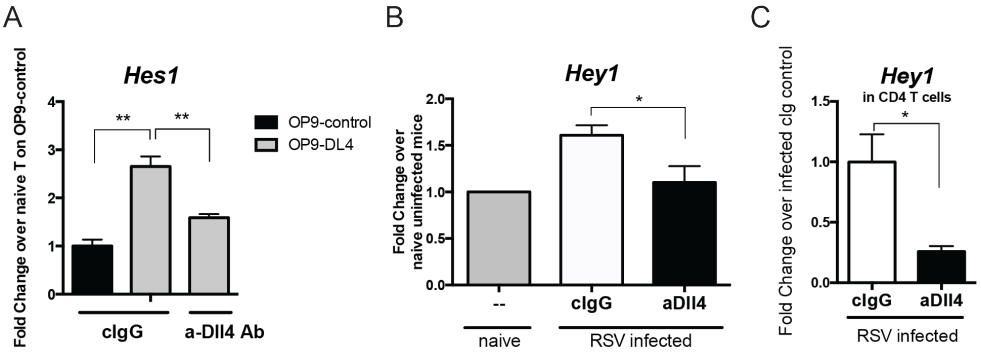

Figure 3.5 Anti-Dll4 neutralization impedes Notch signaling activation demonstrated by Notch target gene expression *in vitro* and *in vivo*

A. OP9 cells (OP9-control) and Dll4-transduced OP-9 cells (OP9-DL4) were cultured in the 10^{5}/ 24 wells and fixed with 4% formaldehyde to provide Notch ligand Dll4 without

mRNA production. After pre-incubating 2 μg of anti-Dll4 antibody or control IgG for 15 minutes, 10^6 of naïve CD4 T cells were culture on OP9-control or OP9-DL4 for 2 hours. CD4 T cells were harvested, and *Hes1* expression was measured.

B. Notch target genes *Hey1* in the lung were measured at 8 dpi to examine the efficacy of Dll4 neutralization.
C. Viable CD4 T cells in mediastinal lymph node from individual mice were sorted, and Notch target gene *Hey1* were measured to examine the efficacy of Dll4 inhibition in CD4 T cells. N=5 in each group.

Data represent mean ± s.e.m. * P<0.05; ** P<0.005; *** P<0.0005; NS: no significance (unpaired two-tailed t-test)

Dll4 blockade increased peribronchial infiltration by mononuclear cell clusters and drove mucus production in the airway as assessed in periodic-acid Schiff (PAS)-stained lung sections **(Figure 3.6A).** As an indication of RSV-induced pathology, expression of the mucus-associated gene *gob5 (mClca3)* was substantially increased **(Figure 3.6B)**, but the viral titer measured with RSV-F and RSV-G didn't have any significant difference at both 6 dpi and 8 dpi (**Figure 3.6C** and data not shown). Thus, Dll4 targeting significantly altered lung immunopathology during RSV infection.

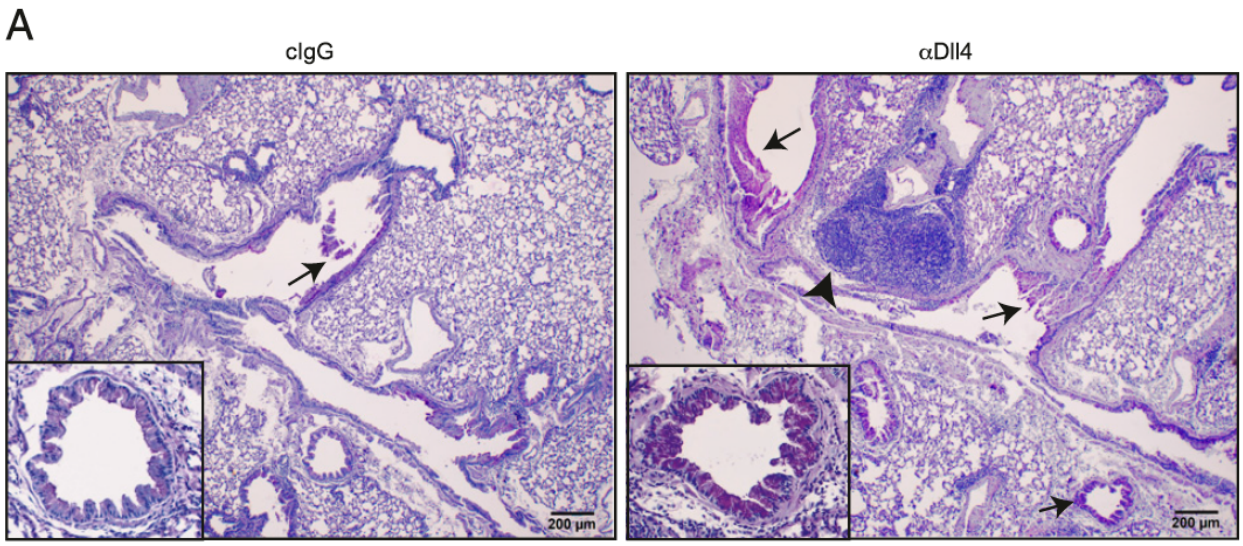

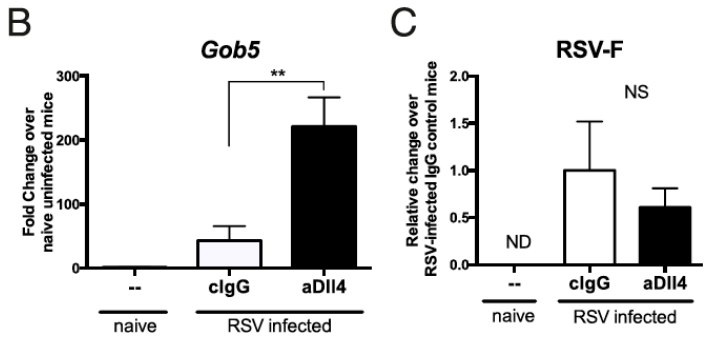

Figure 3.6 Blockade of Dll4 drives mucus production in lung but not affect the abundance of RSV viral gene at 8 dpi of RSV infection

A. Periodic acid-Schiff (PAS) staining of formalin-fixed lung section from 8 dpi. Bar, 200 μm. ↑ indicates the detection of mucin, and ➤ designates mononuclear cells aggregates.
B. *Gob5* expression in the lung at 8 dpi.
C. RSV-F viral fusion protein gene expression in lung at 8 dpi. ND: non-detectable

Besides CD4 T cells, RSV infection also activated ILC2 cells between 4 to 6 dpi in lung to be mucogenic and immunopathogenic [8]. Here we investigate if Notch ligand Dll4 affects ILC2 homeostasis. The gating strategy is shown in **Figure 3.7**. Strikingly, Dll4 inhibition increased the number of $Lin^{-}CD45^{+}CD127^{+}ST2^{+}CD25^{+}$ ILC2 cells in lung (**Figure 3.7**) and and mLN (data not shown) at 6 dpi. Thus, Dll4 targeting significantly altered lung immunopathology during RSV infection. These data suggested that Dll4 blockade enriched ILC2 in airway during RSV infection.

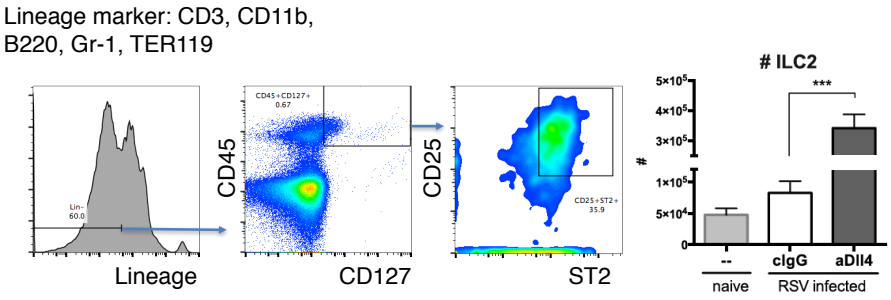

Figure 3.7 Blockade of Dll4 increased the number type 2 innate lymphoid cells (ILC2) at 6 dpi of RSV infection

Balb/c mice were infected with RSV, and Dll4 were inhibited by injecting 2.5 mg of purified anti-Dll4 antibody intraperitoneally (i.p). Lung cells in uninfected mice, cIg-injected RSV-infected mice, and Dll4 neutralized RSV-infected mice were immunostained. $Lineage^{-}$

$CD45^+CD127^+CD25^+ST2^+$ Type 2 Innate lymphoid cells (ILC2) were gated and counted. ***: $p<0.0005$

Excessive cytokine production is one of the key feature leading to RSV pathogenesis. IFNγ promotes viral clearance while IL-4, IL-5, IL-13 and IL-17A are pathogenic [211–213]. Here we determined the effect of Dll4 blockade on cytokine profiles in draining lymph nodes. The same number of mLN cells were cultured and re-stimulated with 10^5 pfu RSV. *In vivo* Dll4 blockade during RSV infection led to significantly increased Th2 cytokines IL-5, IL-13 and IL-17A while IFNγ, IL-4, IL-9, and IL-10 were not significantly affected in RSV re-challenged lymph node cells. **(Figure 3.8)**

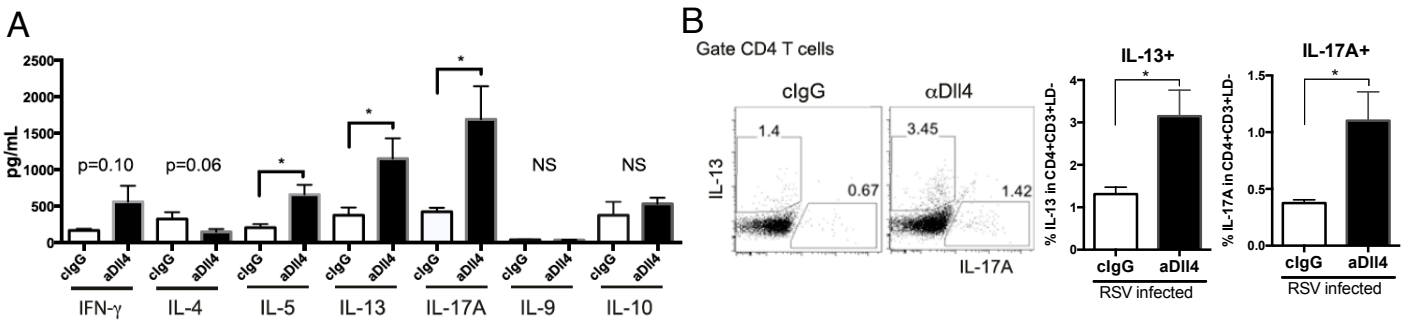

Figure 3.8 Blockade of Dll4 drives accumulation of IL-13 and IL-17A production

A. Mediastinal lymph node cells from control or Dll4 neutralized mice were counted, and $5*10^5$ of mediastinal lymph node cells were restimulated 10^5 pfu of RSV. After 48 hours, cytokines in the supernatant were measured.
B. Mediastinal lymph node cells from control or Dll4 neutralized mice were restimulated with PMA+Ionomycin+Golgi Stop+Golgi plug for 5 hours. Intracellular IL-13 and IL-17A in CD4 were stained.

To specify if Dll4 regulated T helper cell cytokine production in CD4 T cells, mLN cells were re-stimulated with PMA+Ionomycin and CD4 T cells were examined by flow cytometry. Dll4 blockade significantly increased IL-13+ and IL-17A+ CD4 helper T cells in mLN in both 6 dpi

and 8 dpi (data not shown). These data indicated that Dll4 neutralization exacerbated RSV-induced immunopathology, as shown by elevated mucus production, activated CD4 T cells, and Th2-Th17 cytokine over-production.

3.3.3 Dll4 neutralization reduces central Treg and increases Th17-like Treg during RSV infection

Several studies demonstrated that Treg cells quickly accumulate in lymphoid tissues and in the airway to dampen activated T cell infiltration and Th2 responses [39–41], and that RSV infection drove Treg cells to Th2-like effector cells with impaired function [214]. Our group showed that Dll4 inhibition exacerbated type 2 cytokine production and activated T cell infiltration, but little is known about the role of Dll4 in Treg cell development, stability and function. After targeting Dll4 as previously described, total Treg cells did not change in mLN at 6 dpi. However, when gating on CD62L^{hi}CD44^{lo} central CD4 T cells (cT), Dll4 neutralization decreased the cTreg population, while eTreg were not altered in mLN (**Figure 3.9**A~C). CCR7-mediated signals recruit CD62L^{hi}CD44^{lo} T cells to the T cell zone, and CCR7 is a marker of cTreg cells [215]. Here we also found that Dll4 inhibition decreased expression of the CCR7 chemokine receptor on cTreg cells (**Figure 3.9**D, E). These data suggested that Dll4 specifically sustained cTreg cells and their expression in mLN during RSV infection. (**Figure 3.9**)

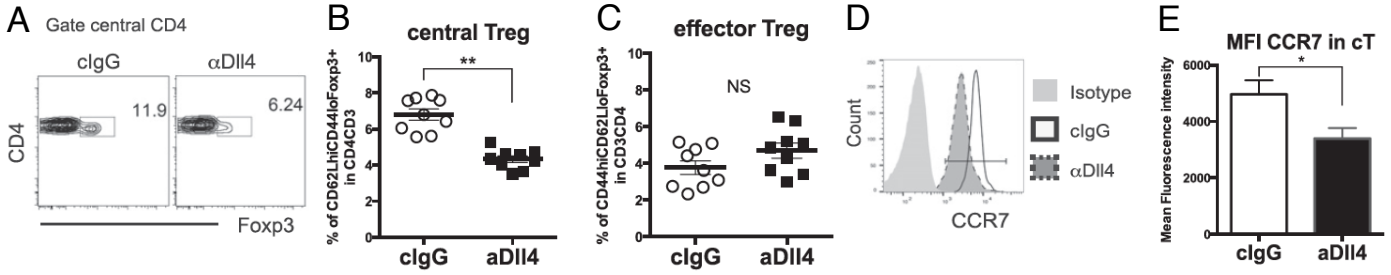

Figure 3.9 Dll4 inhibition impairs the maintenance of central T_{reg} cells in lymph node *in vivo*

A. Percentage of $Foxp3^+$ cells in $CD62L^{hi}CD44^{lo}$ central CD4 T cells harvested from the mLN at 6 dpi
B. Percentage of $CD62L^{hi}CD44^{lo}Foxp3^+$ central Treg cells in mLN at 6 dpi
C. Percentage of $CD44^{hi}CD62L^{lo}Foxp3^+$ effector Treg cells in mLN at 6 dpi
D. Representative flow cytometric analysis showing CCR7 expression in $CD62L^{hi}CD44^{lo}$ central CD4 T cells in mLN at 6 dpi
E. E. Mean fluorescence intensity of CCR7 in $CD62L^{hi}CD44^{lo}$ central CD4 T cells in mLN at 6 dpi

We next examined if Dll4 can also perturb cytokine production in $Foxp3^+$ CD4 T cells. Lung cells harvested at 8 dpi were re-stimulated and stained for intracellular Foxp3, IL-13 and IL-17A before flow cytometric analysis. *In vivo* Dll4 blockade significantly increased the abundance of $IL\text{-}17A^+Foxp3^+$ after PMA+Ionomycin (P+I) re-stimulation. To further characterize if Dll4 regulates either Th17 or Th2 transcription factor co-expression in Treg cells, RORγt or GATA3 were co-stained with Foxp3 after re-stimulation. Dll4 neutralization increased the percentage of $ROR\gamma t^+Foxp3^{lo}$ cells but not $ROR\gamma t^-Foxp3^+$ after 8 dpi **(Figure 3.10)**

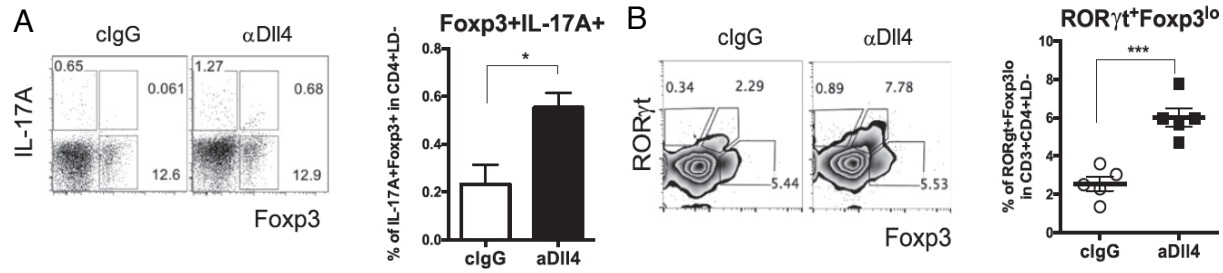

Figure 3.10 Dll4 inhibition enriches Th17-like Treg *in vivo*

A. Gating strategy and percentage of $IL\text{-}17A^+Foxp3^+$ cells in viable CD4 T cells at 8 dpi. Lung cells were re-stimulated with PMA+ Ionomycin+ Golgi Stop+ Golgi plug 5 hours for intracellular cytokine staining
B. Gating strategy and percentage of $ROR\gamma t^+Foxp3^{lo}$ cells in viable CD4 T cells at 8 dpi. No stimulation is applied.

These data suggested that Dll4 inhibition drove a Th17-like effector phenotype in Treg cells during RSV infection *in vivo*. Surprisingly, we didn't detect significant changes in GATA3^{+} Treg cells and even total GATA3^{+} CD4 T cells in both lung and LN after Dll4 inhibition (data not shown).

To further specify the role of Dll4 in cytokines, especially in Foxp3^{-} Tconv cells versus Foxp3^{+} Treg cells, here we switch the mouse strain from Balb/cJ to Foxp3^{EGFP} knock-in mice which have EGFP cassette knocked in downstream of an endogenous STOP codon with no defect in Foxp3 expression and Treg function. Foxp3^{EGFP} knock-in mice were i.t infected with RSV and treated with neutralizing anti-Dll4 antibody. At 6 dpi, viable CD4^{+}Foxp3$^{EGFP-/+}$ cells from mLN were sorted (**Figure 3.11A**). DLL4 neutralization decreased *Foxp3* expression in EGFP^{+} CD4 T cells (**Figure 3.11C**). At both 6 dpi and 8 dpi, *Il17a* mRNA was increased in EGFP^{+} but not EGFP- CD4 T cells (**Figure 3.11B**), whereas DLL4 inhibition increased *Il5* and *Il13* expression in EGFP- but not in EGFP^{+} mice. DLL4 inhibition differentially affected *Ifng* expression in EGFP- versus EGFP^{+} mice(**Figure 3.11D-E**).

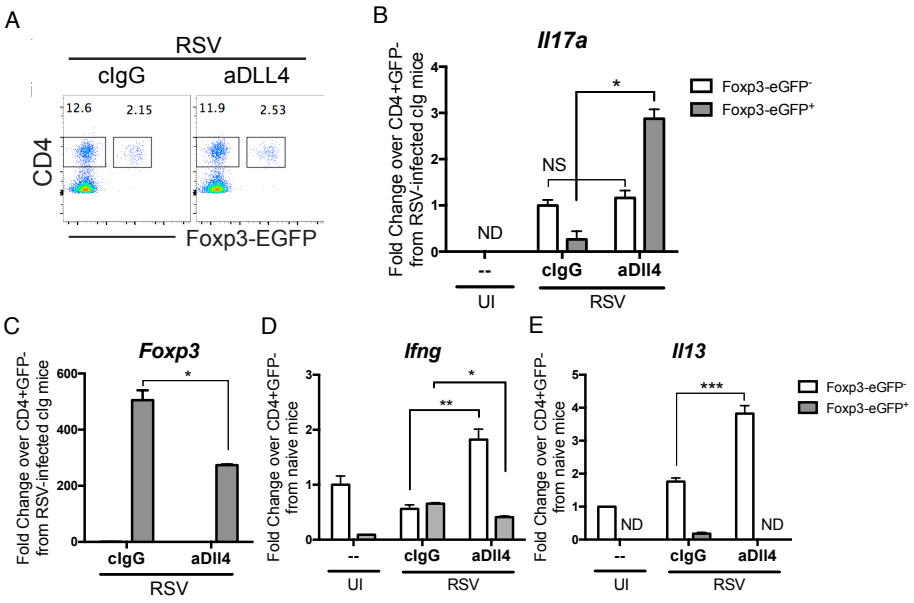

Figure 3.11 Dll4 inhibition enriches more *Il17a* and decreases Foxp3 expression in Foxp3-GFP$^+$ Treg during RSV infection *in vivo*

A. FACS gating strategy for CD4+Foxp3-GFP+ or CD4+Foxp3-GFP- population in mLN at 6 dpi of RSV infection
B. *Il17a* expression in Foxp3-GFP+ and EGFP- population at 6 dpi
C. *Foxp3* expression in Foxp3-GFP+ and EGFP- population at 6 dpi
D. *Ifng* expression in Foxp3-GFP+ and EGFP- population at 6 dpi
E. *Il13* expression in Foxp3-GFP+ and EGFP- population at 6 dpi

To further investigate if Dll4 regulated Treg cell functional markers, several parameters were examined: Inducible T cells co-stimulator (ICOS), Programmed cell death protein 1 (PD-1), Granzyme B (GzmB), and Neuropilin-1 (Nrp1). It was previously shown that during RSV infection, GzmB was the critical functional molecule for Treg cell function to limit the associated immunopathology [42]. After further gating on central vs effector Treg, we found that Dll4 neutralization decreased the frequency of GzmB$^+$ in Foxp3$^+$ Treg cells in the lung after 8 dpi, especially prominently for GzmB$^+$ eTreg cells **(Figure 3.12)**. On the other hand, ICOS, PD-1 and Nrp1 expression were unchanged in Foxp3$^+$ Treg cells.

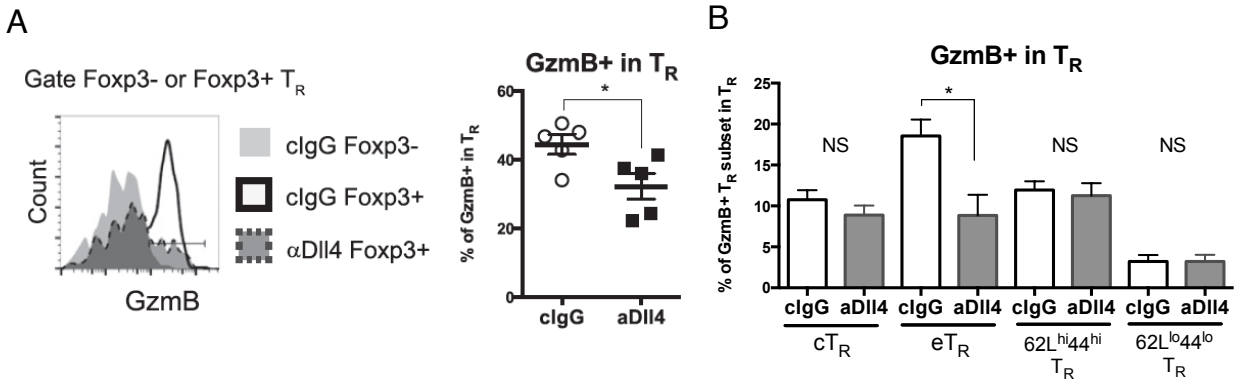

Figure 3.12 Dll4 harnesses cytolytic effector function in Treg, especially in effector Treg during RSV infection *in vivo*

A. Granzyme B (GzmB) staining in Foxp3$^-$CD4$^+$CD3$^+$ or Foxp3$^+$CD4$^+$CD3$^+$ (Treg) cells in lung at 8dpi.
B. Percent of GzmB+ in CD62L^{hi}CD44^{lo} central Treg (cT$_R$), CD44^{hi}CD62L^{lo} effector Treg (eT$_R$), and other two populations.

Our results indicate that Dll4 prevented Foxp3 Treg cell acquisition of Th17-like effector phenotype, and it supported GzmB expression in Treg cells in the lung during RSV infection.

3.3.4 Dll4-knockdown of DC exacerbates RSV immunopathology and Treg cell identity

Figure 3.2~3.3 demonstrated that $CD11c^+$ DC express Dll4 during RSV infection, and Figure 3.6~3.8 showed that Dll4 inhibits RSV immunopathology and sustains Treg cell identity *in vivo*. To further specify if Dll4 on $CD11c^+$ DC is directly responsible for the RSV immunopathology and Treg cell identity, we first tried to breed CD11c-Cre with $Dll4^{f/f}$ mice but obtained no Cre+ offspring. We then switched to UBC-Cre-ERT2 X $Dll4^{f/f}$ to have Cre-ERT2 expressed in all tissue types. ERT2 doesn't bind to the natural ligand of estrogen receptor—17β-estradiol—but binds to synthetic ligand 4-hydroxytamosifen (4-OHT). After 6 days of bone-marrow derived dendritic cells (BMDC) culture, we treated the Cre- control or Cre+ BMDC with 1 μM of 4-OHT. 48 hours later, BMDCs were infected with RSV line 19 with MOI=1 for 24 hours. BMDC were subject to flow cytometry to confirm the knockdown with ~50% efficiency (**Figure 3.13A**). At day 0, we i.t. transferred $2.5*10^5$ Cre- control or Cre+ BMDC into $Foxp3^{EGFP}$ recipients. After 12 days post DC transfer i.t, male or female $Foxp3^{EGFP}$ recipients were re-infected with RSV, and mice were harvest at day 20 (8 dpi) (**Figure 3.13B**). We observed more Muc5ac and Gob5 mucin gene expression in Dll4 knockdown (KD) DC mice, although the p-value was not significant **(Figure 3.13C** and data not shown**)**. PAS positive staining mucin was visualized in lung histology as indicated by arrows **(Figure 3.13D)**. To further investigate the role of Dll4 on DC in Treg cell identities, we stained Foxp3, CTLA-4, OX40, Granzyme B, Lag3 in CD4 T cells in lung. Treg cell markers were not changed by Dll4 KD DC (data not shown). To investigate if deletion of Dll4 in DC could affect Th17 like Treg like cells, we double stained IL-17A and Foxp3 in CD4 T cells. Strikingly, Foxp3 intensity in Treg cells was significantly decreased (**Figure 3.13F**), while there

was no change in IL-17A+ Foxp3- Th17 cells and very few IL-17A+Foxp3+ cells were detected (**Figure 3.13E**). Moreover, mucogenic and pathogenic IL-5 and IL-13 were increased by Dll4 knockdown in DC (**Figure 3.13G**). Note that these CD4 T cells were all from wild type B6 mice. These data strongly emphasize the role of Dll4 in DC that promotes Foxp3 expression in CD4 T cells and impedes pathogenic type 2 cytokine over-production.

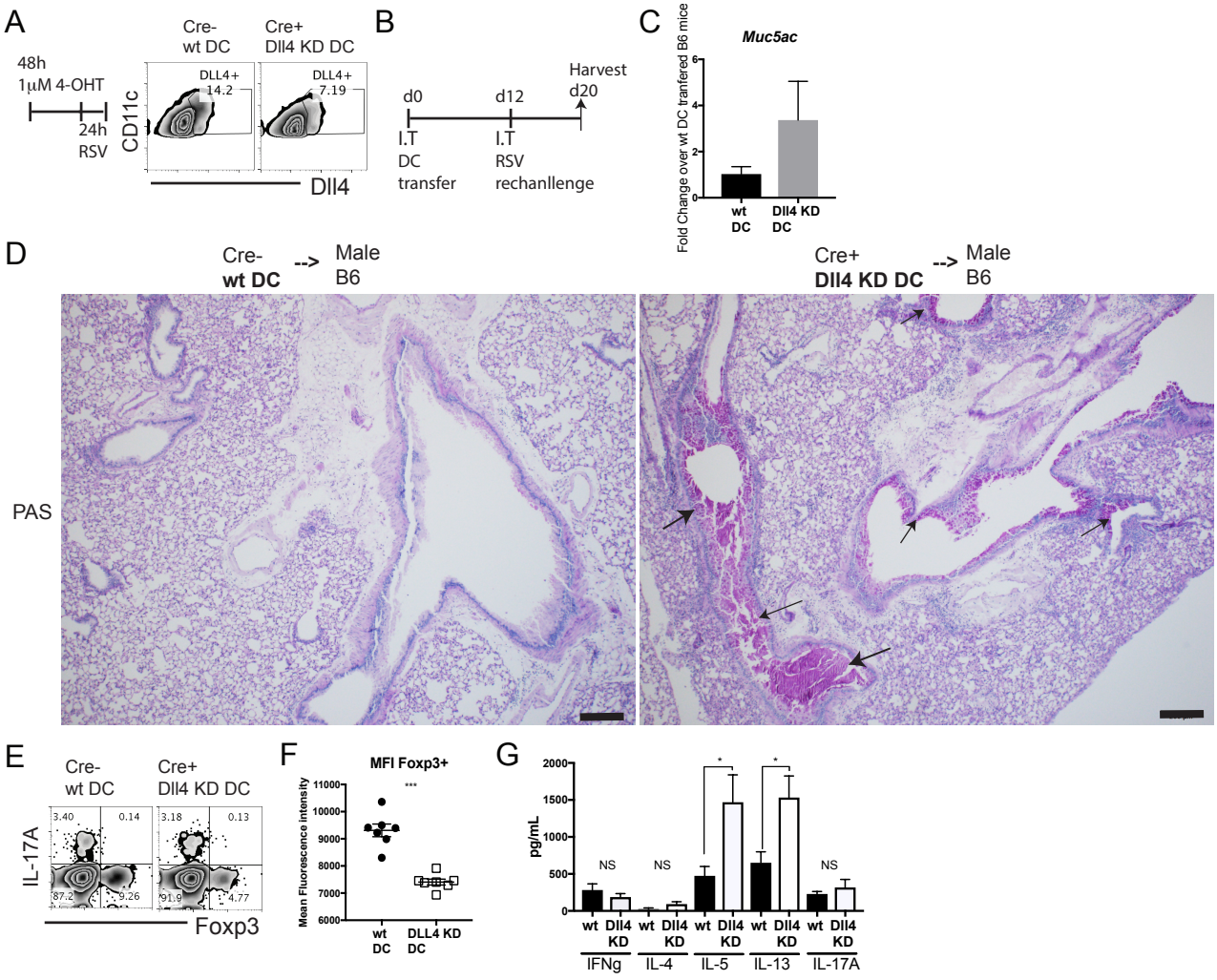

Figure 3.13 Dll4 on DC sustains Treg identity and attenuates RSV Th2 pathology *in vivo*

A. After 6 days of BMDC culture, BMDC were incubated with 1mM 4-OHT for 48 hours, and DC were washed before infection with Line 19 RSV for 24 hours. Dll4 expression on $CD11c^{+}$ BMDC were examined with flow cytometry.
B. Experimental regimen of Dll4 DC transfer experiment. $2.5*10^{5}$ Wt DC or Dll4 KD DC were i.t transferred into wt $Foxp3^{EGFP}$ mice. After 12 days, both DC-transferred $Foxp3^{eGFP}$

mice were re-infected with RSV. After another 8 days (at d20), mice were harvested for analysis.

C. Expression of *Muc5ac* in lung from wt DC or Dll4 KD DC transferred B6 mice were measured at d20.
D. PAS-stained lung section from wt DC or Dll4 KD DC transferred B6 mice to indicate mucin-positive signal in purple (arrows).
E. Viable CD4+ T cells from lung were re-stimulated with P+ I for 5 hours. And IL-17A^{+} Foxp3^{+} cells were stained.
F. Foxp3 mean fluorescence intensity was quantified in the Foxp3^{+}IL-17A^{-} CD4 T cells population.
G. 2*10^{5} mLN cells from either wt DC or Dll4 KD DC transferred B6 mice were re-stimulated with RSV for 48 hours. Cytokines were measured and profiled by Bioplex.

3.3.5 Dll4 activates and maintaines inducible Treg cells *in vitro*

Our data reveal differential effects of Dll4 in Foxp3+ Treg cells in lymphoid vs. non-lymphoid tissue during pulmonary infection. To further investigate Dll4 effects on Treg cell differentiation in a controlled context, splenic CD4^{+}CD25^{-}CD62L^{hi}CD44^{lo} naïve CD4 T cells were activated with anti-CD3/anti-CD28 with or without plate-bound recombinant Dll4, and skewed toward Treg cells with TGF-β and IL-2. We first confirmed that Dll4 was able to activate expression of the Notch target gene *Hes1* in naïve CD4 T cells, Th0 and Treg cells in a dose-dependent manner and activated intracellular domain of Notch1 (N1ICD) cleavage **(Figure 3.20)**.

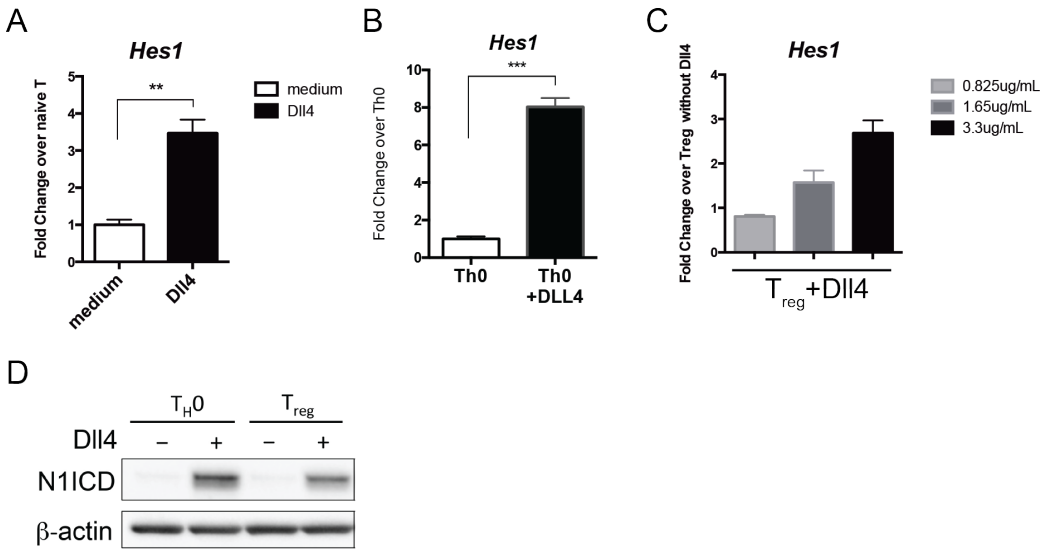

Figure 3.14 Plate-bound recombinant Dll4 activates Notch signaling in both naïve CD4 T cells and Treg differentiation *in vitro*

A. Naïve CD4 T cells were cultured in 96 well round bottom plate only or in a Dll4 coated plate for 24 hours. Notch target gene *Hes1* was measured.
B. Naïve CD4 T cells were cultured in either α-CD3/α-CD28 Th0 conditions +/- plate-bound Dll4 for 24 hours. Notch target gene *Hes1* was measured.
C. Naïve CD4 T cells were cultured in α-CD3/α-CD28/TGF-β/IL-2 iTreg conditions plus plate-bound Dll4 with the indicated concentrations for 24 hours. Notch target gene *Hes1* was measured.
D. Naïve CD4 T cells were cultured in Th0 or iTreg conditions with or without Dll4 for 48 hours. Cleaved Notch 1 intracellular domain (N1ICD) was detected to indicate Notch signaling activation.

Subsequently, naïve T cells were skewed toward Th0 or iTreg cell phenotype. Importantly, Dll4 increased $CD25^{+}Foxp3^{+}$ iTreg cells in a dose-dependent manner only in the presence of TGF-β. Furthermore, *Foxp3* expression was significantly decreased with homozygous *ROSA26*-driven expression of the pan-Notch-inhibitor dominant negative Mastermind-like 1 (DNMAML1), and with inactivation of the *Rbpj* gene, encoding RBP-Jκ **(Figure 3.21).** Since MAML1 and RBP-Jκ mediate transcriptional activation through Notch signaling, these data revealed that Dll4-activated Foxp3 expression was dependent upon canonical RBP-Jκ/MAML-dependent Notch signaling.

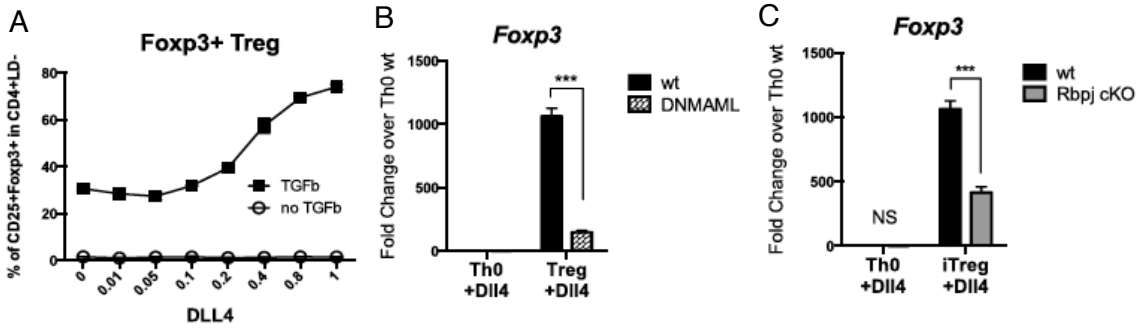

Figure 3.15 Dll4 up-regulates Foxp3$^+$ iTreg differentiation in TGF-β dependent and canonical Notch dependent manner *in vitro*

A. CD25$^+$Foxp3$^+$ iT$_{reg}$ were skewed from naïve CD4 T cells for 72 hours with or without 2 ng/mL of TGF-β and indicated concentration of Dll4 (μg/mL)
B. *Foxp3* expression after 48 hours skewing from either wild type naïve CD4 T cells or naive T cells expressing dominant negative MAML1 (DNMAML)
C. *Foxp3* expression after 48 hours skewing from either wild type or CD4-specific *Rbpj*-deficient naïve CD4 T cells

To further characterize Foxp3+ cells in this differentiation system, primary Dll4-activated iTreg cultures were rested in IL-2 for 3 days without Dll4. Dll4-treated iTreg cells consistently maintained a higher percent of Foxp3+ cells and higher Foxp3 expression **(Figure 3.16)**.

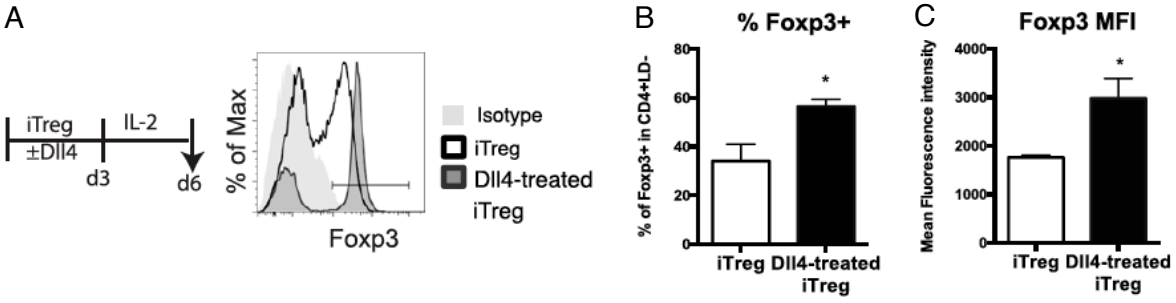

Figure 3.16 Dll4 exposure sustains the percent of Foxp3+ and Foxp3 expression in iTreg *in vitro*

A. Naïve CD4 T cells from wild type B6 mice were skewed toward iT$_{reg}$ with or without Dll4 stimulation for 72 hours (d3), then rested in 10 ng/mL of IL-2 for another 72 hours. Representative flow cytometry showed the expression of Foxp3 in viable CD4 T cells at day 6 (d6).
B. Percentage of Foxp3$^+$ in viable CD4 T cells at day 6.

C. Mean fluorescence intensity of Foxp3 in viable Foxp3^{+} CD4 T cells at day 6

To investigate whether Dll4 affected any homeostatic features on Treg cells during *in vitro* skewing, CD62L and CD44 expression was evaluated before or after sequential dosing of IL-2 during rest. Naïve CD4 T cells that were exposed to Dll4 during primary iTreg cell skewing maintained more CD62L^{hi}CD44^{lo}Foxp3+ cells independent of the dose of IL-2 during the rest period and at multiple time points after primary skewing (**Figure 3.17**).

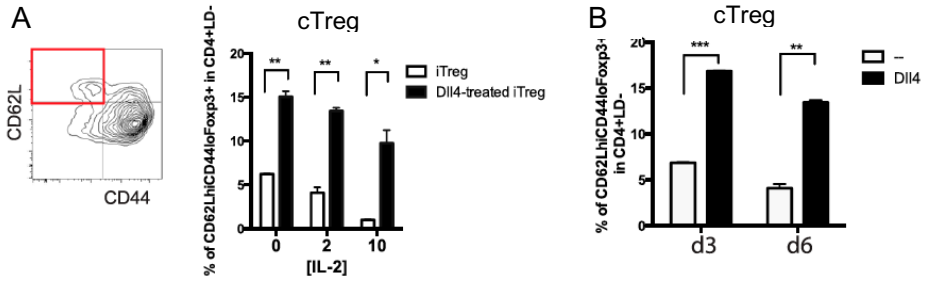

Figure 3.17 Dll4 exposure sustains the percent of central Treg Foxp3+ *in vitro*

A. Percentage of CD62L^{hi}CD44^{lo}Foxp3^{+} central T_{reg} (cT_R) after 0 ng/mL, 2 ng/mL and 10 ng/mL of IL-2 resting at day 6 iT_{reg} culture
B. Percentage of cT_R at day 3 and day 6 with 2 ng/mL of IL-2 in iT_{reg} culture

These data suggest that the presence of Dll4 during iTreg activation and differentiation stabilized Foxp3 expression and sustained more Treg with a CD62L^{hi}CD44^{lo} phenotype *in vitro*.

3.3.6 Dll4-exposed iTreg cells are more suppressive and functional *in vitro*

To further evaluate the function of iTreg cells after Dll4 exposure, we sorted viable, Foxp3-eGFP^{+} iTreg cells from culture on day 6 and co-cultured these cells with CD45.1^{+} naïve CD4 T cells as responders. CD45.1^{+} naïve T cells were labeled with CellTrace Violet (CTV) and stimulated with α-CD3/α-CD28 mouse T cell activator for 72 hours. Viable CD45.1^{+} cells were gated to examine CTV dilution as a readout of cell proliferation. Responder cells that were co-cultured with Dll4-treated iTreg cells were less proliferative, especially at the 1:1 and 1:2 cell ratio of Treg: naïve T,

suggesting that Dll4-treated iTreg cells were more suppressive than iTreg cells without Dll4. **(Figure 3.18).** There data indicated that Dll4-exposed iTreg cells were more functional *in vitro*.

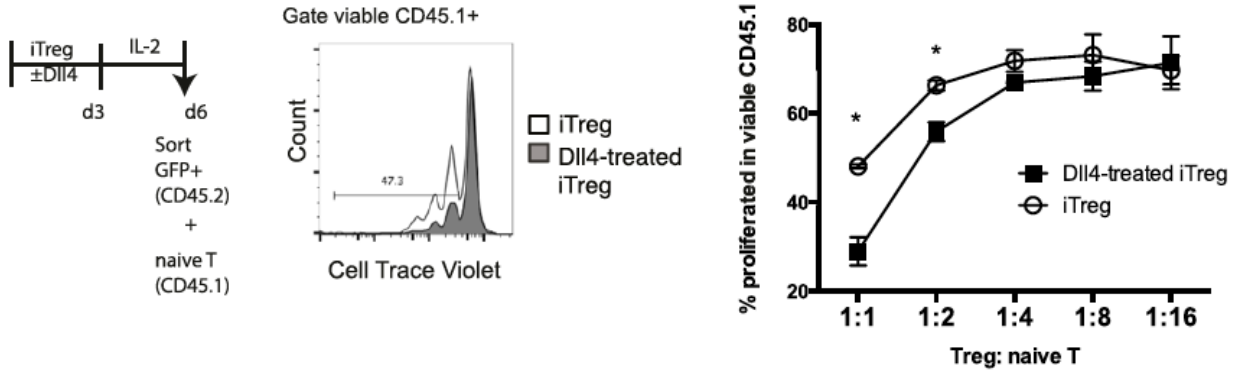

Figure 3.18 Dll4-exposed iTreg cells are more suppressive *in vitro*

Schematic representation of the *in vitro* suppression assay. Naïve CD4 T cells from Foxp3-EGFP knock-in mice underwent iT_{reg} differentiation with or without Dll4 for 72 hours, and resting in 2 ng/mL IL-2 for 72 hours. Viable iT_{reg} or Dll4-exposed iT_{reg} were sorted out as Foxp3-eGFP^{+} DAPI^{-}, and co-cultured with CellTrace violet (CTV) labeled CD45.1^{+} naïve T cells with anti-CD3/anti-CD28 beads. After 3 days in co-culture, proliferation was assessed by CTV dilution in CD45.1^{+} responder cells.

3.3.7 Dll4 and Notch activation strengthen iTreg to be less plastic toward Th17

To examine whether Dll4 and Notch signaling could inhibit acquisition of a Th17 effector phenotype in iTreg cells, naïve CD4 T cells were purified and cultured in iTreg skewing conditions and *Il17a* expression was examined. Inactivation of Notch increased *Il17a* expression during iTreg skewing, while Foxp3 transcripts were decreased. Both DNMAML1 expression and *Rbpj* inactivation in CD4 T cells led to increased IL-17A in iTreg Dll4 skewed cultures **(Figure 3.19).** These data suggest that intrinsic Notch activation inhibited *Il17a* expression while enhancing Foxp3 expression in iTreg cells during differentiation.

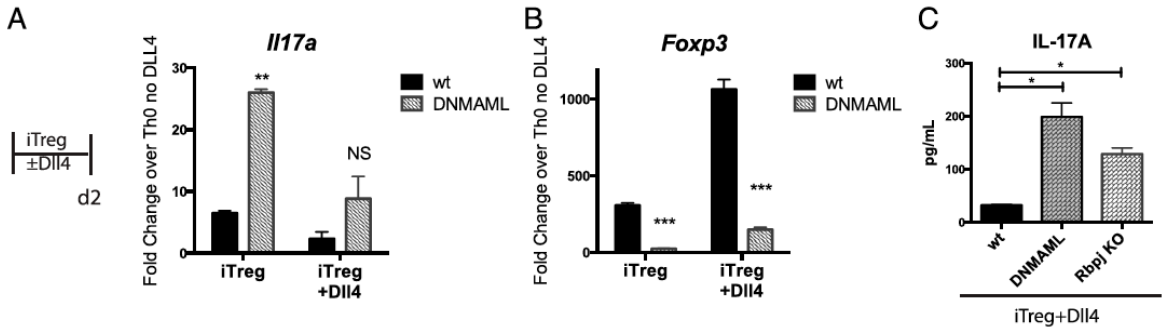

Figure 3.19 Dll4 stimulation and intracellular Notch promotes Foxp3 and impedes IL-17A production during iTreg differentiation *in vitro*

A. Splenic naïve CD4 T cells from DNMAML or wt B6 mice were skewed toward iTreg cells for 48 hours. *Il17a* expression in iTreg cell culture was measured.
B. *Foxp3* expression in iTreg cell culture was measured by realtime PCR after 48 hours of skewing.
C. IL-17A secretion from iTreg cells was measured using the luminax system after 48 hours of skewing.

To further investigate whether Dll4 affects IL-17A production after Treg cell differentiation, the same number of differentiated iTreg were challenged under IL-6 + TGFβ Th17 skewing conditions for 3 more days after the standard 6 day iTreg cell skewing culture. In Th17 re-stimulation, Dll4-treated iTreg cells secreted significantly less IL-17A with associated decreased RORγt+ cells. Furthermore, Dll4-exposed iTreg cells retained a higher percentage and expression level of Foxp3 **(Figure 3.20).**

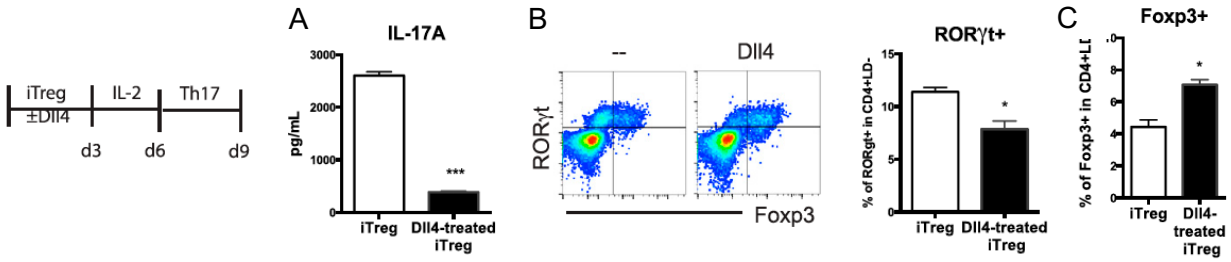

Figure 3.20 Dll4 exposure retains Foxp3 expression and impedes IL-17A production in Th17 re-stimulation *in vitro*

A. Naïve CD4 T cells from wt B6 mice were skewed toward iTreg with or without Dll4 stimulation for 72 hours, then rested in 10 ng/mL of IL-2 for another 72 hours. At day 6,

5 X 10^5 of viable cells were re-stimulated in Th17 conditions. After 3 days, IL-17A in the supernatant was accessed.

B. Percentage of RORγt$^+$ in viable CD4 T cells after Th17 skewing.
C. Percentage of Foxp3$^+$ in viable iTreg or Dll4-exposed iTreg after Th17 skewing.

These data suggest that Dll4-mediated signals during iTreg cell differentiation led to less inflammatory Th17 skewing while maintaining iTreg cell commitment.

To clarify if Dll4-educated Foxp3$^+$ iTreg cells possessed less plasticity to become RORγt$^+$ cells, 10^5 viable Foxp3-eGFP$^+$ iTreg cells were sorted after 6 days of iTreg skewing and cultured in Th17 conditions. Approximately 40% of eGFP$^+$ iTreg cells cultured without Dll4 acquired RORγt$^+$ expression, whereas Dll4-skewed eGFP$^+$ iTreg cells expressed significantly less and RORγt$^+$Foxp3$^+$ cells (**Figure 3.21**). Dll4-treated iTreg cells still retained more percent of Foxp3$^+$RORγt$^-$ during Th17 skewing **(Figure 3.21).**

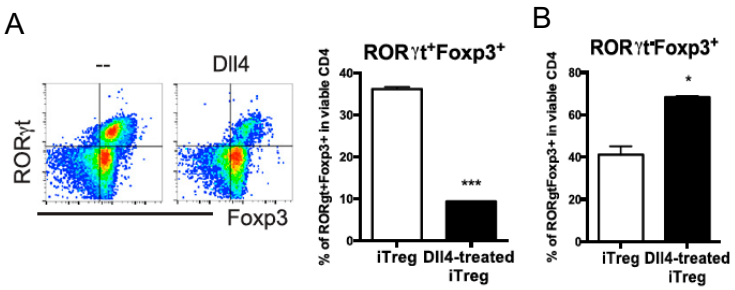

Figure 3.21 Dll4 exposure solidifies iTreg phenotype to be less plastic toward Th17 *in vitro*

Naïve CD4 T cells from wild type B6 mice were skewed toward iTreg cells with or without Dll4 stimulation for 72 hours, then rested in 10 ng/mL of IL-2 for another 72 hours. 5 X 10^5 of viable Foxp3-eGFP$^+$ cells were sorted out and re-stimulated in Th17 skewing conditions at day 6. After 3 days

A. The percentage of RORγt$^+$Foxp3$^+$ was determined.
B. The percentage of RORγt$^-$Foxp3$^+$ was determined.

These data suggest that Dll4-educated iTreg cells are less able to skew toward an inflammatory Th17 phenotype.

3.4 Discussion

The objective of this study was to determine if the Notch ligand Dll4 influenced Foxp3$^+$ Treg cell development, homeostasis, and function during pulmonary infection. Notch signaling has been suggested to be instrumental in Foxp3+ Treg cell formation and maintenance [70,216]. Notch ligands—Dll1, Jagged1 and Jagged2—have been shown to regulate Treg cell expansion and to elicit suppressive activity [93,96,217]. The present study suggests that Dll4 mechanistically regulates the stability of iTreg cells. Previous studies showed that primary RSV infection enhanced Foxp3$^+$ Treg cells in the airway [39,40]. Our data indicate that Dll4 sustained Foxp3 expression especially in central Treg cells, and altered homeostatic features and functional markers of Treg cells. *In vivo* Dll4 inhibition allowed the acquisition of effector cytokine production in Treg cells, increased their effector phenotype (CD44^{hi}CD62L^{lo}), and decreased functional Treg cell markers (GzmB) during infection. *In vitro* skewing of iTreg cells co-stimulated with Dll4 from naïve T cells had enhanced regulatory function, retained their central Treg cell phenotype, and were more stable with less susceptibility to become RORγt$^+$ Th17 cells. Importantly, stable and functional Treg cells prevent autoimmunity and enhance immunity against chronic infection [218]. Thus, identifying Dll4 as one stabilizing factor in autologous Treg cells could potentially further optimize clinical efficacy of treatment protocols [219,220].

Dll4/Notch signaling appears to have differential functions in various disease models. Using systemic blockade, Dll4 inhibition lessened GvHD, Type 1 diabetes, and experimental autoimmune encephalomyelitis [89,98,100,221,222]. In contrast, Dll4 blockade leads to exacerbated allergic airway disease and pulmonary RSV infection responses, as well as to increased BCG-induced granuloma formation [82,83]. These different results could be reconciled with a revised model

that Notch signaling fine-tunes T cell responses to different environmental cues [76], and thereby plays a distinct role in different diseases, such as antigen driven/infectious vs. autoimmune or allogeneic responses. Recently, a study demonstrated that intrinsic Notch signaling limited peripheral Treg cell maintenance during steady state and in GvHD [70]. In contrast to their finding, our results suggests that Dll4 and canonical Notch signaling sustained iTreg cell differentiation and stability to prevent immunopathogenesis of pulmonary infection. Recent evidence supports that iTreg cells are important for mucosal homeostasis, suppression of immune responses to environmental and food antigens, and to impede mucosal inflammation. In contrast, nTreg cells prevent autoimmunity and alter the threshold of immune activation [154,223]. Notch signaling and Dll4 restrain nTreg cell development *in vivo* [98], and GvHD was mainly prevented by nTreg [224,225] but not iTreg due to lineage instability of the latter [226]. To answer the question if Dll4 differentially affect nTreg versus iTreg cells, we used Neuropilin-1 (Nrp1) to distinguish nTreg versus iTreg cells *in vivo* as described [113–115,227]. Our preliminary findings showed that Dll4 inhibition decreased $Nrp1^-$ Treg cells during RSV infection but increased $Nrp1^+$ Treg cells in spleen (data not shown). Therefore, we speculate that Dll4/Notch may have a differential role on nTreg versus iTreg cells, thereby limiting Treg cells in GvHD but enhancing them in RSV infection. Additional research needs to be done to elucidate this intriguing hypothesis.

Pathogenic RSV infection also exhibits a type 2-biased immune response [228]. Our group has shown that Dll4 prevent Th2 cytokine secretion in CD4 T cells during RSV infection. Since both Notch signaling and Treg cells have been reported to be involved in the Th2 program, it raised the question: Does Dll4 regulates Th2 cytokine production directly or indirectly through Treg cells. Our data presented a dysfunctional Treg and Th17-like effector phenotype but not Th2-like after Dll4 inhibition. Since IL-17A aggravated Th2 responses in RSV infection and other pulmonary

inflammation, these results suggest that Dll4 mostly exacerbated Th2 cytokine production indirectly. Beside Th2 cells, recent studies demonstrated that RSV infection activated ILC2 cells with a concurrent IL-13 increase [8]. The present study indicated that Dll4 inhibition drove the number of ILC2 cells and corresponded with elevated IL-5 and IL-13 levels. Dll1/Notch has been shown to support ILC2 progenitor cell development *in vitro* [216,229], but the *in vivo* role of Dll4 in ILC2 biology during infection has not been described. Our novel finding further highlights the importance of Dll4 in ILC2 homeostasis *in vivo*, but it is not clear whether the regulation is direct or indirect. Since iTreg cells inhibit ILC2 cells and attenuate pulmonary inflammation [230], future studies will be necessary to specify the indirect contribution of iTreg cells in restraining ILC2 cells during pulmonary infection.

The homeostatic features of $Foxp3^+$ Treg cells were characterized with CD62L, CD44, and CCR7. $CD62L^{hi}CD44^{lo}CCR7^+$ cTreg cells are quiescent, long-lived, and dependent on IL-2, whereas $CD44^{hi}CD62L^{lo}Foxp3^+$ eTreg cells appear to be shorter lived [116,215]. These two subpopulations favored distinct compartments, as cTreg cells homing to SLO to be suppressive for autoimmunity [231]. Lymph node sensitization is critical to mount a proper immune response since insufficient lymph node formation led to impaired Foxp3 Treg cell function, promoted IL-17A-mediated pulmonary pathology, and initiated lymphoid cell clusters in the lung [31,232]. In the present study, the data showed that Dll4 sustained the cTreg cell population in SLO while preventing Th17 effector phenotype during RSV infection, representing a novel role for Dll4 in cTreg cell maintenance.

In addition to the alteration of the Treg cell cytokine phenotype, the present study further suggests that Dll4 sustained Treg cell function by influencing GzmB *in vivo* and CD25 *in vitro*. Intriguingly, GzmB in Foxp3+ Treg cells controlled RSV-induced T cell infiltration in airways [42],

and GzmB has been postulated to be a better functional marker of iTreg cells during viral infection [233]. Further investigation on the function of Treg subsets during RSV infection needs to be undertaken. Here, our findings with GzmB may provide a mechanistic explanation for how Dll4 inhibition exacerbates RSV-induced CD4 and CD8 T cells infiltration[82].

Taken together, our study demonstrates that Dll4/Notch promotes iTreg cell development, homeostasis, stability/plasticity, and functions *in vitro* and *in vivo* during RSV infection. Dll4 prevented RSV pathogenesis and supported iTreg cell development *in vitro*. The effects of Dll4 on Treg cells are an example of how Notch signaling can promote T cell homeostasis and disease regulation. By extending our understanding of Dll4 in Treg cell stability and function, our results may provide a road for future translational research leading to a better therapeutic strategy.

Chapter 4 SMYD3: a Methyltransferase that Supports Dll4-enhanced Treg Cell Differentiation

4.1 Abstract

Notch ligand Dll4 has been shown to regulate CD4 T cell differentiation, including Treg cells. Epigenetic alterations, which include histone modifications, are critical in cell differentiation decisions. Recent genome-wide studies demonstrated that Treg cells have increased tri-methylation on histone H3 at lysine 4 (H3K4me3) around the Treg master transcription factor, *Foxp3* loci. Here we report that Dll4 dynamically increased H3K4 methylation around the Foxp3 locus that was dependent upon up-regulated SET and MYDN domain containing protein 3 (SMYD3). Dll4 promoted *Smyd3* through the canonical Notch pathway—RBP-Jκ in iTreg cells during *in vitro* differetiation. Smyd3 were enriched in TGF-β dependent Th (iTreg and Th9) *in vitro*, and more abundant in lung than lymphoid tissue (thymus and spleen). Deletion of Smyd3 in CD4 cells perturbed IL-17A cytokine production and exacerbated RSV immunopathology *in vivo*. Using genome-wide unbiased mRNA sequencing, a novel set of Dll4- and *Smyd3*-dependent differentially expressed genes was discovered (e.g. Lag3). Together, our data demonstrate a novel mechanism of Dll4/Notch-induced Smyd3 pathway activation that regulates and stabilizes immunomodulatory environment in viral infections.

4.2 Introduction

Many infectious and chronic inflammatory diseases are characterized by inappropriate or dysregulated CD4+ T cell immunity. CD4+ T cell immunity underlies successful immune responses with diverse cytokine expression profiles and distinct effector functions. Naïve CD4 T cells differentiate into subsets of CD4 T helper cell (Th) upon T cell receptor activation, cell associated co-stimulatory proteins, and cytokine stimulation. The different Th subsets, type 1 Th (Th1), type 2 Th (Th2), IL-17–producing Th (Th17), IL-9-producing Th (Th9) cells, produce a unique set of cytokines (IFN-γ for Th1; IL-4, IL-5, and IL-13 for Th2; IL-17A for Th17, IL-9 for Th9). Treg cells, especially iTreg cells, constrain airway allergic inflammation [154,234,235] and immunopathology upon RSV infection[39,41,42]. Foxp3 is the master transcription factor of Treg cells that is induced by TCR activation in the presence of TGF-β [150,236]. Both transcription factors and post-translational modifications can fine-tune the activity of Foxp3 promoter or conserved non-coding DNA sequence (CNS) 1, 2, 3 to control the expression of Foxp3 and the function, composition, and stability of Treg populations [140,236].

Post-translational modifications that alter gene expression without changing the bases of DNA sequence, are called "epigenetic modifications". Epigenetic alterations, including histone modifications, DNA methylation, chromatin remodeling, and microRNAs, are indispensable for optimized Th differentiation [176,177]. One of the permissive epigenetic marks—histone 3 lysine 4 tri-methylation (H3K4me3) is enriched around the activated gene promoters while the suppressive marks—H3K27me3 are removed compared to uncommitted naïve CD4 T cells [185]. In Treg cells, H3K4me3 are mostly enriched around Foxp3 CNS1 and its promoter but not as significantly around CNS2 and CNS3 [140]. Another mechanism, DNA methylation on CpG motif was reported to contribute to Foxp3 instability [160,162], while Tet methylcytosine dioxygenase 1(TETs) facilitated

CpG motif de-methylation and enhanced Foxp3+ Treg cell stability [183]. Histone modification by Ezh2 demonstrated that removal of H3K27me3 around Foxp3-bound genes stabilizes Treg cell identity [186] and enhances its suppressive function in response to inflammation[187]. Our lab previously identified that SMYD3, which is a H3K4 di- and tri-methyltransferase [189], was induced by TGF-β and supported iTreg cell differentiation to lessen immunopathogenesis in pulmonary viral infections [192]. In a separate study we have also identified that Dll4/Notch leads to stabilization of the iTreg phenotype *in vivo* and *in vitro*[120]. The present studies further extend those earlier findings by identifying the Notch-mediated epigenetic mechanism in regulating Treg cell function.

Notch signaling is well-conserved throughout metazoans and orchestrates T cell differentiation decisions[237–239]. In CD4 T cells, Notch signaling influenced CD4 T helper cell differentiation, including Th1, Th2, Th17, and Th9 cells, by directly initiating Th signature transcription. Compelling evidence showed that Notch activation directly drives Th programs in part through downstream transcription complex binding. In Th1, Notch1 directly interacts with *Ifng* CNS22 to cooperate with T-bet [76]; in Th2 cells, Notch1 and its downstream DNA-binding transcription factor—RBP-Jκ—directly interact with *Il4* and *Gata3* promoters during Th2 differentiation[81]; RBP-Jκ interacts with *Il17a* and *Rorc* promoter [87], and with the *Il9* promoter during Th9 cell differentiation [62]. Together, Notch orchestrates multiple Th differentiation pathways [76]. The mechanism of Notch in Treg cell differentiation is more complex. Notch directly induces Treg master transcription factor, Foxp3, through RBP-Jκ in iTreg differentiation [63], while constitutively active Notch1 in developed Foxp3+ Treg destabilized peripheral Treg in part through CpG motif methylation on Foxp3 CNS2 [70]. These studies are the first to demonstrate that Notch and its ligand regulates iTreg differentiation through an epigenetic mechanism.

Here we report that Notch signaling through its ligand Dll4 directly regulated *Smyd3* expression during iTreg differentiation leading to H3K4me3 around the *Foxp3* locus to stabilize *Foxp3* expression. Dll4 inhibition and/or Smyd3 deletion introduced cytokine dysregulation including increased IL-17A and decreased IL-10 to confer immunopathology upon viral infection. Using genome wide RNA sequencing, we further identified Treg cell signature genes —including *Lag3* and *Tgm2*—that are regulated by Dll4 and Smyd3. These latter studies also strongly suggest that these same signals have an overall effect on the immune environment by altering both Foxp3+ Treg and Foxp3- T cells. Together, our study reveals a novel pathway—Dll4→Smyd3—that can control Treg differentiation and function and affect the overall immune environment.

4.3 Results

4.3.1 Notch ligand Dll4 promotes gene activation and histone modification around the *Foxp3* gene during iTreg cell differentiation *in vitro*

Dll4/Notch activation through the canonical Notch signaling pathway enhances Treg differentiation by stimulating *Foxp3* gene expression [63,120]. H3K4me3 is a permissive histone mark that represents gene activation and is enriched around the Foxp3 locus in Foxp3+ Treg cells [180,240]. Here we hypothesized that Dll4 may enrich H3K4me3 around the *Foxp3* gene to enhance iTreg differentiation. Given that iTreg differentiation accompanies *Foxp3* expression while Th0 activation lacks *Foxp3* expression, we examined the role of Dll4 on H3K4me3 marks around the *Foxp3* promoter and functional enhancers, CNS1, CNS2, and CNS3, in iTreg compared to Th0 cells. Using chromatin immunoprecipitation (ChIP), the data showed that Dll4 stimulation drove the enhancement of H3K4me3 around *Foxp3* promoter as well as in CNS1, CNS2 and CNS3 at 72 hours specifically in iTreg but not in Th0 cells (**Figure 4.1A**). To characterize the relative enrichment of H3K4 mono-methylation (H3K4me) and H3K4me3 in the *Foxp3* promoter and enhancers during early iTreg differentiation, we immunoprecipitated both H3K4me and H3K4me3 at 48 hours of iTreg differentiation. Dll4 decreased H3K4me while it increased H3K4me3 around the *Foxp3* promoter as well as in CNS1, 2, and 3 regions (**Figure 4.1B**). *Foxp3* induction in the presence of TGF-β-Smad3 is dependent on CNS1 [150,154,236], allowing us to focus on the dynamics of H3K4me3 on *Foxp3* CNS1. Dll4 stimulation first decreased but then inversely increased H3K4me3 at 48 and 72 hours post differentiation at the CNS1 enhancer (**Figure 4.1C**). These data suggested that Notch ligand Dll4 activation changed the H3K4me3 around *Foxp3* promoter and its functional CNS1 enhancer during iTreg differentiation.

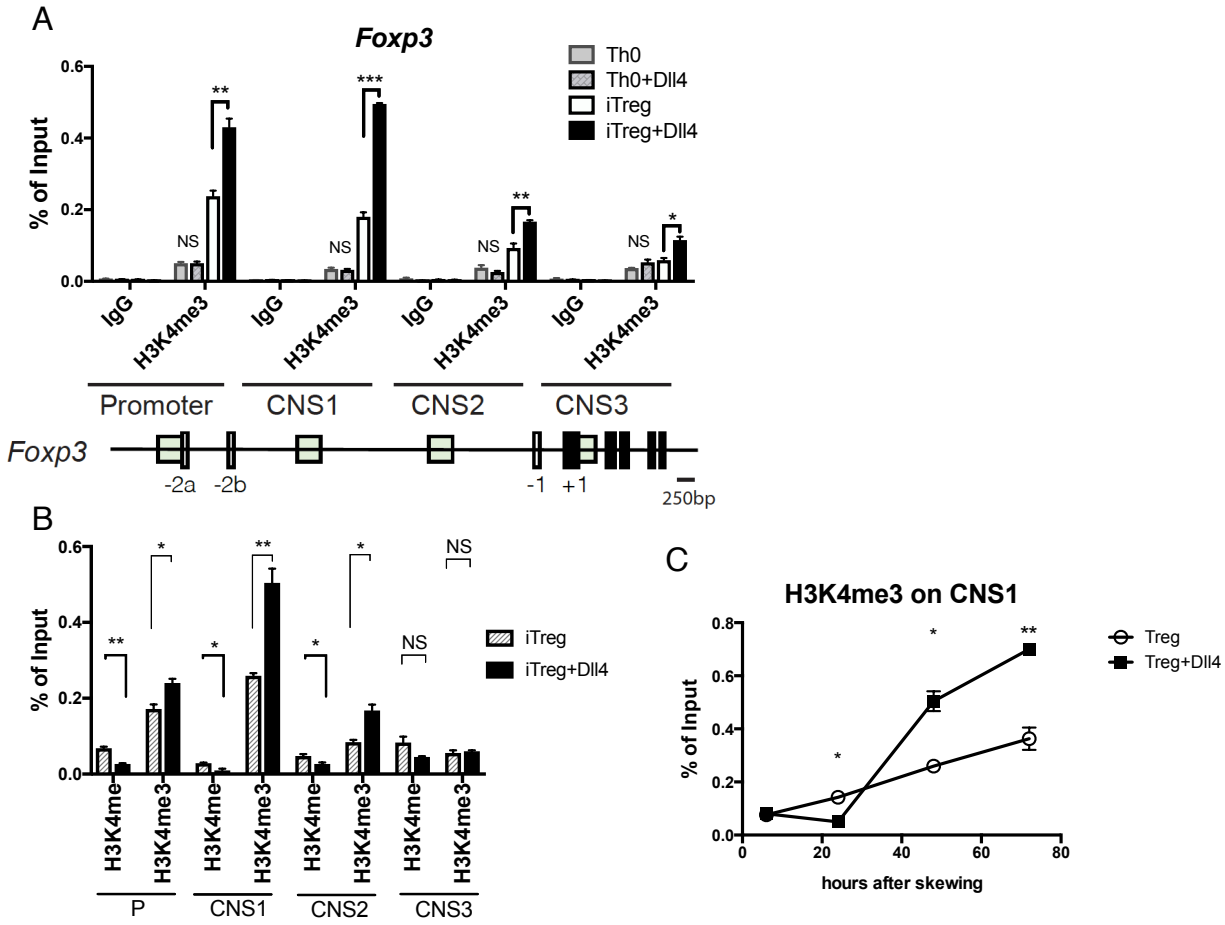

Figure 4.1 Dll4 enriches H3K4me3 around Foxp3 promoters and consensus-non-coding sequences (CNS)1, 2, 3

A. 2X10^6 of naïve CD4 T cells were skewed toward Th0 or iTreg cell differentiation with or without Dll4 stimulation *in vitro*. ChIP was performed to detect H3K4me3 around the *Foxp3* promoter and CNS 1, CNS2 and CNS3 after 72 hours.

B. Changes of H3K4me and H3K4me3 by Dll4 stimulation during iTreg cell differentiation was detected at 48 hours of skewing.

C. H3K4me3 kinetics at *Foxp3* CNS1 after 6 hours, 24 hours, 48 hours and 72 hours post iTreg cell differentiation were measured with or without Dll4 stimulation *in vitro*.

Data represent mean ± SEM. Data were from one experiment representative of two to three experiments. * P<0.05; ** P<0.005; *** P<0.0005; NS: no significance (unpaired two-tailed t-test)

4.3.2 Dll4 promoted SMYD3 during iTreg cell differentiation

The addition of methyl groups on H3K4 is mediated by histone lysine methyltransferases [241]. Therefore, we hypothesized that Dll4 would regulate an epigenetic enzyme to catalyze H3K4me3 around the *Foxp3* locus during iTreg cell differentiation. To investigate if Dll4 up-regulated any epigenetic enzymes in iTreg cells, especially histone methyltransferases, we performed an epigenetic enzyme PCR array to compare the Dll4-stimulated gene profile in iTreg differentiation at 48 hours. The array analysis indicated that *Smyd3* was the most up-regulated candidate in the iTreg+Dll4 activation (**Figure 4.2A**). It was also the most highly up-regulated methyltransferase when examining all methyltransferases in the array across multiple experiments (**Figure 4.2B**). *Smyd3* expression was significantly increased by Dll4 stimulation in iTreg cells but not in Th0 or in unstimulated iTregs as determined by RT-PCR (**Figure 4.2C**). Consistently, Dll4 stimulation also increased SMYD3 protein expression at 48 hours (**Figure 4.2D**). These data suggested that Dll4 facilitates Smyd3 expression in iTreg cell differentiation *in vitro*.

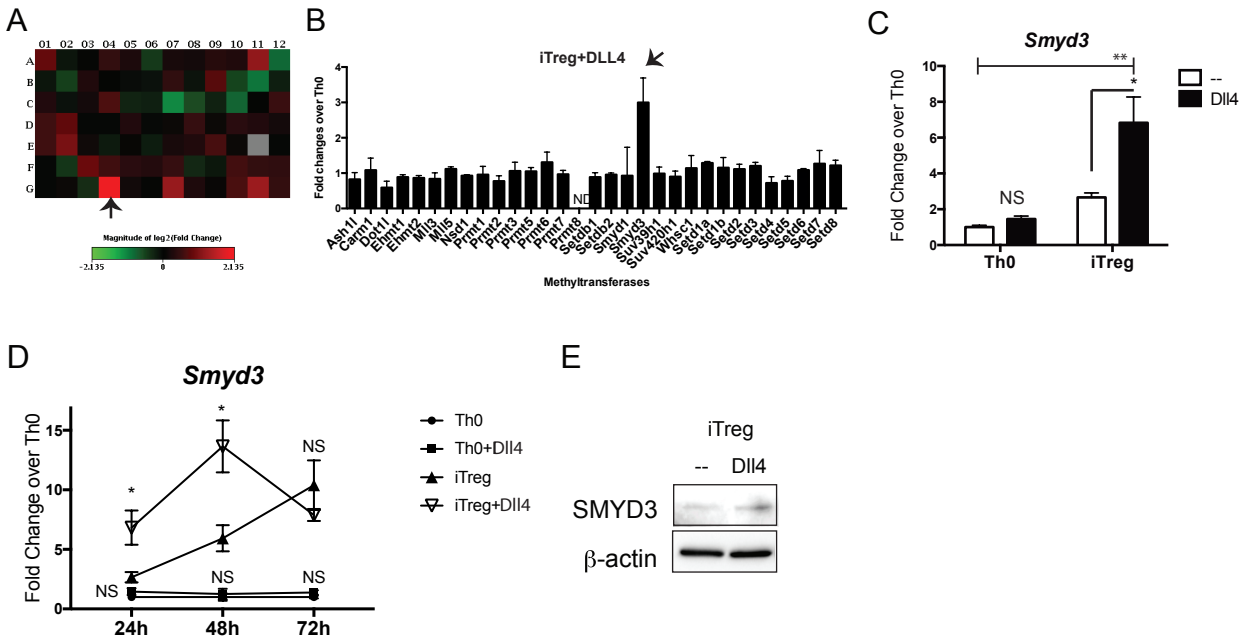

Figure 4.2 Dll4 up-regulates SMYD3 methyltransferase in iTreg cell differentiation

A. The expression of 87 epigenetic enzymes in epigenetic PCR array (SA Bioscience, PAMM-085) were measured in DLL4-stimulated iTreg cells compared to Th0 cells after 48 hours of skewing. Fold changes were indicated with a heatmap. The following genes were either up or down-regulated more than two-fold: *Dnmt1* (A11), *Hdac9* (C7), *Nek6* (E2), *Smyd3* (G4), *Ube2a* (G7), *Usp21* (G11)
B. All the methyltransferases in the PCR array are shown. The arrow indicated *Smyd3* as the most-expressed methyltransferase *in vitro*
C. *Smyd3* expression levels were measured after 24 hours of Th0 and iTreg cell differentiation with or without Dll4 activation *in vitro*.
D. *Smyd3* expression time course shows the relative expression of Smyd3 normalized to Gapdh and then compared to Th0 cell control at every time point.
E. SMYD3 expression was blotted after 48 hours of iTreg cell differentiation with or without Dll4 stimulation.

Data represent mean ± SEM. Data were from one experiment representative of two to three experiments. PCR array is one-time experiment. * $P<0.05$; ** $P<0.005$; *** $P<0.0005$; NS: no significance (unpaired two-tailed *t*-test)

4.3.3 Intracellular Notch signaling promoted SMYD3 in a RBP-Jκ dependent manner during iTreg differentiation

To further investigate if Dll4-upregulated *Smyd3* expression is Notch-dependent, we used CD4-specific *Rbpj* knockout mice and CD4-specific dominant-negative MAML1 mice (DNMAML) that deleted canonical Notch transcription factor and inactivated intracellular Notch signaling activation, respectively. The expression of *Smyd3* was significantly decreased in $Rbpj^{-/-}$ CD4 T and DNMAML CD4 T cells in Dll4-stimulated iTreg differentiation (**Figure 4.3A~B**), suggesting that *Smyd3* expression is dependent on intracellular Notch signaling activation. To investigate if *Smyd3* is a potential target gene of canonical Notch signaling, we examined the *Smyd3* promoter and found 5'-TGGGAA-3' RBP-Jκ consensus binding sites [87,242] upstream of Smyd3 transcription start site (TSS) using *in silico* analysis (**Figure 4.3C**). We performed a promoter walk, and representative primer sets 0 (P0) and P2 showed that RBP-Jκ directly bound to the *Smyd3* promoter, with Dll4 stimulation further enriching RBP-Jκ binding at 6 hours of early iTreg differentiation

(**Figure 4.3C**). Together, these data demonstrated that Dll4 and intracellular Notch signaling facilitated *Smyd3* expression in iTreg differentiation.

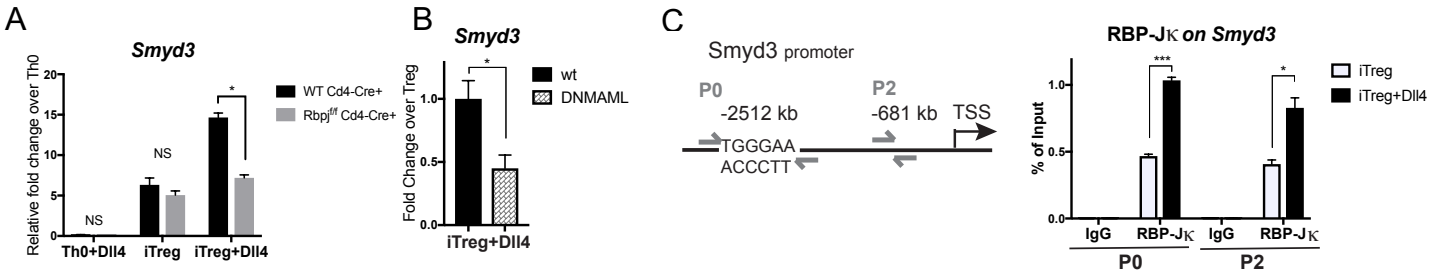

Figure 4.3 Dll4 promotes Smyd3 expression through canonical Notch and RBP-Jκ in iTreg differentiation

A. Naïve CD4 T cells were isolated from CD4-specific Rbpj knockout mice or wt un-floxed littermate controls. Activated (Th0) or iTreg differentiation with or without Dll4 were performed. After 48 hours, CD4 T cells were harvested and *Smyd3* were measured.
B. Naïve CD4 T cells were isolated from wt B6 or CD4-specific DNMAML mice. *Smyd3* were measured after 48 hours of iTreg differentiation+Dll4 stimulation *in vitro*.
C. $2X10^6$ of naïve CD4 T cells were isolated from wild type B6 mice. After iTreg differentiation with or without Dll4 stimulation for 6 hours, RBP-Jκ were precipitated and RBP-Jκ-bound DNA sequence were PCR with Smyd3 primer P0 and P2.

Data represent mean ± SEM. Data were from one experiment representative of two to three experiments. PCR array is a one-time experiment. * $P<0.05$; ** $P<0.005$; *** $P<0.0005$; NS: no significance (unpaired two-tailed *t*-test)

4.3.4 SMYD3 was enriched in TGF-β mediated T helper cells differentiation

SMYD3 is enriched in TGF-β-induced iTreg cells [190]. To further investigate the relative expression level of SMYD3 in differentiated T helper cells subsets (Th), we skewed naïve T cells to Th1, Th2, Th17, Th9, iTreg and IL-27 Treg1. Here we found that both iTreg and Th9 (TGF-β+IL-4) had enriched SMYD3 protein levels, but not much was expressed in naïve CD4, Th0, Th1, Th2, Th17, and IL-27 cells *in vitro* (Fig 3A).

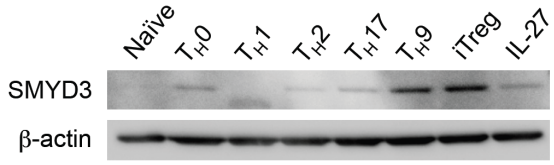

Figure 4.4 SMYD3 is enriched in iTreg and Th9 only slightly in activated CD4 T cells (Th0) and Th1, Th2, Th17, and IL-27 type 1 regulatory T cells (Treg1)

4.3.5 Dll4-facilitated Foxp3 expression was SMYD3-dependent

Since Dll4 upregulates *Foxp3* expression during iTreg differentiation and further, that Dll4/Notch upregulated *Smyd3*, we hypothesized that Dll4 and *Smyd3* cooperatively upregulated *Foxp3*. We first confirmed that Cre+ cKO expressed minimal amount of SMYD3 compared to Cre- controls in iTreg cell differentiation at 72 hours (**Figure 4.5A**). Here the data showed that Dll4 facilitated *Foxp3* expression in Cre- control, whereas deletion of *Smyd3* decreased *Foxp3* expression in the presence of Dll4 at 48 hours during iTreg cell differentiation (**Figure 4.5B**). Consistent with wt B6 mice, Dll4 stimulation up-regulated H3K4me3 around the Foxp3 promoter as well as in CNS1, 2, and 3 in Cre- control, but Dll4 did not increase H3K4me3 in Cre+ *Smyd3* knockout CD4 T cells (**Figure 4.5C**). These data suggested that *Smyd3* mediated Dll4-enriched H3K4me3 around Foxp3 regulatory elements—promoter, CNS1 and CNS2. Thus, Dll4 appears to support Foxp3 expression through induction of SMYD3 leading to histone modification and expression of *Foxp3*.

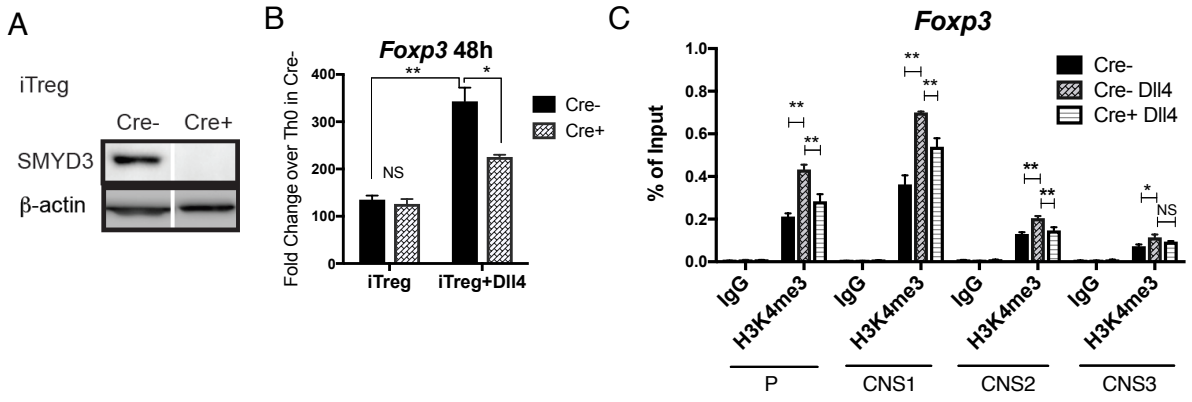

Figure 4.5 Dll4-enhanced H3K4me3 enrichments are SMYD3 dependent

A. 10^6 naïve CD4 T cells from Cre- control or Cre+ CD4-specific SMYD3 conditional knockout (cKO) were differentiated to iTreg cells. After 72 hours, SMYD3 levels were quantified by Western blotting.
B. Smyd3 mRNA levels were measured in iTreg cells and Dll4-stimulated iTreg cells post 48 hours.
C. 2*10^6 of naïve CD4 T cells from Cre- control with or without Dll4 stimulation or Cre+ CD4-specific SMYD3 were differentiated to iTreg cells. After 72 hours, H3K4me3 was immune precipitated, and *Foxp3* promoter and CNS1, 2, 3 were qPCR quantified compared to input control

Next, we determined if *Smyd3* was also involved in Dll4-facilitated iTreg cell differentiation and maintenance by flow cytometric analysis of the differentiated cell populations. Dll4-increased Foxp3+ iTreg cells were compromised in Smyd3 cKO mice at 3 days post iTreg differentiation (**Figure 4.6**) and continued to be impaired after 6 days both with and without Dll4 with no increase in Treg cell development in the presence of Dll4 without SMYD3 (**Figure 4.7**).

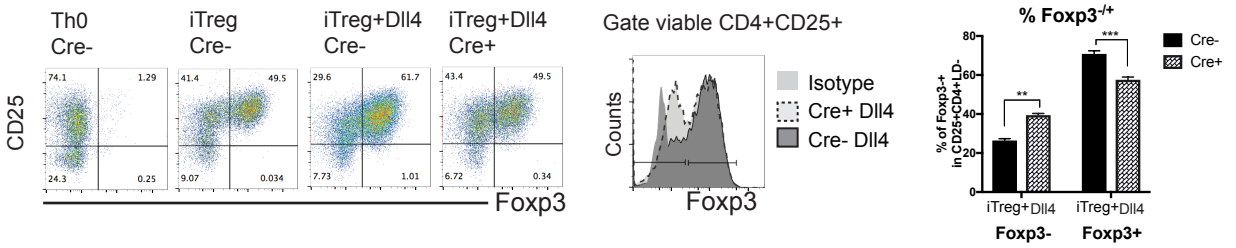

Figure 4.6 SMYD3 modulates and supports Foxp3$^+$ iTreg primary differentiation *in vitro*

10^6 of naïve CD4 T cells from Cre- control or Cre+ SMYD3 cKO were activated (Th0) or differentiated to iTreg with or without Dll4. After 72 hours of skewing, Foxp3 and CD25 were labeled and quantified by flow cytometry

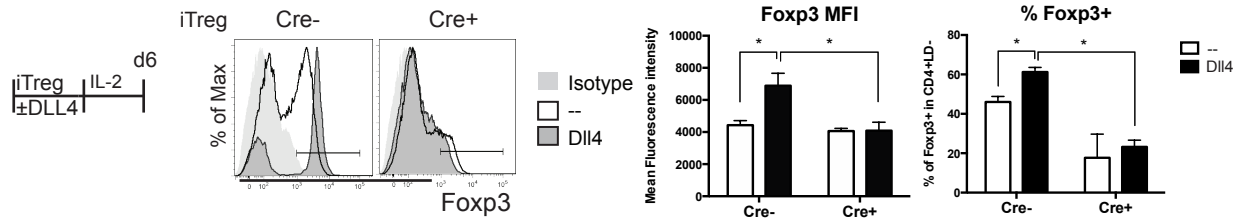

Figure 4.7 SMYD3 maintains Dll4-enhanced Foxp3$^+$ iTreg cells after incubation with IL-2 *in vitro*

10^6 of naïve CD4 T cells from Cre- control or Cre+ SMYD3 cKO were activated (Th0) or differentiated to iTreg cells with or without Dll4. After 72 hours of skewing, both Th0 and iTreg were rested in IL-2 (10 ng/mL) for another 72 hours. Foxp3 and CD25 were detected and quantified by flow cytometry.

Data represent mean ± SEM. Data were from one experiment representative of two to three experiments. * P<0.05; ** P<0.005; *** P<0.0005; NS: no significance (unpaired two-tailed t-test).

To further explore if the methyltransferase function of SMYD3 is responsible for iTreg cell differentiation and maintenance, we collaborated with Epizyme to test their SMYD3 inhibitor—EPZ030456. This small molecule inhibitor is specific to SMYD3 and has an IC^{50}=40nM. After testing that 50 nM and 200 nM didn't affect T cell viability, we performed H3K4me3 ChIP around the Foxp3 locus. Both 50 nM and 200 nM EPZ030456 decreased H3K4me3 on the Foxp3 promoter, CNS1, and CNS2 (**Figure 4.8A** and data not shown), similar to Smyd3 knockout mice shown in Figure 4.5. Surprisingly, both 50 nM and 200 nM of EPZ030456 Smyd3 inhibitor did not affect

iTreg cell differentiation at 3 days (data not shown). Since previous reports indicatethat epigenetic changes regulate long-term and later cell differentiation decisions, we turned to a longer regimen where we inspected the differentiation based on cell proliferation status. When we performed 6 days iTreg maintenance regimen with Smyd3 inhibitor at day 0 and day 3, the inhibitor increased Foxp3- undifferentiated cells in slowly-proliferative generations (labeled as CTV generation 1 to 5) (**Figure 4.8B**), especially in Dll4-exposed iTreg (**Figure 4.8C**). These data indicate that Smyd3 methyltransferase activity indeed catalyzed H3K4me3 around the Foxp3 gene but only slightly modulated iTreg differentiation.

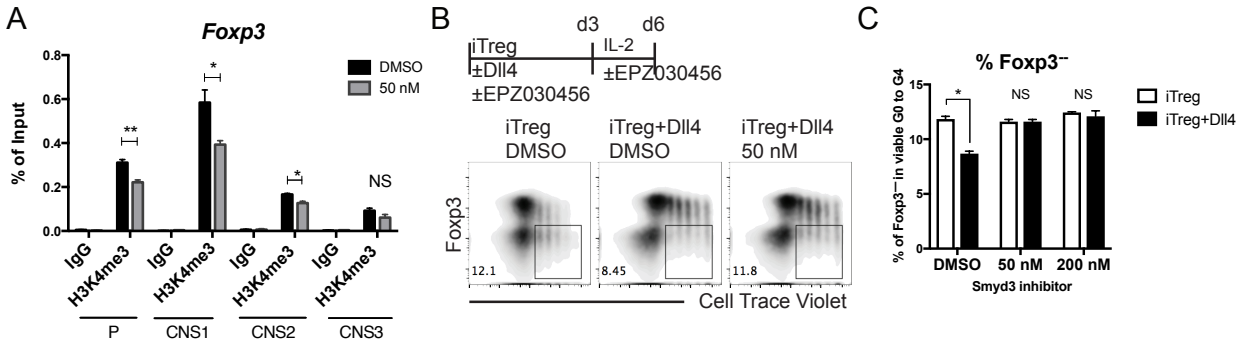

Figure 4.8 SMYD3 inhibitor EPZ030456 decreases H3K4me3 around Foxp3 locus, increases Foxp3- undifferentiated and slowly proliferative CD4 T cells *in vitro*

A. 2*10^6 naïve CD4 T cells were differentiated toward iTreg phenotype for 72 hours in the presense of DMSO alone or with SMYD3 inhibitor—EPZ030456. H3K4me3 (abcam) or control IgG were immunoprecipitated with ChIP and the Foxp3 loci were amplified.
B. 2*10^5 naïve CD4 T cells were incorporated with Cell Trace Violet (CTV) and were differentiated toward the iTreg phenotype with or without Dll4 and/or SMYD3 inhibitor for 72 hours. The iTreg cell culture were maintained in IL-2 (10 ng/mL) and fresh SMYD3 inhibitor as above. After another 72 hours, Foxp3- undifferentiated G1-G4 slowly proliferative populations were gated
C. Foxp3- undifferentiated CD4 gated in B. were quantified.

After knowing that SMYD3 itself supports iTreg differentiation, we next determined whether SMYD3 in CD4 support Treg function, both in peripheral nTreg and iTreg cells. *In vivo* pTreg

were enriched by sorting viable CD4+CD25+ Treg cells from inguinal lymph nodes (**Figure 4.9A**), and CD45.2 peripheral nTreg were co-cultured with CD45.1 naïve CD4 T cells labeled with CTV. After 72 hours of stimulation with anti-CD3/anti-CD28 beads, we measured Treg suppression by gating proliferation of naïve T cells. The data showed that Smyd3 knockout nTreg cells have similar functions to control cells, suggesting that Smyd3 did not control nTreg cell function (**Figure 4.9B**). Instead, Smyd3 KO iTreg cells were less functional at 1:1 Treg: naïve T culture (**Figure 4.9C**). There was a greater percent of CTV-diluted CD45.1 responder cells when co-cultured with Cre+ Smyd3 KO iTreg cells(**Figure 4.9 D**). These data suggest that Smyd3 moderately contributes to iTreg cell function *in vitro*.

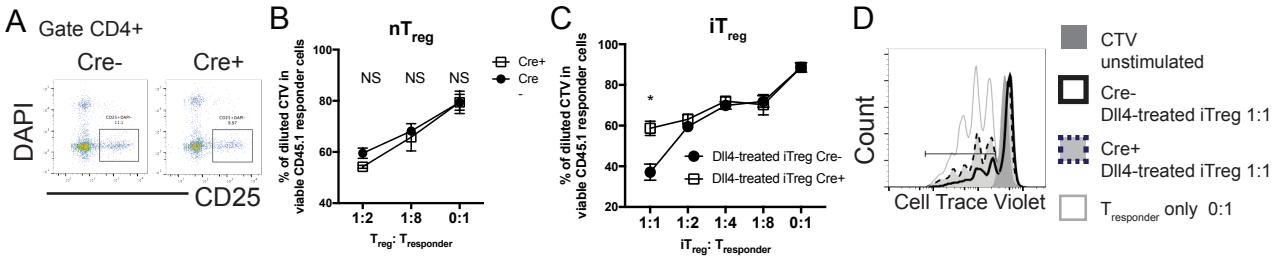

Figure 4.9 SMYD3-depleted iTreg are less suppressive in an *in vitro* suppression assay

A. DAPI-CD4+CD25+ viable nTreg and iTreg cells were flow sorted.
B. 2.5*10^4 CD45.1+ naïve CD4 T cells were labeled with CTV and co-cultured with serial-diluted nTreg cells. 2.5*10^4 of anti-CD3/anti-CD28 mouse T cell activator beads were added to cell culture. After 72 hours, CTV dilution in viable CD45.1 responders were gated to represent Treg cell suppression ability.
C. iTreg cells were cultured as described in Figure 4.7. 2.5*10^4 CD45.1+ naïve CD4 T cells were labeled with CTV and co-cultured with serial-diluted iTreg cells. 2.5*10^4 of anti-CD3/anti-CD28 mouse T cellactivator beads were added in co-culture. After 72 hours, CTV dilution in viable CD45.1 responders were gated to represent Treg suppression ability
D. CTV in CD45.1 T cell responders are shown. The groups were: T cell responder only without mouse T cell activator (CTV unstimulated), T cell responder only with mouse T cell activator (T responder only 0:1), T cell responder+ Dll4-treated Cre- iTreg + mouse T cell activator (Cre-), T cell responder+ Dll4-treated Cre+ iTreg+ mouse T cell activator (Cre+).

Data represent mean ± SEM. Data were from one experiment representative of two experiments with 3 to 5 mice per time point, with samples from each mouse processed and

analyzed separately. * $P<0.05$; ** $P<0.005$; *** $P<0.0005$; NS: no significance (unpaired two-tailed *t*-test)

As Figure 3.1 shows, RSV infection in lung enriches Dll4 on DC. To examine if RSV infection in the lung is a good model to study Smyd3 function, we first measured Smyd3 expression in lung versus other lymphoid tissues. Lungs have much higher baseline expression of Smyd3 than thymus and spleen (**Figure 4.10A**). And RSV infection further induced Smyd3 expression in the lungs at both 4 dpi and 6 dpi (**Figure 4.10B**). These results imply that RSV infection in lungs could induce not only Dll4 but Smyd3 and thus, is an optimal model to study their regulation in pTreg *in vivo*.

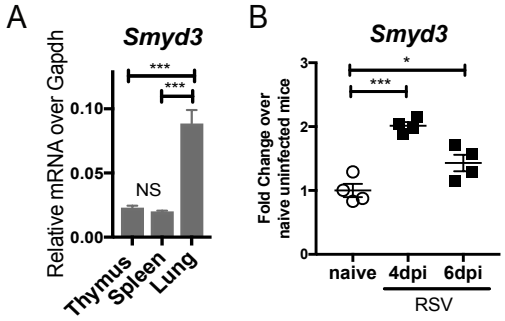

Figure 4.10 Smyd3 is enriched in lung non-lymphoid tissue and is further up-regulated by RSV infection

A. Smyd3 expression in primary lymphoid organ--thymus, secondary lymphoid organ--spleen, and non-lymphoid tissue--lung from uninfected wt B6 mice were measured. N=4
B. Smyd3 expression in lungs of uninfected naïve mice and i.t. RSV infected mice at 4 dpi and 6 dpi was measured. N=4

4.3.6 Smyd3 lessened RSV lung immunopathology and regulated Treg cells and cytokine production in CD4 T cells

Next we investigated Smyd3 function in pTreg cells, CD4 cytokines and RSV pathology. Using Smyd3 cKO, more mucin-positive staining and globlet cell hyperplasia in lung was observed, indicating the more severe immunopathology in cKO at 8dpi (**Figure 4.11A**), while the viral

clearance was maintained in Cre+ knockout post RSV infection (data not shown). Smyd3 cKO had decreased CD25+Foxp3+ Treg cells (**Figure 4.11B**) as described [190]. Treg cell functional markers including CTLA-4, OX40 and ICOS were not changed between Cre- control and Cre+ Smyd3 cKO mice at both 6 dpi and 8 dpi (data not shown). Granzyme B in both Foxp3+ Treg cells and CD8 T cells was not altered at 8 dpi (data not shown). However, deletion of Smyd3 led to increased IL-17A in mLN after RSV restimulation (**Figure 4.11C**). Type 1 cytokine IFNγ was unchanged, but type 2 cytokine IL-5 was increased in Smyd3 cKO (**Figure 4.11D~E**). Both $Foxp3^{+}$ Treg and $Foxp3^{-}$IL-10-producing type 1 Treg have been shown to be suppressive in RSV infection [39,50,51]. Here we further found that *Smyd3* cKO mice secreted less anti-inflammatory cytokine IL-10 in re-stimulated mLN at 8 dpi (**Figure 4.11F**). These data suggested that *Smyd3* in T cells supported regulatory cells phenotype and key cytokines to alleviate RSV immunopathology.

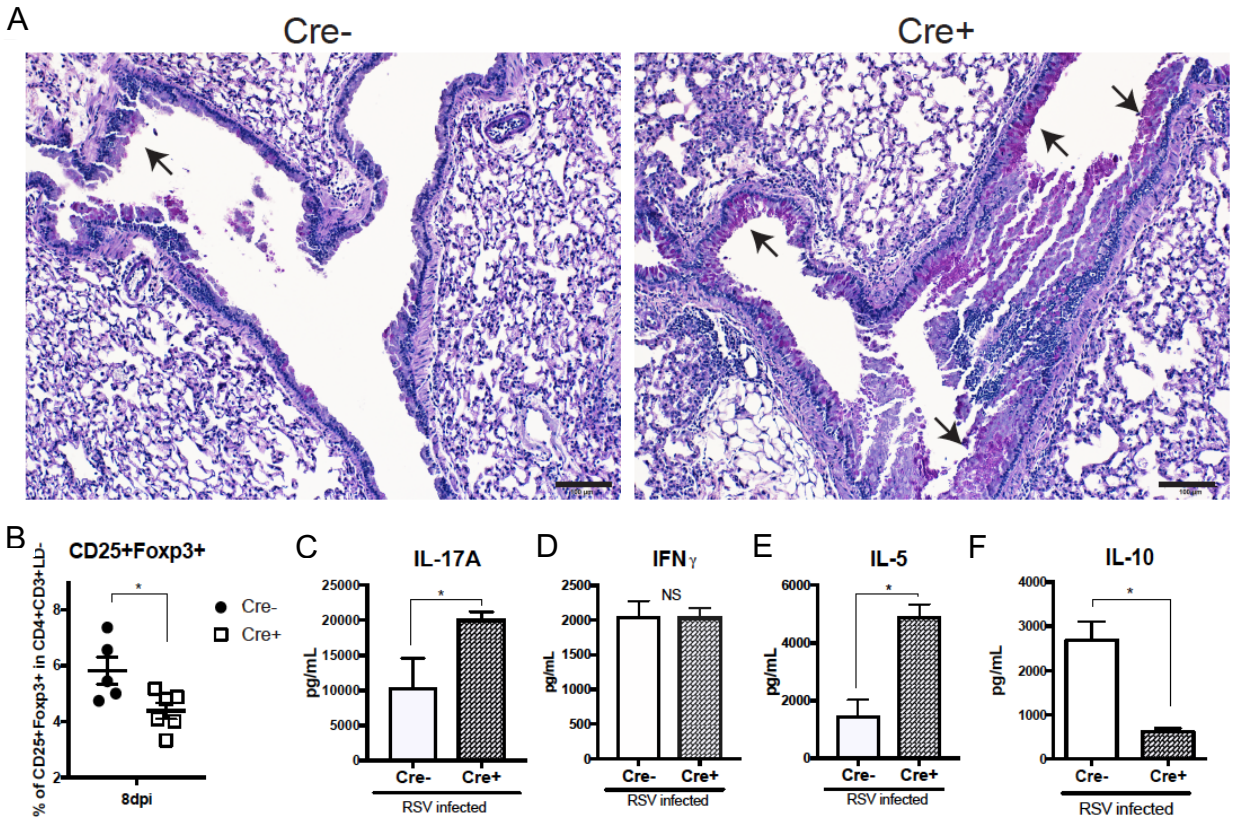

Figure 4.11 Smyd3 in T cells impedes RSV immunopathology

A. CD4-specific *Smyd3* knockout (Cre+ *Smyd3* cKO) and Cre- littermate control were i.t infected with RSV. PAS staining of formalin-fixed lung section from 8 dpi. Bar, 100 μm. ↑ indicates the detection of mucin. N=5~6.
B. Percent of viable CD25+Foxp3+ Treg cells in lungs were gated and quantified at 8dpi.
C- F. mLN cells were harvested at 8dpi and re-stimulated with RSV for 48 hours. The following cytokines were measured in the supernatants: C.) IL-17A; D.) IFN-γ; E.) IL5; F.)IL10.
Data represent mean ± SEM. Data were from one experiment representative of two experiments with 4 to 6 mice per group, with samples from each mouse processed and analyzed separately. * $P<0.05$; ** $P<0.005$; *** $P<0.0005$; ND: not-detectable; NS: no significance (unpaired two-tailed *t*-test)

4.3.7 Notch and Smyd3 promote *Il10* and inhibit *Il17a in vitro* during iTreg cell differentiation

To better understand if Dll4 and intracellular Notch regulated IL-10 and IL-17A in iTreg cells, naïve CD4 T cells from wild type B6 mice were skewed towards iTreg cells. Dll4 stimulation enhanced *Il10* expression and inhibited *Il17a* at 24 hours post iTreg differentiation, but the observations were reversed using a pan-Notch inhibitor of gamma-secretase (gsi) (**Figure 4.11A~B**). More specifically, naïve CD4 T cells from Notch-inactivated DNMAML and canonical Notch deleted *Rbpj* cKO mice secreted less IL-10 in the presence of Dll4 (**Figure 4.11C**) and more IL-17A in iTreg+Dll4 conditions (**Figure 4.11D**). To further understand if Dll4 regulated *Il10* and *Il17a* expression in a Smyd3 dependent manner, naïve CD4 T cells from Cre+ *Smyd3* cKO and Cre- littermate controls were activated toward iTreg phenotype. Dll4-upregulated *Il10* expression was partially Smyd3-dependent during primary iTreg diffentiation (**Figure 4.11E**), and Smyd3 inhibited Il17a expression in primary iTreg cell differentiation (**Figure 4.11F**). Finally, we determined whether the presence of *Smyd3* regulated IL-17A secretion using a Th17 plasticity assay. After resting, Dll4-activated iTreg cultures were re-stimulated under Th17 skewing conditions. Dll4-exposed Smyd3 cKO secreted more IL-17A than Cre- controls (**Figure 4.11G**).

These data indicate that Dll4 and Smyd3 cooperatively promoted *Il10* and inhibited *Il17a*. In contrast, since Smyd3 deleted T cells have significant increases in IL-17 and Dll4 reduces the level of IL-17 in both WT and Smyd3 KO, the two signals may also have differential effects on IL-17 regulation.

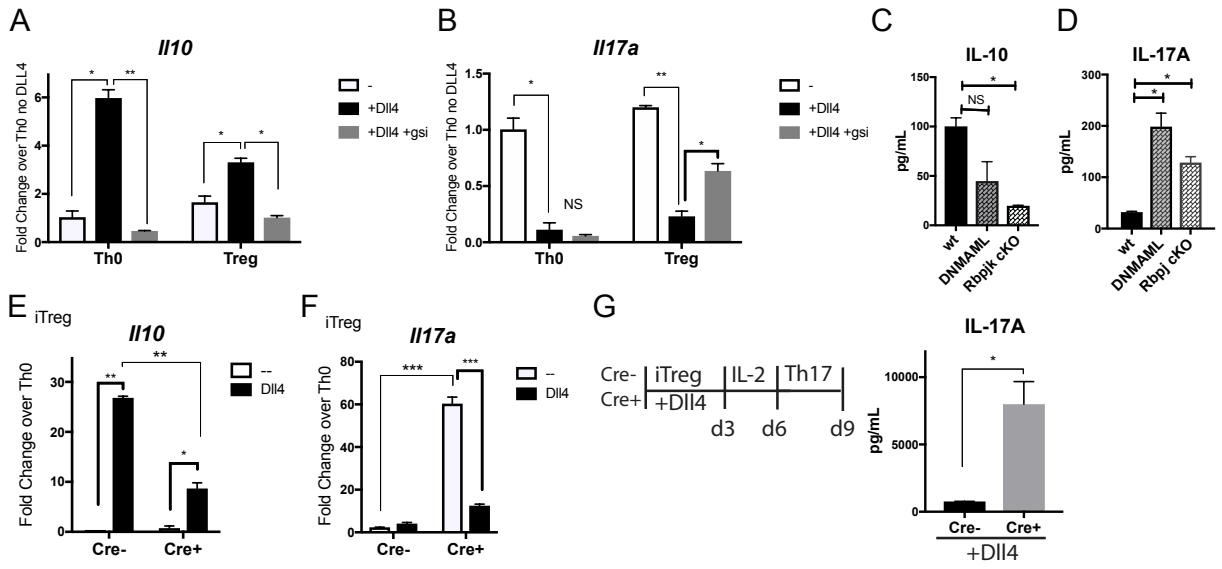

Figure 4.12 Intracellular Notch and Smyd3 in CD4 T cells support IL-10 production and inhibit IL-17A production in iTreg cells *in vitro*

A. Naïve CD4 T cells were isolated and incubated with DMSO or 1 μM of gamma-secretase inhibitor (gsi) and proceed to Th0 or iTreg differentiation with or without Dll4 for 24 hours. *Il10* mRNA was measured;
B. Naïve CD4 T cells were isolated and incubated with DMSO or 1 μM of gamma-secretase inhibitor (gsi) and proceed to Th0 or iTreg differentiation with or without Dll4 for 24 hours. *Il17a* mRNA was measured.
C. Naïve CD4 T cells from DNMAML mice and Rbpj cKO mice were activated with Dll4 for 48 hours. IL-10 production in supernatant was measured.
D. Naïve CD4 T cells from DNMAML mice and Rbpj cKO were differentiated to iTreg cells with Dll4 for 48 hours. IL-17A production in supernatant was measured.
E. Naïve CD4 T cells from Cre- control or Smyd3 cKO were differentiated to iTreg cells with or without Dll4 for 48 hours. *Il10* expression was measured;
F. Naïve CD4 T cells from Cre- control or Smyd3 cKO were differentiated to iTreg cells with or without Dll4 for 48 hours. *Il17a* mRNA was measured.
G. Naïve CD4 T cells from Cre- control or Cre+ Smyd3 cKO micewere differentiated to iTreg cells with Dll4 stimulation for 72 hours then rested in IL-2 (10 ng/mL) for another 72 hours. 5*10^5 of viable rested iTreg cells were re-stimulated under Th17 skewing condition for 72 hours. IL-17A in Th17 re-stimulation culture was measured.

Data represent mean ± SEM. Data were from one experiment representative of two to three experiments. * $P<0.05$; ** $P<0.005$; *** $P<0.0005$; NS: no significance (unpaired two-tailed *t*-test)

4.3.8 Dll4 and Smyd3 regulated gene expression profile in iTreg differentiation

In the above studies we identified that Dll4 increased Treg cell differentiation as well as promoted maintenance of the Treg phenotype that was enhanced by a Smyd3 mechanism. Interestingly, Figure 4.12 showed that Notch inactivation and Smyd3 deletion produced changes in *Il10* and *Il17a* expression (24 to 48 hours) before Smyd3 protein induction (48 to 72 hours) and Foxp3 protein dysregulation (72 to 144 hours). Thus, while some of the Treg characteristics were enhanced by Dll4/Notch through a *Smyd3*-dependent mechanism, others were not. Therefore, we hypothesized that Dll4 and *Smyd3* could regulate additional genes independent of Foxp3 during iTreg cell differentiation. To discover novel genes that are regulated by Dll4 and/or *Smyd3* dependent pathways, we performed whole genome RNA sequencing in early iTreg cell differentiation (48 hours after skewing). To distinguish the results between four groups, principle component analysis (PCA) was performed in DESeq2. Dll4 stimulation introduced substantial variance (76%) in gene expression profile, and *Smyd3* deletion changed the global gene expression on its own but was especially dramatic in the presence of Dll4 (**Figure 4.13A**). These results demonstrated the interdependence of Dll4 and *Smyd3*. Next, we investigated what genes were differentially expressed by Dll4 stimulation. Some of the significantly up-regulated (dots in red) or down-regulated (dots in blue) differentially expressed genes (DEGs) were labeled in black text (**Figure 4.13B**). *Smyd3* was significantly up-regulated by Dll4 along with several reported Treg cell functional genes including *Ctla4, Gzmb, Ox40* (**Figure 4.13B**). Furthermore, Notch-related genes (*Dtx1, Notch3, Jag2*) and anti-inflammatory cytokine *Il10* were also up-regulated by Dll4 (*Dtx1*: 2.43 fold; *Notch3*: 1.98 fold; *Jag2*: 2.77 fold; *Il10*: 1.42 fold) (**Figure 4.13B**). Data also

identified DEGs that were significantly up-regulated (adjusted p value<0.05 and absolute fold change more than two folds) between wildtype iTreg+Dll4 and control iTreg. These differences were examined by comparing overlapping Treg cell signature genes [175] and Foxp3-dependent genes [174]. A venn diagram illustrates the number of genes that were Dll4-stimulated DEGs, Treg signature genes, Foxp3-dependent genes, and the number of genes that were in two or even all three groups. Results indicate that only 5.3 % of Dll4-stimulated DEGs were also Treg cell signature genes, and 3.3 % of these DEGs were Foxp3-dependent (**Figure 4.13C**). These results indicated that the majority of the Dll4-stimulated DEGs were neither Treg-signatures nor Foxp3-dependent, and that Dll4 stimulation introduced novel DEGs that may have a previously undefined role for Treg cells. To get a more informed understanding of the molecular function of Dll4 DEGs, we performed gene ontology analysis of the 781 Dll4 DEGs and plotted a treemap. The most significant Gene Ontology (GO) term was cytokine activity with the p-value: $1.8*10^{-8}$. The p-value of each GO term and their area in treemap were in inverse proportion (**Figure 4.13D**). Together, these data revealed that Dll4 not only regulated reported Treg signatures and Foxp3-dependent genes but also broadly impacted cytokine responses during differentiation. To further identify specific DEGs that were both regulated by Dll4 stimulation and *Smyd3*, we normalized the counts and did unsupervised cluster with the Pearson distribution of a heatmap showing the Z-score of DEGs. There were 95 DEGs that were significantly [BH adjust p-value (padj)<0.05] regulated with a greater than 2 fold change (log2FC > 1) in Dll4 stimulation, and down-regulated more than 1.5 fold (log2FC < -0.6) in *Smyd3* knockout mice (**Figure 4.13E**). Heatmap analysis then clustered with row Means identified the top 20 DEGs. Using this analysis, 2 Treg signature genes, *Tgm2* and *Lag3,* were highly up-regulated by Dll4 stimulation and down-regulated in *Smyd3* knockout (**Figure 4.13E**). Interestingly, Notch target gene Deltex1 (*Dtx1*) was also decreased in Smyd3

depletion. These data uncovered a new set of DEGs that were Dll4 and *Smyd3* dependent. These results will help us further define functional gene differences in future studies.

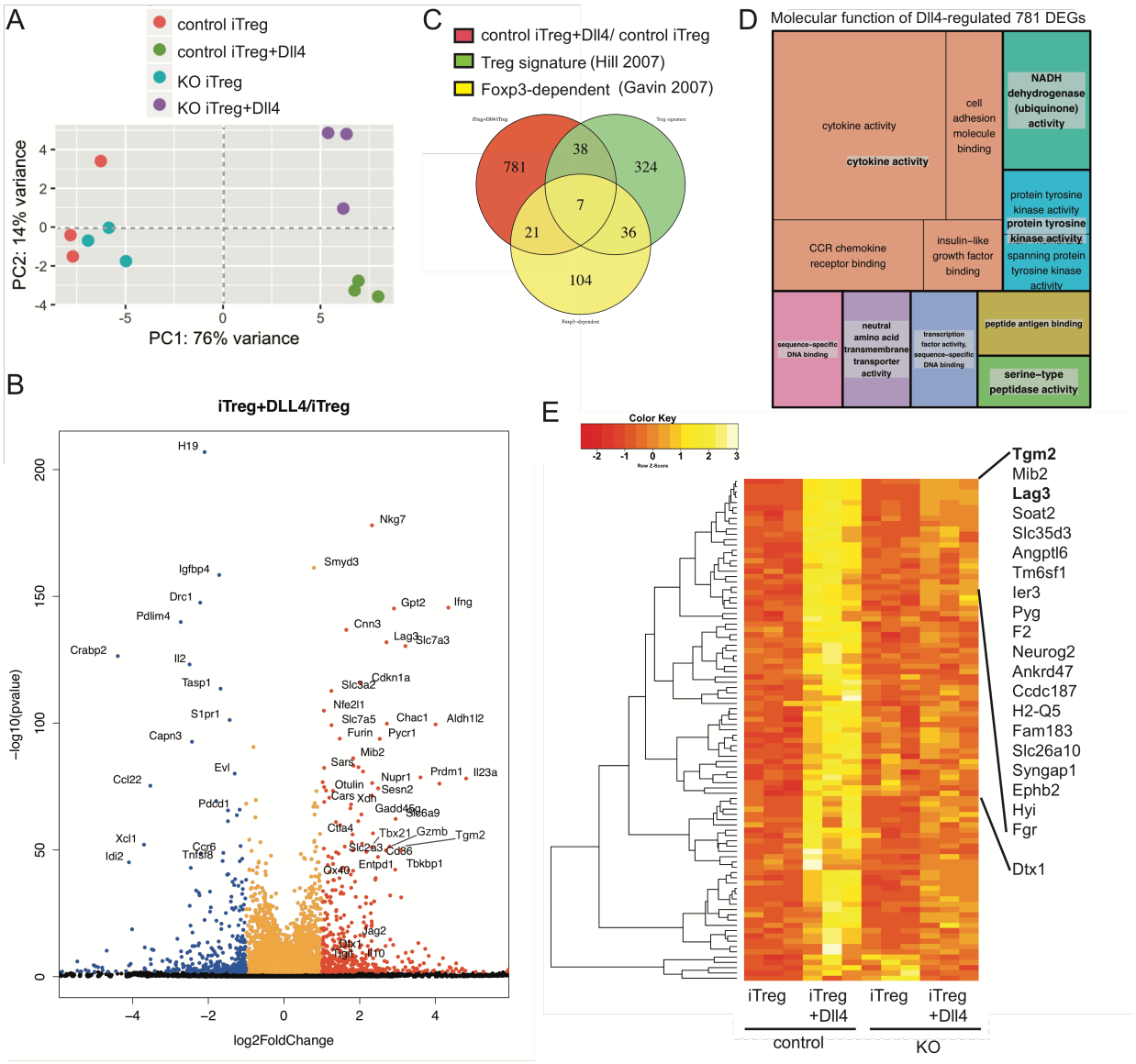

Figure 4.13 Smyd3 deletion changes gene expression profile in iTreg cells in the presence of Dll4 stimulation

A. Principle-component analysis of RNA-seq data sets of iTreg cells from Cre- control or Cre+ Smyd3 cKO, with or without Dll4 stimulation, was assessed using the top 500 genes with the highest variance. Each symbol represented a single mouse. Each group have three biological triplicates.

B. Volcano plot showed the differentially expressed genes (DEGs) in control iTreg+Dll4 over control iTreg cells; red dots indicated genes that were significantly (BH-adjusted p-value < 0.05) up-regulated by Dll4 more than 2 fold (log2FoldChange>1), and blue dots

represent genes that were significantly down-regulated by Dll4 more than 2 fold. y-axis represents the significance of the differential analysis by showing -log10(BH-adjusted p-value).

C. Venn diagram demonstrated the overlap between current Dll4-regulated DEGs and published dataset of Treg signatures and Foxp3-dependent genes.
D. Gene Ontology (GO) of un-overlapped Dll4-regulated DEGs (781 genes). Treemap showed the significant GO term with False-discovery-rate (FDR)-adjusted global P value < 0.05. P value is inversely proportional to area for each GO term.
E. Normalized expression of all the DEGs that were significantly up-regulated by Dll4 stimulation more than 2.00 fold, and down-regulated more than 1.51 fold by Smyd3 deletion. Heatmap presents Z-score in a dendrogram cluster by Pearson distribution and ranked based on row Means. Top 20 DEGs and Deltex1 are indicated.

4.4 Discussion

Previous studies showed that infection and inflammation-experienced Treg cells were more stably maintained, and they acquired changes in chromatin modifications correlated with gene expression profiles [243]. Chromatin modifications contribute to long-term responses of Treg cell differentiation, subset specification, and cytokine-producing potential, such as histone 3 lysine 4 methylation and its methylase [188], But how infection and environmental cues epigenetically instruct Treg cell differentiation is relatively undefined. Our labs and others have previously identified that Notch ligand Dll4 was induced during pulmonary infection and inflammation to enhance Treg cell differentiation [120,244]. Here we report one specific methyltransferase, SMYD3 [189,245], that could be directly regulated by Dll4/Notch. The present study demonstrates several novel findings and concepts: 1) Epigenetic enzymes are a part of the mechanism by which RSV infection modifies CD4 T cells lineage specification, including Treg cell differentiation; 2) Dll4/Canonical Notch signaling directly facilitates SMYD3 expression *in vitro* and *in vivo* during RSV infection; 3) Dll4 stimulation directed gene activation epigenetic mark, H3K4me3, around Foxp3 functional promoters and enhancers that is SMYD3 dependent; 4) Dll4 confers cytokine expression changes in Treg cells, and SMYD3 regulates additional gene expression in the presence of Dll4. Together, our data unravel the broad impact of Dll4/Notch in Foxp3+ Treg cells and have identified a novel stabilization mechanism through methyltransferase SMYD3-mediated histone modification.

SMYD3 was reported to be regulated by estrogen receptor (ER), androgen receptor (AR) and TGF-β [190,196,200,246]. Here we reported another novel regulatory signal—Notch. It is noteworthy that Dll4 stimulation and intracellular Notch inactivation alone does not activate Smyd3 expression in Th0 cells, suggesting that iTreg cell environmental cues including TGF-β and/or IL-2 are required. One explanation is intracellular Notch inactivation inhibited TGF-β1 dependent Foxp3

expression since Smad3 and RBP-Jκ together bind to Foxp3 promoter [63]. Given that Smad3 binds to the Smyd3 promoter [190] and the present study also showed RBP-Jκ binding on the Smyd3 promoter, these data suggest that TGF-β signaling and canonical Notch pathways may cooperatively facilitate Smyd3 expression.

Treg suppression is tailored to fit in specific tissue and inflammatory settings using multiple suppressive mechanisms. For example, Foxp3/T-bet could suppress Th1 effector responses [247], Foxp3/IRF4 suppresses Th2[165], and Foxp3/STAT3 suppresses Th17 [167]. But little is known about the direct role of Foxp3 for Treg cell specification. The RNA-seq results showed that *Ifng* was up-regulated more than 16 fold by Dll4 in iTreg cells, suggesting that Dll4 stimulation provided a Th1-like profile in iTreg differentiation similar to previous observations in Th1 differentiation [69,248,249]. Although Dll4 neutralization did not significantly perturb IFN-γ secretion in mLN post RSV infection, here we found that it decreased *Ifng* in Foxp3-eGFP+ Treg while *Ifng* in eGFP- Tconv was increased. These *in vitro* and *in vivo* data suggest a novel paradigm that Dll4 may favor a Th1-like suppressive program in Treg cells. It would be intriguing to further investigate if Dll4 regulated effector T cell cytokine production through T-bet+Foxp3+ Th1-like Treg cells. This program may have a significant advantage in a viral infection, such as RSV, where IFN-mediated programs are required for viral clearance yet control more pathogenic Th2 and Th17 responses necessary to protect tissue function.

Besides Foxp3+ Treg cells, the RNA-seq results suggested that Dll4 stimulation promote a substantial amount of DEGs (819, 96.7% of total Dll4 DEGs) that are not Foxp3-dependent. The RNA-seq results further showed two other Dll4 and Smyd3 dependent gene candidates, namely *Tgm2* and *Lag3*. Tgm2 encodes the TG2 protein that covalently crosslinks latent TGF-β1-binding protein and controls TGF-β1 maturation and activity [250,251] and therefore increases TGF-β1 mRNA

levels [252]. In cancer cells, TGF-β-induced Tgm2 promotes epithelial to mesenchymal transition (EMT) [253,254]. These latter studies suggest that Dll4/Notch and Smyd3 may reinforce the positive feedback loop of TGF-β signaling to facilitate iTreg cell differentiation. Another Treg signature gene that was shown to be Dll4 and Smyd3 dependent was Lymphocyte activation gene 3 (Lag3). Lag3 is required for maximal regulatory function of CD25+Foxp3+ Treg cells [255] and is a biomarker for IL-10 producing Treg1 cells that enhance suppressor function to lessen mucosal inflammation and autoimmunity [256,257]. The present study also found that both Dll4 and SMYD3 supported IL-10 production *in vitro* and *in vivo* during RSV infection, together suggesting that Dll4 and SMYD3 may promote Treg1 functional markers to support an overall tolerogenic environment along with Foxp3+ Treg cells. Future studies need to be performed to dissect the mechanism of Dll4/Notch and Smyd3 in Tgm2 and Lag3 regulation. Since Lag3 is a checkpoint inhibitor now targeted in cancer immunotherapy trials, it will be exciting to investigate the efficacy of targeting Smyd3 in Notch-active cancers, including lymphomas and leukemias that have Notch activation signals.

Together, these studies offer new and exciting data that demonstrate the role of a central and conserved developmental pathway, Notch, which promotes Treg cell differentiation through a SMYD3 mediated epigenetic mechanisms that includes not only direct but indirect effects on *Foxp3* and other critical Treg cell associated genes (Figure 4.14).

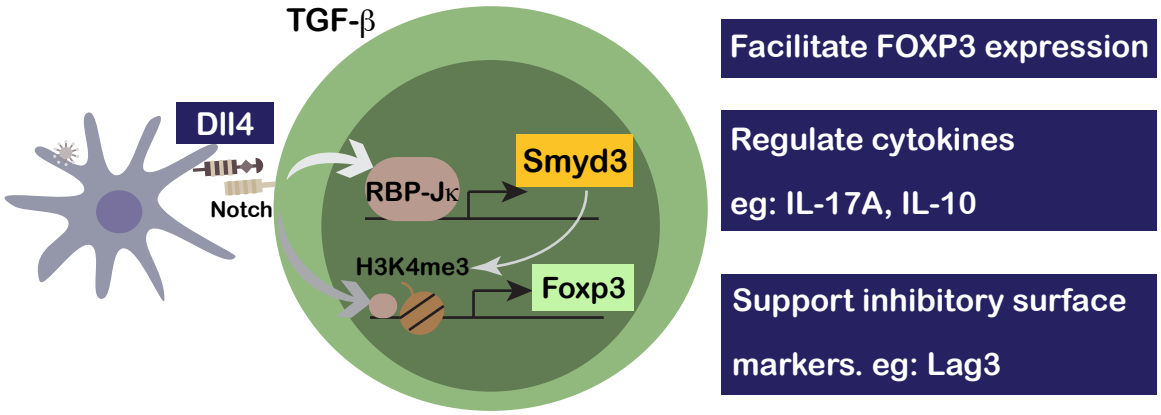

Figure 4.14: **Schematic summary of how Dll4 promoted Smyd3 expression to leverage regulatory features of CD4 T cells**[7]

[7] This figure was created by Hung-An (Anna) Ting

Chapter 5 Conclusions and Discussion

5.1 Significance of studying regulatory T cells in RSV pathogenesis

The high prevalence and pervasive nature of respiratory infections receives a disproportionate level of attention from the public. In fact, WHO reported that respiratory infections count for more than 6% of the total global burden of disease that count in mortality, morbidity and financial cost [258,259]. Among pulmonary infections, RSV is the most common and often serious infections in pediatric clinics because more than 90% of children have been infected before 2 years of age. The current effective therapy is supportive care, hydration, and there's no strong evidence supporting the use of any pharmacologic agents such as steroid had little effect. To date, there is no active prophylaxis such as vaccine to control this prevalent infection. Since the exacerbated inflammation is not only the clinical manifestation of RSV infection but also the life-threatening predisposition in 1960 RSV vaccine trial[260], understanding the regulation of RSV immunopathogenesis is in a critical unmet need.

RSV clinical manifestations of bronchiolitis aren't driven by viral replication and direct viral toxicity but exacerbated immune responses. Scientist tried to scrutinize the reason of vaccine trial failure that led to severe exacerbated disease in the 1960's RSV vaccine using mice[260]. These studies not only showed that a predominant Th2 response resulted, but also showed that the vaccine led to a complete absence of Treg cells in the airways, enhanced lung inflammation and augmented clinical severity upon RSV infection[260]. Moreover, increasing the number of Treg cells in the airways recruited by IL-27 which is a type 1 Treg-inducing cytokine reversed the enhanced lung

inflammation and weight loss[261]. Recent studies in mice using RSV clinical isolates also demonstrate the importance of both Foxp3+ Treg cells and IL-10-producing type 1 Treg cells in limiting pulmonary immunopathology (e.g. mucogenic cytokine secretion). These results highlight the significance of regulatory T cells in RSV pathogenesis, and inform the follow up question of by what mechanism. Knowing how regulatory T cells are regulated may introduce new insights for therapeutic development to control RSV immunopathogenesis.

Adaptive immunity that includes B cells and T cells is essential for viral clearance. However, RSV clearance has been shown to be predominantly dependent on T cells responses[262,263]. Unfortunately, RSV does not mount good T cells memory responses resulting in the possibility of secondary re-infection, even with the same strain[10]. Thus, one conundrum is how are T cell memory responses suppressed by RSV. Recent evidence strongly suggests that Foxp3+ Treg cells impede memory responses to viral infections[264,265]. . The studies in this thesis provides new insights of how Treg are promoted in primary RSV infection, regulated by Dll4-induced Smyd3. By knowing how Treg are regulated during RSV infection, we may be able to more precisely control CD4 regulation to mount appropriate and long-term immune memory against RSV re-infection and shed light on future vaccine development.

5.2 Notch regulation is context-dependent in Foxp3$^+$ Treg cell differentiation and function

Treg cell differentiation and suppressive function are regulated by Notch and its ligand Dll4 in RSV infection, although the results differ in various disease models with no unified mechanism concluded. In autoimmune hepatitis, intracellular inhibition of pan-Notch activation using a gamma-secretase inhibitor demonstrates the supportive role of Notch in Foxp3+ Treg cell development and function[63]. As we and others have shown Notch induced Foxp3+ Treg cells play

a seminal role in allergic airway disease and in a RSV pulmonary infection model [120,244]. In contrast, systemic blockade of Notch ligand Dll4 enriches Foxp3+ Treg numbers and function in autoimmune encephalitis and autoimmune diabetes[89,98]. We think this inconsistency may arise from two underlying conditions of Notch signaling and Treg cell biology: 1. The context-dependent nature of Notch signaling; and 2. The heterogeneity of Foxp3+ Treg cells.

The evidence for context dependent regulation of Treg cells by Notch is supported by 4 different lines of evidence. **First**, the expression and the role of the Notch ligands may vary in different immune responses. In our RSV infection model, only the Dll4 ligand is up-regulated and its expression peaking at 6 dpi and this occurred mainly on CD11b+ pulmonary DC. Notch ligand Dll1 was expressed but not gradually up-regulated by RSV infection, while Jag1 and Jag2 weren't up-regulated and undetectable by flow (**Figure 3.1** and data not shown). In contrast, all four Notch ligands are expressed on DC in a GvHD model[221]. Moreover, Dll1/4 are also expressed on fibroblastic stromal cells in GvHD[266], while Dll1 and Jag1 are reported to be present on microglia[267,268] that initiate neuroinflammation in EAE. Given that Delta and Jagged elicit distinct immune responses[69,269], these different combinations of Notch ligand expression patterns present in different cell types in different disease scenarios introduce layers of complexity that subverts any one-for-all theory of Notch activation *in vivo*. **Second**, increasing evidence demonstrates that Notch receptor and ligand can be modified by post-translational modifications to fine-tune signaling status. For example, Lunatic Fringe (Lfng) which is a glycosyltransferase that adds N-acetyl glucosamine to *O*-fucose on the extracellular domain of Notch receptors could inhibit Jagged-mediated Notch activation but promoting Dll-mediated Notch activation[270,271]. In T cell development, Notch1, 2 and 3 are all expressed in the thymus but Notch1 is preferentially used to interact with Delta like ligands (e.g. Dll4) after Lfng activitiy[272]. In an RSV infection, exacerbated

allergic airway model, *Lfng* promotes Dll4-Notch binding and Notch activation for Th2 responses[85]. **Third,** intracellular Notch signaling was maintained in an inactive state. For instance, a novel zinc finger protein--LRF--could prevent lineage fate decisions of hematopoietic stem cells to T cells either through inhibiting intracellular Notch activation[273] or repressing Notch ligand Dll4[274]. **Last but not least**, unknown mediators in a certain inflammatory environment can compensate for the absence of Notch in T cells. For example, DNMAML mice are resistant to *Leishmania major* (type 1 parasite infection) but susceptible to *Trichuris muris* (type 2 parasite infection)[58]. Together these studies serve as evidence to demonstrate the entanglement of Notch signaling in the context of other important aspects (e.g. other signals, cell types, disease) with both spatial and temporal layers of regulation.

Treg in peripheral lymphoid organ and non-lymphoid tissue (pTreg) consist of not only nature-occuring Foxp3+ Treg (nTreg) but induced Treg (iTreg) that were Foxp3- before disease on-set. The iTreg constitute 10~30% of the total pTreg that is tissue dependent *in vivo*[275–277]. Using $Foxp3^{Cre}$ to delete Notch1 or by overexpressing NICD in differentiated Foxp3+ Treg cells, a recent study argues that Notch impedes Foxp3+ Treg cell maintenance and function in GvHD[70]. These should not be mis-interpreted since GvHD is mainly prevented by nTreg cells [224,225], not iTreg cells due to lineage instability[226]. Using Neuropilin-1 (Nrp1) to distinguish nTreg versus iTreg cells *in vivo* as described [113–115,227], our finding showed that Dll4 inhibition decreased $Nrp1^{-}$ Treg cells during RSV infection (**Appendix Figure A.1**). Therefore, we speculate that Dll4/Notch may have a differential role in nTreg versus iTreg. Additional research needs to be done to test this hypothesis.

5.3 Distinct methods of Dll4 inhibition share similar outcomes in Foxp3 regulation

We used two different methods to study the role of Dll4 in regulatory T cells and RSV immunopathology. One is systemic neutralization of Dll4 with anti-Dll4 antibody, and another is knocking down Dll4 on i.t transferred DC with the following RSV infection. Based on the data that RSV infection enriches Dll4 expression on DC but not on other cells types (e.g. alveolar macrophages) (**Figure 3.1-3.3** and data not shown), we hypothesize that the Dll4 neutralization targets DC-presented Dll4 to tamp down Notch signaling activation in CD4 T cells (**Figure 3.5C**). However, we can't ignore the possibility that other cell types could also present Dll4 that are involved in exacerbated RSV immunopathology. In GvHD, our collaborator Maillard lab and others found that systemic blockade of Dll ligand decreased GvHD mortality. Surprisingly, deletion of Dll1 and Dll4 in the hematopoietic system had minimal effects on T cell pro-inflammatory cytokines. In contrast, Dll1 and Dll4 deletion in stromal cells impaired donor T cell production of IFNγ and IL-2 and also impaired protection from GvHD[278]. With Dll4 neutralization, we found decreased development of central Treg cells by Foxp3 MFI and reduced function of effector Treg cells by GzmB. To further examine our hypothesis that the Dll4 on DC regulates Treg, we sensitized mice into the airway with RSV-infected Dll4-deleted DC versus control DC and examined the immune response of re-infection with RSV. Dll4 on DC supported Foxp3 expression in total Treg populations, both central and effector Treg cells (**Figure 3.13**). Moreover, the absence of Dll4 on DC exacerbated the RSV immunopathology with increased mucus production, goblet cells hypertrophy, and mononuclear cell infiltration (**Figure 3.13**). These overlapping results support the notion that indeed, Dll4 on DC support Foxp3 expression and suppress RSV pathology. But unlike Dll4 systemic neutralization, we didn't detect any Th17 cell plasticity phenotype in Foxp3+ Treg by sorting Foxp3-GFP+ for *Il17a* expression or by staining

IL-17A+Foxp3+ in Dll4 DC knockdown (data not shown), suggesting that DC-presented Dll4 may not involve in Treg-Th17 plasticity. We didn't find a GzmB+ Treg decrease either in Dll4 knockdown DC transfer mice. In this experiment, 12 days after transfer of Dll4 knockdown DC mice are re-infected with RSV and sacrificed 8 days later. Thus, it's possible that this 20 day time point had passed IL-17A peak production and also was involved in the exacerbated responses. While our study revealed a novel model that Dll4 on DC sustained Foxp3+ Treg cells and impeded RSV immunopathology, future studies need to be performed to further establish the role of Dll4 on DC in Th17-Treg plasticity and additional aspects of Treg function.

5.4 The role of Dll4 in regulating CD4 T cell co-stimulation and co-inhibition: beyond Foxp3$^+$ Treg

Previous studies have shown that Notch could regulate T cell co-stimulation, known as signal 2. First, Notch could directly regulate CD28 expression in T cell acute lymphoma (T-ALL)[279]. Second, several Notch target genes including HES inhibit PTEN expression that is a negative regulator of co-stimulation[280]. Third, Notch/Dll1 boosts the activation of TCR at Double Negative stage 3 (DN3) pre-T cell development[281,282] and Notch/Dll4 promotes CD4SP naïve T cell activation[74], both through the same downstream co-stimulation pathway of the PI3K/Akt/mTOR. However, the role of Notch and Dll4 in the expression of other co-stimulators and co-inhibitors remains elusive. However, Notch regulates co-activator/co-inhibitor in have not been elucidated during pulmonary infection. Here our **Figure 4.13** reports multiple co-stimulators and co-inhibitors that are differentially expressed by Dll4 stimulation during Treg differentiation, including co-stimulator OX40 and co-inhibitors CTLA-4, TIGIT, PD-1 and Lag3. These molecules are highly expressed on Treg cells in the homeostatic state and have been called "Treg

functional markers", while they are also functionally present in conventional Foxp3- CD4 SP cells[283–285]. Binding of OX40 and PD-1 to their ligands (OX-40L, PD-L1) modulates type 1 versus type 2 cytokine production and RSV pathogenesis in vivo[286,287], but the function of other co-stimulator/co-inhibitor in RSV infection are still unknown. Here we reported CTLA-4, OX40 and Lag3 are regulated by Dll4 *in vitro* in iTreg cells and *in vivo* during RSV infection. Systemic neutralization of Dll4 perturbed the percent of CTLA-4, OX-40 and Lag3 expression on Foxp3+ Treg (**Appendix Figure A.2 and A.3**). It will be intriguing to investigate the contribution of T cells' co-stimulation/co-inhibitors in Notch/Dll4 regulated RSV immunopathology in the future.

5.4.1 Notch and Dll4 support type 1 regulatory T cells (Treg1) marker—Lag3

Among all the co-inhibitors, Lag3 may be the most interesting one because of the its important role in modulating T cell tolerance. In fact, Lag3 is a structural homolog of CD4, and it could bind to the MHC-II complex in a competitive manner. There is an inhibitory "KIEELE" domain to inhibit T cell receptor (TCR) activation and mediate Treg function in both Foxp3+ Treg cells and Foxp3- IL-10 producing type 1 T regulatory cells (Treg1)[255,256,288]. Here we found the novel regulation of Notch and Dll4 in Lag3. Lag3 is one of the top candidates in RNA-seq experiment with small p-value and high fold changes regulated by both Dll4 stimulation and SMYD3 deletion. Dll4 stimulation up-regulated Lag3 expression not just in iTreg differentiation assessed by RNA-seq has shown but also in Th0, Th2, and Th17 (**Figure A.3.A**). And Lag3 expression was RBP-Jκ canonical Notch dependent (**Figure A.3.B**). Dll4 enriched H3K4me3 at the Lag3 promoter, and the stimulation increased % Lag3+ cells in different Th (**Figure A.3.C~D**). *In vivo*, Lag3 expression was up-regulated after RSV infection (**Figure A.3.E**), and Dll4 neutralization enriched the percent Lag3 + cells in T cells but not APC at 6 dpi in primary RSV infection (**Figure A.3.F**).

Although Lag3 were expressed on both CD8+CD3+ and CD4+CD3+ T cells, Dll4 neutralization only enriched % Lag3+ on CD4 T cells, both Foxp3+ Treg and Foxp3- Tconv (**Figure A.3.G**). On the other hand, Dll4 KD DC displayed decreased percentages of Lag3+ T cells in RSV re-infection (**Figure A.3.H**). So far our current data suggest that Notch/Dll4 regulates Lag3 on CD4 T cells, but the role of Dll4 on Lag3 is context-dependent. Future studies need be performed after overcoming the low binding efficacy of anti-Lag3 antibody with a new and better generation of monoclonal antibody that Merck and other companies are working on (personal conversation with Dr. Dan Cua at ICMI 2017). With better tools, we will be able to determine the precise role of Notch in Lag3 RSV pathogenesis and beyond.

5.5 Redundancy of H3K4 methylase in Foxp3 and Treg cell regulation

Our research shows that Dll4-facilitated H3K4me3 on Foxp3 promoter and CSN elements was SMYD3-dependent (Figure 4.5C). One important observation is that Smyd3 gene deletion and Smyd3 inhibition don't completely abrogate all H3K4me3 on all Foxp3 regulatory element (**Figure 4.5C** and **Figure 4.8A**). It is possible that other histone methyltransferases also contribute to the H3K4me3 around Foxp3 regulatory elements. Besides Smyd3, KMT2B (MLL4) is the only other histone methyltransferase that is reported to involve in Foxp3+ Treg development[188]. But the mechanism associated with MLL4 is not able to explain the residual H3K4me3 since MLL4 mainly catalyzes H3K4 mono-methylation (H3K4me). It will be interesting to explore if other H3K4 tri-methylase are involved in Treg cell development and maintenance. Preliminary results from Drs. Kunkel and Schaller indicates that another H3K4 tri-methylase, namaely MLL1, could potentially regulate Foxp3+ Treg development *in vivo* and maintain immune tolerance from inflammatory bowel phenotype (unpublished data in Schaller lab). Future studies will be

performed to elucidate other methyltransferase in Treg and immune tolerance in mucosal surface (e.g. lung, gut, skin).

5.6 SMYD3 may also function as a protein methylase that regulates histone sites other than H3K4

One caveat about SMYD3 function is that SMYD3 is not only a H3K4 di- and tri-methylase but also a H4K20 methylase as well as protein methylase [191,245]. Therefore, it is likely that Dll4/Notch-driven Smyd3 not only regulates Foxp3+ Treg cell differentiation through H3K4 trimethylation on *Foxp3*, but may also have broad effects on gene expression and possibly protein function, as indicated by our RNA-seq analysis demonstrating a diverse set of genes altered in Smyd3 deficient Treg cells. For example, *Il10* expression is supported by both Dll4 and Smyd3 *in vitro* in iTreg cells and *in vivo* during RSV infection. Unlike the Foxp3 results shown in Figure 4.5C that H3K4me3 around *Foxp3* locus are Smyd3-dependent, we didn't detect abrogation of H3K4me3 on *Il10* promoter in Smyd3-deleted iTreg cells. Another example is Lag3. Our RNA-seq results and data in **Appendix Figure A.3** highlight the strong influence of Dll4/Notch in Lag3 gene expression, while Smyd3 cKO have decreased Lag3 expression. But again we can't detect a decrease of H3K4me3 on the Lag3 promoter in Smyd3-deleted iTreg cells (data not shown). These negative result suggest an alternative function or an indirect effect of Smyd3 in *Il10* and *Lag3* regulation. Future studies need to further investigate the mechanism of how Smyd3 affects the anti-inflammatory cytokine, IL-10 and the Treg1 marker, Lag3 in CD4 T cells for more precise regulation of tolerance.

5.7 SMYD3 modulates CD4 tolerance at another mucosal surface: gut

SMYD3 deletion supports tolerogenic CD4 T cells including Foxp3+ Treg cells and IL-10 production in pulmonary infection. We are also curious if these phenotypes exist in a steady state without inflammation or infection. We had investigated the Treg in thymus and periphery and found no significant differences in Treg development in unmanipulated SPF mice (data not shown) . SMYD3 Cre+ KO mice have a similar number and percent of Foxp3+ CD4 T cells in the thymus compared to wildtype mice (**Figure A.4.A**). Unlike the phenotype in Foxp3 *scurfy* mice and Foxp3 depleted mice, Smyd3-deleted mice have no splenomegaly, lymphomegaly or other autoimmunity disease (**Figure A.4.B**). Treg cell development in the spleen was slightly compromised (**Figure A.4.C**), and Foxp3-inhibited cytokines, namely IL-4, IL-5, IL-13 and IL-17A, were up-regulated after 24 hours of T cells activation with P + I (**Figure A.4.D**). These data suggest that Smyd3 deletion in CD4 T cells has a minimal effect in SLO. Since Dll4 is highly expressed on lacteal lymphatic vessels in gut lamina propria[289], and multiple cell types (eg., epithelial cells, gut dendritic cells, Treg cells) in the gut lamina propria express TGF-β[290,291]. More recently, CD103+ DC in gut lamina propria were shown to participate in TGF-β mediated induction of pTreg cells[292,293]. Here we isolated colon lamina propria lymphocyte(LPL) that is enriched with IL-10 producing and Foxp3+ Treg cells[126,132]. CD4-specific Smyd3 knockout mice have significantly fewer Foxp3+ Treg in colon LPL in 6 to 7 weeks old adult mice compared to wt control mice (**Figure A.4.E~F**). Moreover, decreased percentages and numbers of Foxp3+ Treg cells were detected in 23-26 weeks old mice (data not shown). Meanwhile, *Foxp3* expression in colon LPL was significantly decreased in 6-7 weeks old CD4-specific Smyd3 KO mice, as well as *Il10* expression (**Figure A.4.G~H**). These data suggested that Smyd3 supported *Foxp3* and *Il10* expression *in vivo* in the colon. Previous studies show that DC elicit IL-17A+ CD4 T cells and

Foxp3+ Treg cells in small intestine lamina propria[292,294]. Here we further investigate IL-17A and found that Smyd3 deletion enriched *Il17a* expression in LPL, and IL-17A+ CD4 T cells from small intestine lamina propria (**Figure A.4.I-J**). Thus, Smyd3 appears to be important for supporting Treg differentiation and stability in other mucosal sites like gut.

5.8 SMYD3 may also regulate anti-tumor immunity in lung carcinoma model

Smyd3 can regulate multiple oncogenic pathways including RAS, Estrogen receptor, and E-caderin-driven tumorogenesis to promote epithelial to mesenchymal transition (EMT) and be a transcription potentiator [199,200,245]. Although Smyd3 promotes transformed cell growth and inhibits apoptosis as a cancer potentiator [193,194,199,295], we didn't find that Smyd3 affected non-transformed CD4 T cell proliferation in CFSE-labeling experiment with iTreg cell differentiation (data not shown).

Due to the correlation of Smyd3 expression with poor prognosis in multiple cancers including colorectal carcinoma, breast cancer, hepatocellular carcinoma (HCC), lung adenocarcinoma, and pancreatic cancer[193–198,245], the question remains whether Smyd3 in immune compartment may have a role in cancer progression. . In particular, our hypothesis was that overexpression of Smyd3 in T cells may provide a repressive immune environment that allows the tumor to grow in an immunosuppressed environment. To investigate if Smyd3 cells plays a role in CD4 T not only in lung infection but also in anti-tumor immunity against lung carcinoma, we collaborated with Peter Chockley and Dr. Venkat Keshamouni to subcutaneously inject Lewis lung carcinoma (LLC) cells under the two lateral back of Cre- control or Cre+ Smyd3 cKO mice. Surprisingly, CD4-specific Smyd3 KO that have impaired Smyd3 expression in both CD4 and CD8 T cells had more LLC tumor lung metastasis than control (**Figure A.4.A**). The metastatic lungs had higher pro-metastatic

cytokine *Il22* with no increase in *Il17a, Il10, and Tgfb* in Smyd3 KO mice (**Figure A.5.B**), indicating a potential role of IL-22 in LLC metastasis. The percent and number of Foxp3+ Treg cells in draining inguinal LN were decreased (**Figure A.4.C**) as we had observed in other models. In sorted CD4 and CD8 T cells, there was less *Il2* in CD4 and less *Ifng* in CD8 T cells (**Figure A.4.D**). While Smyd3 cKO mice again had fewer Foxp3+ Treg cells compared to control mice, our data did not find more *Ifng* in CD8 T cells in Smyd3 cKO, a result that challenges the paradigm of Treg cells as inhibitors of anti-tumor cytotoxicity. Instead, Less Ifng from CD8 T cells and more Il22 from CD4 T cells were observed to support more LLC lung metastasis. These results strongly suggest that Smyd3 in T cells regulate LLC metastasis, and the consequence of not having Smyd3 during tumorigenesis appears to be detrimental due to other effects of the Smyd3 regulation on the immune responses. Thus, our understanding of Smyd3 can not be generalized and need to be further defined.

Together, the data presented in my dissertation addresses new and exciting findings that demonstrate a conserved pathway, Notch, that epigenetically promotes Foxp3+ Treg cell differentiation through SMYD3 and harnesses Treg tolerogenic identities (e.g. IL-10, Lag3) to dampen immunopathogenesis in pulmonary viral infection. Furthermore, current thesis also open up new and excited questions to be tested in the future.

Appendix

Additional observations of Dll4 and SMYD3 in regulatory T cells

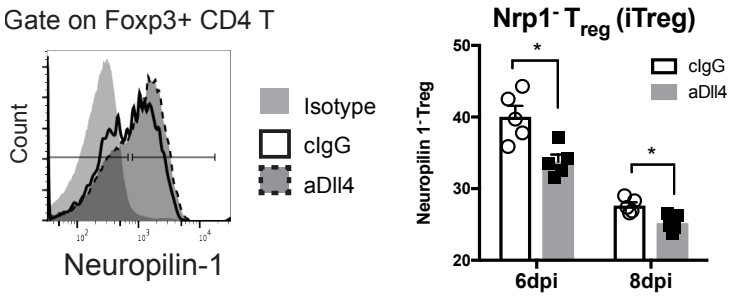

Figure A.1 Dll4 neutralization decreases Nrp1$^-$ adaptively induced Treg (iTreg) in RSV infection

Balb/c mice were intratracheally infected with Line19 RSV, and Dll4 were neutralized by anti-Dll4 antibody every other day (same experimental procedure as described in Chapter 3.3.2). Splenic Foxp3+ CD4 T cells (Foxp3+CD4+CD3+LD-) were stained with Neuropilin-1 (Nrp1) antibody that is a marker of tTreg but not iTreg. Nrp1- iTreg were gated at 6 dpi and 8 dpi after Dll4 neutralization.

Data represent mean ± SEM. Data were from one experiment representative of two to three experiments. * P<0.05; ** P<0.005; *** P<0.0005; NS: no significance (unpaired two-tailed t-test)

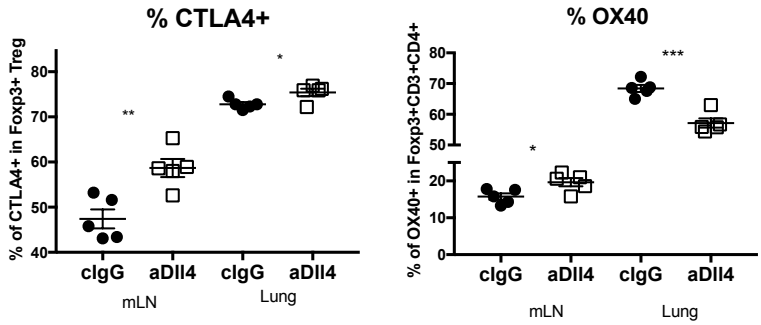

Figure A.2: Co-inhibitor CTLA-4 and co-stimulator OX40 are differentially regulated by Dll4 neutralization in RSV infection

Balb/c mice were intratracheally infected with Line19 RSV, and Dll4 were neutralized by anti-Dll4 antibody every other day (same experimental procedure as described in Chapter 3.3.2). At 8 dpi, Foxp3+ CD4 T cells (Foxp3+CD4+CD3+LD-) in lung and mediastinal lymph node (mLN) were stained with intracellular CTLA-4 and extracellular OX-40 antibody that are both functional marker of Treg.
Data represent mean ± SEM. Data were from one experiment representative of two to three experiments. * P<0.05; ** P<0.005; *** P<0.0005; NS: no significance (unpaired two-tailed t-test)

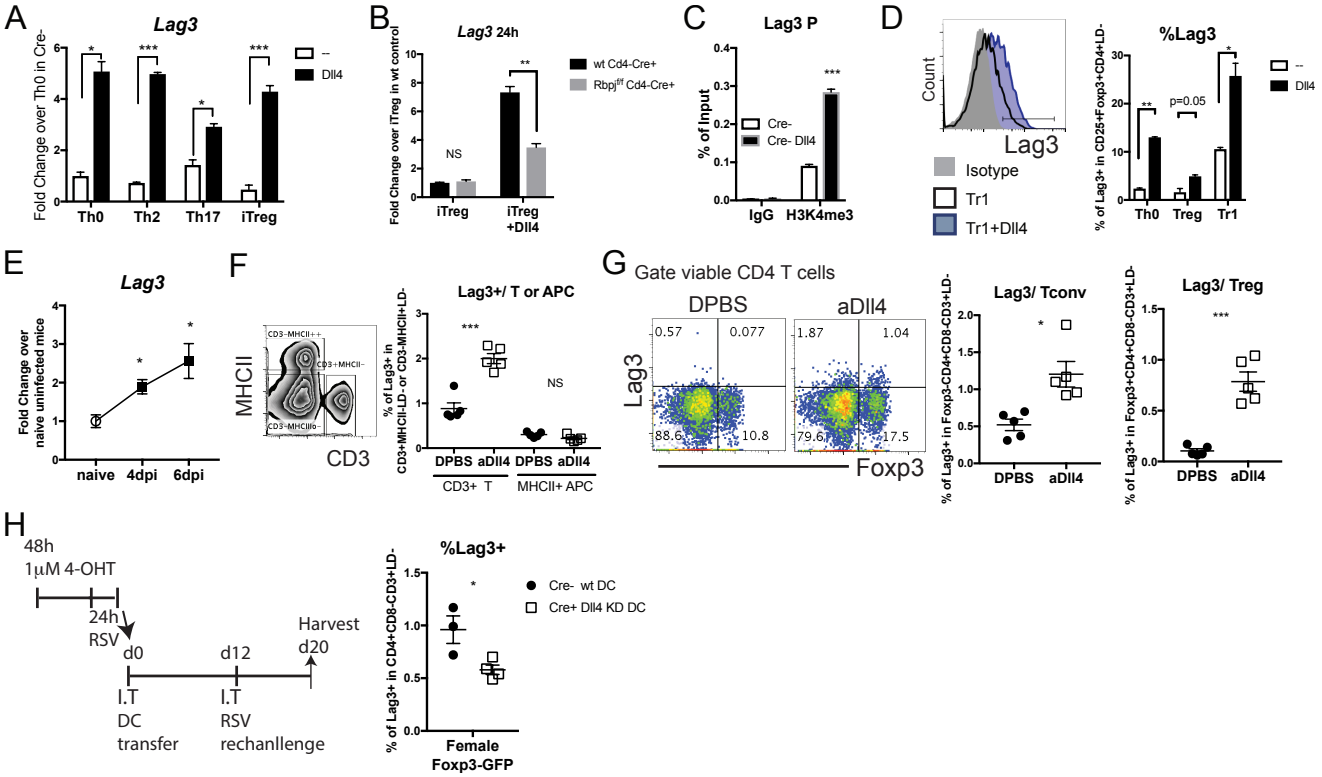

Figure A.3: TCR co-inhibitor Lag3 is dependent on Dll4 and intracellular Notch signaling *in vivo* and *in vitro*

A. Naïve CD4 T cells were isolated from Cre- control B6 mice and skewed toward Th0, Th2, Th17, and iTreg with or without Dll4 stimulation. After 48 hours, Lag3 mRNA were measured.
B. Naïve CD4 T cells were isolated from wt control or CD4-specific Rbpj KO mice, and skewed toward iTreg with or without Dll4 stimulation. After 24 hours, Lag3 mRNA were measured.
C. Naïve CD4 T cells were isolated from Cre- control B6 mice and skewed toward iTreg with or without Dll4 stimulation. After 72 hours, chromatin and DNA were crosslinked and H3K4me3 were immunoprecipitated. Lag3 promoter were then PCR

to quantified the H3K4me3 modification on Lag3 promoter with or without Dll4 stimulation.

D. Naïve CD4 T cells were isolated from Cre- control B6 mice and skewed toward Th0, iTreg and type 1 Treg (Tr1 here were skewed in IL-27 20ng/mL and TGF-β 2 ng/mL here) with or without Dll4 stimulation. After 72 hours, Lag3 protein on CD4 T cells surface were stained and quantified by flow cytometry.
E. Balb/c mice were intratracheally infected with RSV Line19. After 4 days post infection (dpi) and 6 dpi, lung were harvest and Lag3 expression were measured.
F. Balb/c mice were intratracheally infected with RSV Line19, and Dll4 were neutralized by anti-Dll4 antibody every other day. At 6 dpi, Lung T cells (CD3+MHCII-) and APC (MHCII+CD3-) were gated. Lag3 on T cells or APC were stained.
G. Naïve CD4 T cells from Cre- control or Smyd3 cKO were differentiated to iTreg cells with or without Dll4 for 48 hours. *Il17a* mRNA was measured.
H. UBC-Cre/ERT2 mice were bred with $Dll4^{F/F}$ mice to have inducible Dll4 knockdown mice on C57BL6 background. After taking bone marrow and culture into DC for 6 days, these BMDC were incubated with 1 mM 4-OHT for 48 hours to knockdown (KD) Dll4. After infected with RSV MOI=0.5 for 24 hours, control or Dll4-KD RSV-infected BMDC were intratracheally transferred into same recipient of $Foxp3^{eGFP}$ mice. After 12 days, both wt BMDC and Dll4 KD BMDC transferred recipients were rechallenged with RSV infection. After another 8 days, CD4 T cells in lung were harvest and Lag3 on CD4 T cells were stained.

Data represent mean ± SEM. Data were from one experiment representative of two to three experiments. * $P<0.05$; ** $P<0.005$; *** $P<0.0005$; NS: no significance (unpaired two-tailed *t*-test)

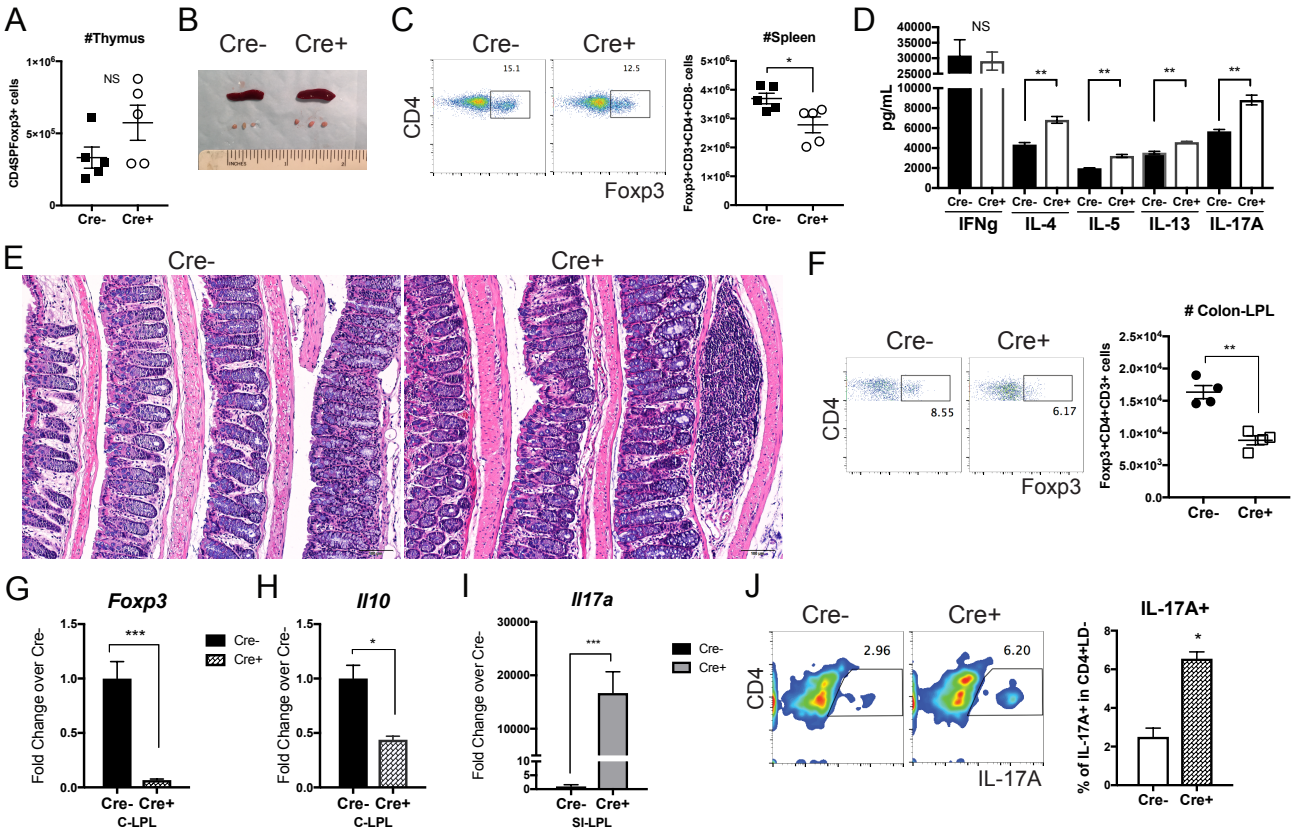

Figure A.4: SMYD3 in T cells maintains gut immune tolerance in un-manipulated SPF mice

A. 5~6 week old Cre- littermate control and Cre+ CD4-specific Smyd3 knockout (Smyd3 cKO) were sacrificed, and the number of thymic Treg (CD4+CD8-Foxp3+) were measured.
B. 19 week old Cre- littermate control and Cre+ CD4-specific Smyd3 knockout (Smyd3 cKO) were sacrificed. The size of spleen, inguinal lymph node, axillary lymph node, and cervical lymph node were compared.
C. 16~19 week old Cre- littermate control and Cre+ CD4-specific Smyd3 knockout (Smyd3 cKO) were sacrificed. Number of splenic peripheral Treg (CD3+CD4+Foxp3+) were measured.
D. 23~26 week old splenocytes were re-stimulated with PMA+Ionomycin without Golgi Stop and Golgi plug for 24 hours. T cells cytokines in supernatant were measured.
E. 26 week old Cre- littermate control and Cre+ CD4-specific Smyd3 knockout (Smyd3 cKO) were sacrificed. Colon were longitudinally opened, fixed and rolled. Cross section of colon were stained by H&E to visualize histopathology of colon inflammation.
F. 6 week old Cre- littermate control and Cre+ CD4-specific Smyd3 knockout (Smyd3 cKO) were sacrificed. Colon lamina propria lymphocytes (C-LPL) were enriched, and Foxp3+CD4+CD3+ Treg were stained and counted.

G. 6 week old Cre- littermate control and Cre+ CD4-specific Smyd3 knockout (Smyd3 cKO) were sacrificed. Colon lamina propria lymphocytes were enriched, and *Foxp3* expression in C-LPL were measured. N=4 in each group
H. 6 week old Cre- littermate control and Cre+ CD4-specific Smyd3 knockout (Smyd3 cKO) were sacrificed. Colon lamina propria lymphocytes were enriched, and *Il10* expression in C-LPL were measured. N=4 in each group
I. 6 week old Cre- littermate control and Cre+ CD4-specific Smyd3 knockout (Smyd3 cKO) were sacrificed. Small intestine lamina propria lymphocytes were enriched, and *Il17a* expression in SI-LPL were measured. N=4 in each group
J. 17 week old Cre- littermate control and Cre+ CD4-specific Smyd3 knockout (Smyd3 cKO) were sacrificed. Small intestine lamina propria lymphocytes were enriched, and *Il17a* expression in SI-LPL were measured.

Data represent mean ± SEM. Data were from one experiment representative of two to three experiments. * $P<0.05$; ** $P<0.005$; *** $P<0.0005$; NS: no significance (unpaired two-tailed *t*-test)

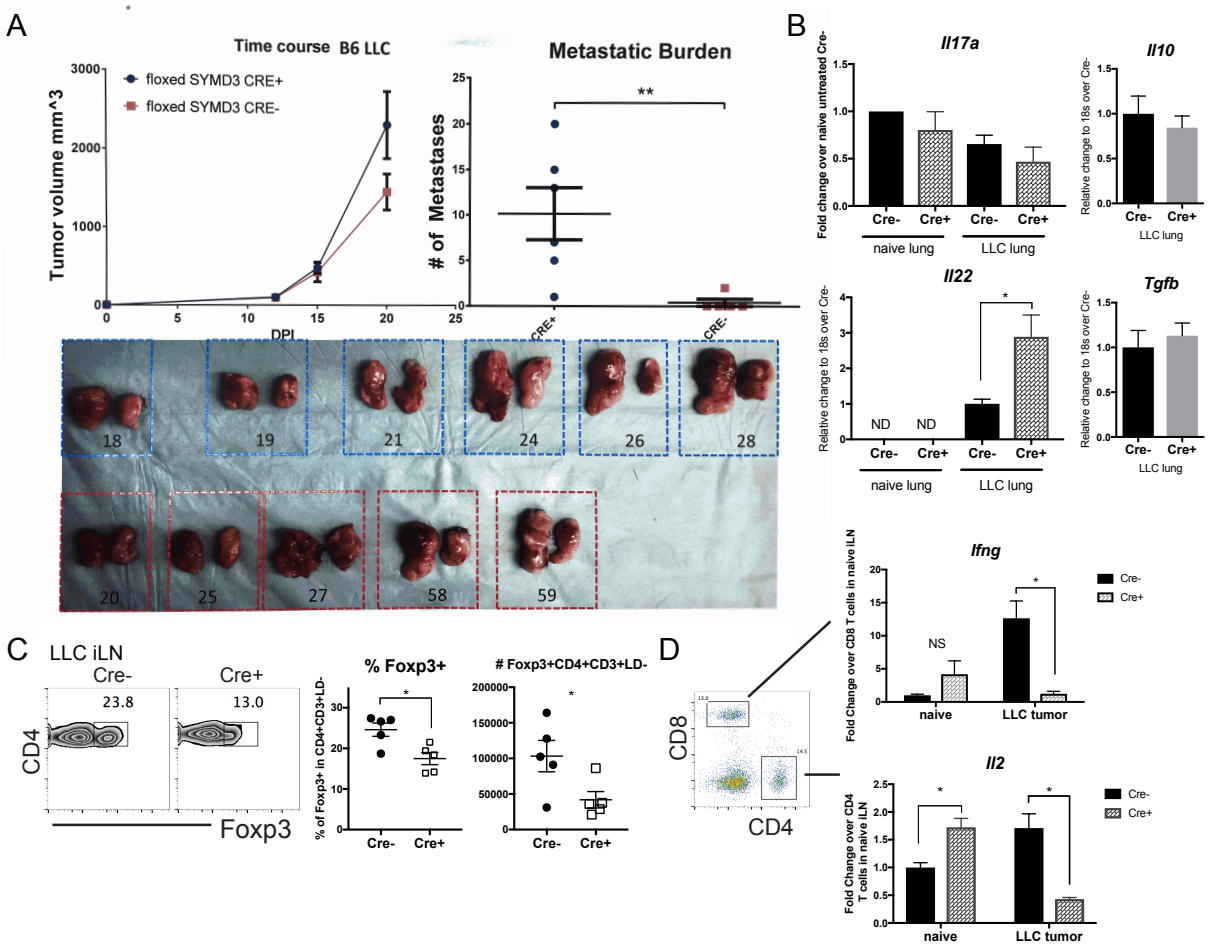

Figure A.5: SMYD3 in T cells limits lung cancer metastasis and anti-tumor immunity *in vivo*

A. 10^6 Lewis lung carcinoma (LLC) were subcutaneously injected into the left and right flank of Cre- littermate control and Cre+ Smyd3 cKO. LLC proliferated and the size of local LLC were measured. Mice were sacrificed at day 21, and the number of LLC metastatic nodule in lung were counted.
B. At day 21 of LLC transfer, Cre- littermate control and Cre+ Smyd3 cKO mice were sacrificed, and *Il17a, Il10, Il22,* and *Tgfb* expression in metastatic lung were measured.
C. At day 21 of LLC transfer, the draining lymph node—inguinal lymph node (iLN)—were harvest. The percent and number of CD3+CD4+Foxp3+ Treg were gated and measured in Cre- littermate control and Cre+ Smyd3 cKO.
D. At day 21 of LLC transfer, CD4 T cells and CD8 T cells in iLN were sorted. The expression of *Ifng* in CD8 T cells and *Il2* in CD4 T cells were measured in either LLC transfer Cre-/Cre+ or un-transferred naïve Cre-/Cre+.

Data represent mean ± SEM. Data were from one experiment representative of two to three experiments. * $P<0.05$; ** $P<0.005$; *** $P<0.0005$; NS: no significance (unpaired two-tailed *t*-test)

Bibliography

1. Simoes, E. A. Treatment and prevention of respiratory syncytial virus lower respiratory tract infection. Long-term effects on respiratory outcomes. *Am. J. Respir. Crit. Care Med.* **163,** S14-17 (2001).
2. Yorita, K. L., Holman, R. C., Sejvar, J. J., Steiner, C. A. & Schonberger, L. B. Infectious disease hospitalizations among infants in the United States. *Pediatrics* **121,** 244–252 (2008).
3. Borchers, A. T., Chang, C., Gershwin, M. E. & Gershwin, L. J. Respiratory syncytial virus--a comprehensive review. *Clin. Rev. Allergy Immunol.* **45,** 331–379 (2013).
4. Collins, P. L. & Graham, B. S. Viral and host factors in human respiratory syncytial virus pathogenesis. *J. Virol.* **82,** 2040–2055 (2008).
5. Hall, C. B. *et al.* The burden of respiratory syncytial virus infection in young children. *N. Engl. J. Med.* **360,** 588–598 (2009).
6. Stensballe, L. G., Devasundaram, J. K. & Simoes, E. A. Respiratory syncytial virus epidemics: the ups and downs of a seasonal virus. *Pediatr. Infect. Dis. J.* **22,** S21-32 (2003).
7. Piedimonte, G. & Perez, M. K. Respiratory syncytial virus infection and bronchiolitis. *Pediatr. Rev.* **35,** 519–530 (2014).
8. Stier, M. T. *et al.* Respiratory syncytial virus infection activates IL-13-producing group 2 innate lymphoid cells through thymic stromal lymphopoietin. *J. Allergy Clin. Immunol.* **138,** 814–824.e11 (2016).

9. Lukens, M. V., Kruijsen, D., Coenjaerts, F. E. J., Kimpen, J. L. L. & van Bleek, G. M. Respiratory syncytial virus-induced activation and migration of respiratory dendritic cells and subsequent antigen presentation in the lung-draining lymph node. *J. Virol.* **83,** 7235–7243 (2009).
10. Henderson, F. W., Collier, A. M., Clyde, W. A. & Denny, F. W. Respiratory-syncytial-virus infections, reinfections and immunity. A prospective, longitudinal study in young children. *N. Engl. J. Med.* **300,** 530–534 (1979).
11. Wagner, D. K. *et al.* Serum immunoglobulin G antibody subclass response to respiratory syncytial virus F and G glycoproteins after first, second, and third infections. *J. Clin. Microbiol.* **27,** 589–592 (1989).
12. Graham, B. S., Bunton, L. A., Wright, P. F. & Karzon, D. T. Role of T lymphocyte subsets in the pathogenesis of primary infection and rechallenge with respiratory syncytial virus in mice. *J. Clin. Invest.* **88,** 1026–1033 (1991).
13. Connors, M. *et al.* Pulmonary histopathology induced by respiratory syncytial virus (RSV) challenge of formalin-inactivated RSV-immunized BALB/c mice is abrogated by depletion of CD4+ T cells. *J. Virol.* **66,** 7444–7451 (1992).
14. Hussell, T., Baldwin, C. J., O'Garra, A. & Openshaw, P. J. CD8+ T cells control Th2-driven pathology during pulmonary respiratory syncytial virus infection. *Eur. J. Immunol.* **27,** 3341–3349 (1997).
15. Openshaw, P. J. M. & Tregoning, J. S. Immune responses and disease enhancement during respiratory syncytial virus infection. *Clin. Microbiol. Rev.* **18,** 541–555 (2005).
16. Bui, R. H. *et al.* Virus-specific IgE and IgG4 antibodies in serum of children infected with respiratory syncytial virus. *J. Pediatr.* **110,** 87–90 (1987).

17. Welliver, R. C. *et al.* The development of respiratory syncytial virus-specific IgE and the release of histamine in nasopharyngeal secretions after infection. *N. Engl. J. Med.* **305,** 841–846 (1981).

18. Garofalo, R., Kimpen, J. L., Welliver, R. C. & Ogra, P. L. Eosinophil degranulation in the respiratory tract during naturally acquired respiratory syncytial virus infection. *J. Pediatr.* **120,** 28–32 (1992).

19. Tripp, R. A. *et al.* Peripheral blood mononuclear cells from infants hospitalized because of respiratory syncytial virus infection express T helper-1 and T helper-2 cytokines and CC chemokine messenger RNA. *J. Infect. Dis.* **185,** 1388–1394 (2002).

20. You, D. *et al.* IL-4Rα on CD4+ T cells plays a pathogenic role in respiratory syncytial virus reinfection in mice infected initially as neonates. *J. Leukoc. Biol.* **93,** 933–942 (2013).

21. Taylor, S. & Bryson, Y. J. Impaired production of gamma-interferon by newborn cells in vitro is due to a functionally immature macrophage. *J. Immunol. Baltim. Md 1950* **134,** 1493–1497 (1985).

22. Srikiatkhachorn, A. & Braciale, T. J. Virus-specific CD8+ T lymphocytes downregulate T helper cell type 2 cytokine secretion and pulmonary eosinophilia during experimental murine respiratory syncytial virus infection. *J. Exp. Med.* **186,** 421–432 (1997).

23. Schwarze, J. *et al.* Critical roles for interleukin-4 and interleukin-5 during respiratory syncytial virus infection in the development of airway hyperresponsiveness after airway sensitization. *Am. J. Respir. Crit. Care Med.* **162,** 380–386 (2000).

24. Johnson, T. R. & Graham, B. S. Secreted respiratory syncytial virus G glycoprotein induces interleukin-5 (IL-5), IL-13, and eosinophilia by an IL-4-independent mechanism. *J. Virol.* **73,** 8485–8495 (1999).

25. Lukacs, N. W. *et al.* Differential immune responses and pulmonary pathophysiology are induced by two different strains of respiratory syncytial virus. *Am. J. Pathol.* **169,** 977–986 (2006).

26. Johnson, T. R., Parker, R. A., Johnson, J. E. & Graham, B. S. IL-13 is sufficient for respiratory syncytial virus G glycoprotein-induced eosinophilia after respiratory syncytial virus challenge. *J. Immunol. Baltim. Md 1950* **170,** 2037–2045 (2003).

27. Moore, M. L. *et al.* STAT1 negatively regulates lung basophil IL-4 expression induced by respiratory syncytial virus infection. *J. Immunol. Baltim. Md 1950* **183,** 2016–2026 (2009).

28. Stokes, K. L. *et al.* Differential pathogenesis of respiratory syncytial virus clinical isolates in BALB/c mice. *J. Virol.* **85,** 5782–5793 (2011).

29. Tabarani, C. M. *et al.* Novel inflammatory markers, clinical risk factors and virus type associated with severe respiratory syncytial virus infection. *Pediatr. Infect. Dis. J.* **32,** e437-442 (2013).

30. Mukherjee, S. *et al.* IL-17-Induced Pulmonary Pathogenesis during Respiratory Viral Infection and Exacerbation of Allergic Disease. *Am. J. Pathol.* **179,** 248–258 (2011).

31. Kallal, L. E., Hartigan, A. J., Hogaboam, C. M., Schaller, M. A. & Lukacs, N. W. Inefficient lymph node sensitization during respiratory viral infection promotes IL-17-mediated lung pathology. *J. Immunol. Baltim. Md 1950* **185,** 4137–4147 (2010).

32. de Almeida Nagata, D. E. *et al.* IL-27R-mediated regulation of IL-17 controls the development of respiratory syncytial virus-associated pathogenesis. *Am. J. Pathol.* **184,** 1807–1818 (2014).

33. Newcomb, D. C. *et al.* IL-13 regulates Th17 secretion of IL-17A in an IL-10-dependent manner. *J. Immunol. Baltim. Md 1950* **188,** 1027–1035 (2012).

34. Chen, Y. *et al.* Stimulation of airway mucin gene expression by interleukin (IL)-17 through IL-6 paracrine/autocrine loop. *J. Biol. Chem.* **278,** 17036–17043 (2003).

35. Fujisawa, T. *et al.* NF-κB mediates IL-1β- and IL-17A-induced MUC5B expression in airway epithelial cells. *Am. J. Respir. Cell Mol. Biol.* **45,** 246–252 (2011).

36. Dodd, J. S. *et al.* IL-9 regulates pathology during primary and memory responses to respiratory syncytial virus infection. *J. Immunol. Baltim. Md 1950* **183,** 7006–7013 (2009).

37. McNamara, P. S. *et al.* Interleukin 9 production in the lungs of infants with severe respiratory syncytial virus bronchiolitis. *Lancet Lond. Engl.* **363,** 1031–1037 (2004).

38. Schuurhof, A. *et al.* Interleukin-9 polymorphism in infants with respiratory syncytial virus infection: an opposite effect in boys and girls. *Pediatr. Pulmonol.* **45,** 608–613 (2010).

39. Fulton, R. B., Meyerholz, D. K. & Varga, S. M. Foxp3+ CD4 regulatory T cells limit pulmonary immunopathology by modulating the CD8 T cell response during respiratory syncytial virus infection. *J. Immunol. Baltim. Md 1950* **185,** 2382–2392 (2010).

40. Lee, D. C. P. *et al.* CD25+ natural regulatory T cells are critical in limiting innate and adaptive immunity and resolving disease following respiratory syncytial virus infection. *J. Virol.* **84,** 8790–8798 (2010).

41. Durant, L. R. *et al.* Regulatory T cells prevent Th2 immune responses and pulmonary eosinophilia during respiratory syncytial virus infection in mice. *J. Virol.* **87,** 10946–10954 (2013).

42. Loebbermann, J. *et al.* Regulatory T cells expressing granzyme B play a critical role in controlling lung inflammation during acute viral infection. *Mucosal Immunol.* **5,** 161–172 (2012).

43. Hoebee, B. *et al.* Influence of promoter variants of interleukin-10, interleukin-9, and tumor necrosis factor-alpha genes on respiratory syncytial virus bronchiolitis. *J. Infect. Dis.* **189,** 239–247 (2004).

44. Wilson, J. *et al.* Genetic variation at the IL10 gene locus is associated with severity of respiratory syncytial virus bronchiolitis. *J. Infect. Dis.* **191,** 1705–1709 (2005).

45. Schuurhof, A. *et al.* Local interleukin-10 production during respiratory syncytial virus bronchiolitis is associated with post-bronchiolitis wheeze. *Respir. Res.* **12,** 121 (2011).

46. Murai, H. *et al.* IL-10 and RANTES are elevated in nasopharyngeal secretions of children with respiratory syncytial virus infection. *Allergol. Int. Off. J. Jpn. Soc. Allergol.* **56,** 157–163 (2007).

47. Legg, J. P., Hussain, I. R., Warner, J. A., Johnston, S. L. & Warner, J. O. Type 1 and type 2 cytokine imbalance in acute respiratory syncytial virus bronchiolitis. *Am. J. Respir. Crit. Care Med.* **168,** 633–639 (2003).

48. Sun, J. *et al.* Autocrine regulation of pulmonary inflammation by effector T-cell derived IL-10 during infection with respiratory syncytial virus. *PLoS Pathog.* **7,** e1002173 (2011).

49. Loebbermann, J. *et al.* IL-10 regulates viral lung immunopathology during acute respiratory syncytial virus infection in mice. *PloS One* **7,** e32371 (2012).

50. Weiss, K. A., Christiaansen, A. F., Fulton, R. B., Meyerholz, D. K. & Varga, S. M. Multiple CD4+ T cell subsets produce immunomodulatory IL-10 during respiratory syncytial virus infection. *J. Immunol. Baltim. Md 1950* **187,** 3145–3154 (2011).

51. Loebbermann, J. *et al.* IL-10 regulates viral lung immunopathology during acute respiratory syncytial virus infection in mice. *PloS One* **7,** e32371 (2012).

52. Thornburg, N. J., Shepherd, B. & Crowe, J. E. Transforming growth factor beta is a major regulator of human neonatal immune responses following respiratory syncytial virus infection. *J. Virol.* **84,** 12895–12902 (2010).

53. Bakre, A. *et al.* Human respiratory syncytial virus non-structural protein NS1 modifies miR-24 expression via transforming growth factor-β. *J. Gen. Virol.* **96,** 3179–3191 (2015).

54. Morgan, T. H. The Theory of the Gene. *Am. Nat.* **51,** 513–544 (1917).

55. Andersson, E. R., Sandberg, R. & Lendahl, U. Notch signaling: simplicity in design, versatility in function. *Dev. Camb. Engl.* **138,** 3593–3612 (2011).

56. Axelrod, J. D., Matsuno, K., Artavanis-Tsakonas, S. & Perrimon, N. Interaction between Wingless and Notch signaling pathways mediated by dishevelled. *Science* **271,** 1826–1832 (1996).

57. Ramain, P. *et al.* Novel Notch alleles reveal a Deltex-dependent pathway repressing neural fate. *Curr. Biol. CB* **11,** 1729–1738 (2001).

58. Tu, L. *et al.* Notch signaling is an important regulator of type 2 immunity. *J. Exp. Med.* **202,** 1037–1042 (2005).

59. Auderset, F. *et al.* Redundant Notch1 and Notch2 signaling is necessary for IFNγ secretion by T helper 1 cells during infection with Leishmania major. *PLoS Pathog.* **8,** e1002560 (2012).

60. Zavadil, J., Cermak, L., Soto-Nieves, N. & Böttinger, E. P. Integration of TGF-beta/Smad and Jagged1/Notch signalling in epithelial-to-mesenchymal transition. *EMBO J.* **23,** 1155–1165 (2004).

61. Blokzijl, A. *et al.* Cross-talk between the Notch and TGF-beta signaling pathways mediated by interaction of the Notch intracellular domain with Smad3. *J. Cell Biol.* **163,** 723–728 (2003).

62. Elyaman, W. *et al.* Notch Receptors and Smad3 Signaling Cooperate in the Induction of Interleukin-9-Producing T Cells. *Immunity* **36,** 623–634 (2012).

63. Samon, J. B. *et al.* Notch1 and TGFbeta1 cooperatively regulate Foxp3 expression and the maintenance of peripheral regulatory T cells. *Blood* **112,** 1813–1821 (2008).

64. Cho, O. H. *et al.* Notch regulates cytolytic effector function in CD8+ T cells. *J. Immunol. Baltim. Md 1950* **182,** 3380–3389 (2009).

65. Pearce, E. L. *et al.* Control of effector CD8+ T cell function by the transcription factor Eomesodermin. *Science* **302,** 1041–1043 (2003).

66. Intlekofer, A. M. *et al.* Effector and memory CD8+ T cell fate coupled by T-bet and eomesodermin. *Nat. Immunol.* **6,** 1236–1244 (2005).

67. Maekawa, Y. *et al.* Notch2 integrates signaling by the transcription factors RBP-J and CREB1 to promote T cell cytotoxicity. *Nat. Immunol.* **9,** 1140–1147 (2008).

68. Ito, T. *et al.* The critical role of Notch ligand Delta-like 1 in the pathogenesis of influenza A virus (H1N1) infection. *PLoS Pathog.* **7,** e1002341 (2011).

69. Amsen, D. *et al.* Instruction of distinct CD4 T helper cell fates by different notch ligands on antigen-presenting cells. *Cell* **117,** 515–526 (2004).

70. Charbonnier, L.-M., Wang, S., Georgiev, P., Sefik, E. & Chatila, T. A. Control of peripheral tolerance by regulatory T cell-intrinsic Notch signaling. *Nat. Immunol.* **16,** 1162–1173 (2015).

71. Hozumi, K. *et al.* Delta-like 4 is indispensable in thymic environment specific for T cell development. *J. Exp. Med.* **205,** 2507–2513 (2008).

72. Adler, S. H. *et al.* Notch signaling augments T cell responsiveness by enhancing CD25 expression. *J. Immunol. Baltim. Md 1950* **171,** 2896–2903 (2003).

73. Eagar, T. N. *et al.* Notch 1 signaling regulates peripheral T cell activation. *Immunity* **20,** 407–415 (2004).

74. Laky, K., Evans, S., Perez-Diez, A. & Fowlkes, B. J. Notch signaling regulates antigen sensitivity of naive CD4+ T cells by tuning co-stimulation. *Immunity* **42,** 80–94 (2015).

75. Sun, J., Krawczyk, C. J. & Pearce, E. J. Suppression of Th2 cell development by Notch ligands Delta1 and Delta4. *J. Immunol. Baltim. Md 1950* **180,** 1655–1661 (2008).

76. Bailis, W. *et al.* Notch simultaneously orchestrates multiple helper T cell programs independently of cytokine signals. *Immunity* **39,** 148–159 (2013).

77. Minter, L. M. *et al.* Inhibitors of gamma-secretase block in vivo and in vitro T helper type 1 polarization by preventing Notch upregulation of Tbx21. *Nat. Immunol.* **6,** 680–688 (2005).

78. Jurynczyk, M., Jurewicz, A., Raine, C. S. & Selmaj, K. Notch3 inhibition in myelin-reactive T cells down-regulates protein kinase C theta and attenuates experimental autoimmune encephalomyelitis. *J. Immunol. Baltim. Md 1950* **180,** 2634–2640 (2008).

79. Amsen, D. *et al.* Instruction of distinct CD4 T helper cell fates by different notch ligands on antigen-presenting cells. *Cell* **117,** 515–526 (2004).

80. Amsen, D. *et al.* Direct regulation of Gata3 expression determines the T helper differentiation potential of Notch. *Immunity* **27,** 89–99 (2007).

81. Fang, T. C. *et al.* Notch directly regulates Gata3 expression during T helper 2 cell differentiation. *Immunity* **27,** 100–110 (2007).

82. Schaller, M. A. *et al.* Notch ligand Delta-like 4 regulates disease pathogenesis during respiratory viral infections by modulating Th2 cytokines. *J. Exp. Med.* **204,** 2925–2934 (2007).

83. Jang, S., Schaller, M., Berlin, A. A. & Lukacs, N. W. Notch ligand delta-like 4 regulates development and pathogenesis of allergic airway responses by modulating IL-2 production and Th2 immunity. *J. Immunol. Baltim. Md 1950* **185,** 5835–5844 (2010).

84. Schaller, M. A. *et al.* Delta-like 4 differentially regulates murine CD4 T cell expansion via BMI1. *PloS One* **5,** e12172 (2010).

85. Mukherjee, S. *et al.* STAT5-induced lunatic fringe during Th2 development alters delta-like 4-mediated Th2 cytokine production in respiratory syncytial virus-exacerbated airway allergic disease. *J. Immunol. Baltim. Md 1950* **192,** 996–1003 (2014).

86. Elyaman, W. *et al.* Notch receptors and Smad3 signaling cooperate in the induction of interleukin-9-producing T cells. *Immunity* **36,** 623–634 (2012).

87. Mukherjee, S., Schaller, M. A., Neupane, R., Kunkel, S. L. & Lukacs, N. W. Regulation of T cell activation by Notch ligand, DLL4, promotes IL-17 production and Rorc activation. *J. Immunol. Baltim. Md 1950* **182,** 7381–7388 (2009).

88. Keerthivasan, S. *et al.* Notch signaling regulates mouse and human Th17 differentiation. *J. Immunol. Baltim. Md 1950* **187,** 692–701 (2011).

89. Bassil, R. *et al.* Notch ligand delta-like 4 blockade alleviates experimental autoimmune encephalomyelitis by promoting regulatory T cell development. *J. Immunol. Baltim. Md 1950* **187,** 2322–2328 (2011).

90. Gurczynski, S. J., Zhou, X., Flaherty, M., Wilke, C. A. & Moore, B. B. Bone marrow transplant-induced alterations in Notch signaling promote pathologic Th17 responses to γ-herpesvirus infection. *Mucosal Immunol.* (2017). doi:10.1038/mi.2017.85

91. Neal, L. M. *et al.* T Cell-Restricted Notch Signaling Contributes to Pulmonary Th1 and Th2 Immunity during Cryptococcus neoformans Infection. *J. Immunol. Baltim. Md 1950* **199,** 643–655 (2017).

92. Barbarulo, A. *et al.* Notch3 and canonical NF-kappaB signaling pathways cooperatively regulate Foxp3 transcription. *J. Immunol. Baltim. Md 1950* **186,** 6199–6206 (2011).

93. Kared, H. *et al.* Jagged2-expressing hematopoietic progenitors promote regulatory T cell expansion in the periphery through notch signaling. *Immunity* **25,** 823–834 (2006).

94. Ou-Yang, H.-F. *et al.* Notch signaling regulates the FOXP3 promoter through RBP-J- and Hes1-dependent mechanisms. *Mol. Cell. Biochem.* **320,** 109–114 (2009).

95. Perumalsamy, L. R., Marcel, N., Kulkarni, S., Radtke, F. & Sarin, A. Distinct spatial and molecular features of notch pathway assembly in regulatory T cells. *Sci. Signal.* **5,** ra53 (2012).

96. Samon, J. B. *et al.* Notch1 and TGFbeta1 cooperatively regulate Foxp3 expression and the maintenance of peripheral regulatory T cells. *Blood* **112,** 1813–1821 (2008).

97. Bassil, R. *et al.* Notch ligand delta-like 4 blockade alleviates experimental autoimmune encephalomyelitis by promoting regulatory T cell development. *J. Immunol. Baltim. Md 1950* **187,** 2322–2328 (2011).

98. Billiard, F. *et al.* Dll4-Notch signaling in Flt3-independent dendritic cell development and autoimmunity in mice. *J. Exp. Med.* **209,** 1011–1028 (2012).

99. Sandy, A. R. *et al.* T cell-specific notch inhibition blocks graft-versus-host disease by inducing a hyporesponsive program in alloreactive CD4+ and CD8+ T cells. *J. Immunol. Baltim. Md 1950* **190,** 5818–5828 (2013).

100. Tran, I. T. *et al.* Blockade of individual Notch ligands and receptors controls graft-versus-host disease. *J. Clin. Invest.* **123,** 1590–1604 (2013).

101. Gershon, R. K. & Kondo, K. Cell interactions in the induction of tolerance: the role of thymic lymphocytes. *Immunology* **18,** 723–737 (1970).

102. Green, D. R. & Webb, D. R. Saying the 'S' word in public. *Immunol. Today* **14,** 523–525 (1993).

103. Brunkow, M. E. *et al.* Disruption of a new forkhead/winged-helix protein, scurfin, results in the fatal lymphoproliferative disorder of the scurfy mouse. *Nat. Genet.* **27,** 68–73 (2001).

104. Sakaguchi, S., Sakaguchi, N., Asano, M., Itoh, M. & Toda, M. Immunologic self-tolerance maintained by activated T cells expressing IL-2 receptor alpha-chains (CD25). Breakdown of a single mechanism of self-tolerance causes various autoimmune diseases. *J. Immunol. Baltim. Md 1950* **155,** 1151–1164 (1995).

105. Thornton, A. M. & Shevach, E. M. CD4+CD25+ immunoregulatory T cells suppress polyclonal T cell activation in vitro by inhibiting interleukin 2 production. *J. Exp. Med.* **188,** 287–296 (1998).

106. Hori, S., Nomura, T. & Sakaguchi, S. Control of regulatory T cell development by the transcription factor Foxp3. *Science* **299,** 1057–1061 (2003).

107. Fontenot, J. D., Gavin, M. A. & Rudensky, A. Y. Foxp3 programs the development and function of CD4+CD25+ regulatory T cells. *Nat. Immunol.* **4,** 330–336 (2003).

108. Fontenot, J. D. *et al.* Regulatory T cell lineage specification by the forkhead transcription factor foxp3. *Immunity* **22,** 329–341 (2005).

109. Walker, M. R. *et al.* Induction of FoxP3 and acquisition of T regulatory activity by stimulated human CD4+CD25- T cells. *J. Clin. Invest.* **112,** 1437–1443 (2003).

110. Chatila, T. A. *et al.* JM2, encoding a fork head-related protein, is mutated in X-linked autoimmunity-allergic disregulation syndrome. *J. Clin. Invest.* **106,** R75-81 (2000).

111. Abbas, A. K. *et al.* Regulatory T cells: recommendations to simplify the nomenclature. *Nat. Immunol.* **14,** 307–308 (2013).

112. Gottschalk, R. A., Corse, E. & Allison, J. P. Expression of Helios in peripherally induced Foxp3+ regulatory T cells. *J. Immunol. Baltim. Md 1950* **188,** 976–980 (2012).

113. Thornton, A. M. *et al.* Expression of Helios, an Ikaros transcription factor family member, differentiates thymic-derived from peripherally induced Foxp3+ T regulatory cells. *J. Immunol. Baltim. Md 1950* **184,** 3433–3441 (2010).

114. Yadav, M. *et al.* Neuropilin-1 distinguishes natural and inducible regulatory T cells among regulatory T cell subsets in vivo. *J. Exp. Med.* **209,** 1713–1722, S1-19 (2012).

115. Weiss, J. M. *et al.* Neuropilin 1 is expressed on thymus-derived natural regulatory T cells, but not mucosa-generated induced Foxp3+ T reg cells. *J. Exp. Med.* **209,** 1723–1742, S1 (2012).

116. Campbell, D. J. Control of Regulatory T Cell Migration, Function, and Homeostasis. *J. Immunol. Baltim. Md 1950* **195,** 2507–2513 (2015).

117. Smigiel, K. S. *et al.* CCR7 provides localized access to IL-2 and defines homeostatically distinct regulatory T cell subsets. *J. Exp. Med.* **211,** 121–136 (2014).

118. Ouyang, W., Beckett, O., Flavell, R. A. & Li, M. O. An essential role of the Forkhead-box transcription factor Foxo1 in control of T cell homeostasis and tolerance. *Immunity* **30,** 358–371 (2009).

119. Sugiyama, D. *et al.* Anti-CCR4 mAb selectively depletes effector-type FoxP3+CD4+ regulatory T cells, evoking antitumor immune responses in humans. *Proc. Natl. Acad. Sci. U. S. A.* **110,** 17945–17950 (2013).

120. Ting, H.-A. *et al.* Notch Ligand Delta-like 4 Promotes Regulatory T Cell Identity in Pulmonary Viral Infection. *J. Immunol. Baltim. Md 1950* **198,** 1492–1502 (2017).

121. Roncarolo, M. G. *et al.* Interleukin-10-secreting type 1 regulatory T cells in rodents and humans. *Immunol. Rev.* **212,** 28–50 (2006).

122. Mempel, T. R. *et al.* Regulatory T cells reversibly suppress cytotoxic T cell function independent of effector differentiation. *Immunity* **25,** 129–141 (2006).

123. Tadokoro, C. E. *et al.* Regulatory T cells inhibit stable contacts between CD4+ T cells and dendritic cells in vivo. *J. Exp. Med.* **203,** 505–511 (2006).

124. Tang, Q. *et al.* Visualizing regulatory T cell control of autoimmune responses in nonobese diabetic mice. *Nat. Immunol.* **7,** 83–92 (2006).

125. Cao, X. *et al.* Granzyme B and perforin are important for regulatory T cell-mediated suppression of tumor clearance. *Immunity* **27,** 635–646 (2007).

126. Kamanaka, M. *et al.* Expression of interleukin-10 in intestinal lymphocytes detected by an interleukin-10 reporter knockin tiger mouse. *Immunity* **25,** 941–952 (2006).

127. Strauss, L. *et al.* A Unique Subset of CD4+CD25highFoxp3+ T Cells Secreting Interleukin-10 and Transforming Growth Factor-β1 Mediates Suppression in the Tumor Microenvironment. *Clin. Cancer Res.* **13,** 4345–4354 (2007).

128. Fiorentino, D. F., Bond, M. W. & Mosmann, T. R. Two types of mouse T helper cell. IV. Th2 clones secrete a factor that inhibits cytokine production by Th1 clones. *J. Exp. Med.* **170,** 2081–2095 (1989).

129. Neumann, C. *et al.* Role of Blimp-1 in programing Th effector cells into IL-10 producers. *J. Exp. Med.* **211,** 1807–1819 (2014).

130. Jankovic, D. *et al.* Conventional T-bet(+)Foxp3(-) Th1 cells are the major source of host-protective regulatory IL-10 during intracellular protozoan infection. *J. Exp. Med.* **204,** 273–283 (2007).

131. Xu, J. *et al.* c-Maf regulates IL-10 expression during Th17 polarization. *J. Immunol. Baltim. Md 1950* **182,** 6226–6236 (2009).

132. Rubtsov, Y. P. *et al.* Regulatory T cell-derived interleukin-10 limits inflammation at environmental interfaces. *Immunity* **28,** 546–558 (2008).

133. Maynard, C. L. *et al.* Regulatory T cells expressing interleukin 10 develop from Foxp3+ and Foxp3- precursor cells in the absence of interleukin 10. *Nat. Immunol.* **8,** 931–941 (2007).

134. Vieira, P. L. *et al.* IL-10-secreting regulatory T cells do not express Foxp3 but have comparable regulatory function to naturally occurring CD4+CD25+ regulatory T cells. *J. Immunol. Baltim. Md 1950* **172,** 5986–5993 (2004).

135. Piccirillo, C. A. *et al.* CD4(+)CD25(+) regulatory T cells can mediate suppressor function in the absence of transforming growth factor beta1 production and responsiveness. *J. Exp. Med.* **196,** 237–246 (2002).

136. Marie, J. C., Liggitt, D. & Rudensky, A. Y. Cellular mechanisms of fatal early-onset autoimmunity in mice with the T cell-specific targeting of transforming growth factor-beta receptor. *Immunity* **25,** 441–454 (2006).

137. Li, M. O., Wan, Y. Y. & Flavell, R. A. T cell-produced transforming growth factor-beta1 controls T cell tolerance and regulates Th1- and Th17-cell differentiation. *Immunity* **26,** 579–591 (2007).

138. Powrie, F., Carlino, J., Leach, M. W., Mauze, S. & Coffman, R. L. A critical role for transforming growth factor-beta but not interleukin 4 in the suppression of T helper type 1-mediated colitis by CD45RB(low) CD4+ T cells. *J. Exp. Med.* **183,** 2669–2674 (1996).

139. Fontenot, J. D., Rasmussen, J. P., Gavin, M. A. & Rudensky, A. Y. A function for interleukin 2 in Foxp3-expressing regulatory T cells. *Nat. Immunol.* **6,** 1142–1151 (2005).

140. Zheng, Y. *et al.* Role of conserved non-coding DNA elements in the Foxp3 gene in regulatory T-cell fate. *Nature* **463,** 808–812 (2010).

141. Ohkura, N. *et al.* T cell receptor stimulation-induced epigenetic changes and Foxp3 expression are independent and complementary events required for Treg cell development. *Immunity* **37,** 785–799 (2012).

142. Floess, S. *et al.* Epigenetic control of the foxp3 locus in regulatory T cells. *PLoS Biol.* **5,** e38 (2007).

143. Ohkura, N., Kitagawa, Y. & Sakaguchi, S. Development and maintenance of regulatory T cells. *Immunity* **38,** 414–423 (2013).

144. Moran, A. E. *et al.* T cell receptor signal strength in Treg and iNKT cell development demonstrated by a novel fluorescent reporter mouse. *J. Exp. Med.* **208,** 1279–1289 (2011).

145. Jordan, M. S. *et al.* Thymic selection of CD4+CD25+ regulatory T cells induced by an agonist self-peptide. *Nat. Immunol.* **2,** 301–306 (2001).

146. Apostolou, I., Sarukhan, A., Klein, L. & von Boehmer, H. Origin of regulatory T cells with known specificity for antigen. *Nat. Immunol.* **3,** 756–763 (2002).

147. Sauer, S. *et al.* T cell receptor signaling controls Foxp3 expression via PI3K, Akt, and mTOR. *Proc. Natl. Acad. Sci. U. S. A.* **105,** 7797–7802 (2008).

148. Kerdiles, Y. M. *et al.* Foxo transcription factors control regulatory T cell development and function. *Immunity* **33,** 890–904 (2010).

149. Long, M., Park, S.-G., Strickland, I., Hayden, M. S. & Ghosh, S. Nuclear factor-kappaB modulates regulatory T cell development by directly regulating expression of Foxp3 transcription factor. *Immunity* **31,** 921–931 (2009).

150. Chen, W. *et al.* Conversion of peripheral CD4+CD25- naive T cells to CD4+CD25+ regulatory T cells by TGF-beta induction of transcription factor Foxp3. *J. Exp. Med.* **198,** 1875–1886 (2003).

151. Xu, L., Kitani, A., Fuss, I. & Strober, W. Cutting edge: regulatory T cells induce CD4+CD25-Foxp3- T cells or are self-induced to become Th17 cells in the absence of exogenous TGF-beta. *J. Immunol. Baltim. Md 1950* **178,** 6725–6729 (2007).

152. Huber, S. *et al.* Cutting edge: TGF-beta signaling is required for the in vivo expansion and immunosuppressive capacity of regulatory CD4+CD25+ T cells. *J. Immunol. Baltim. Md 1950* **173,** 6526–6531 (2004).

153. Wu, C. *et al.* Galectin-9-CD44 interaction enhances stability and function of adaptive regulatory T cells. *Immunity* **41,** 270–282 (2014).

154. Josefowicz, S. Z. *et al.* Extrathymically generated regulatory T cells control mucosal TH2 inflammation. *Nature* **482,** 395–399 (2012).

155. Chinen, T. *et al.* An essential role for the IL-2 receptor in Treg cell function. *Nat. Immunol.* (2016). doi:10.1038/ni.3540

156. Chen, Q., Kim, Y. C., Laurence, A., Punkosdy, G. A. & Shevach, E. M. IL-2 controls the stability of Foxp3 expression in TGF-beta-induced Foxp3+ T cells in vivo. *J. Immunol. Baltim. Md 1950* **186,** 6329–6337 (2011).

157. Burchill, M. A., Yang, J., Vogtenhuber, C., Blazar, B. R. & Farrar, M. A. IL-2 receptor beta-dependent STAT5 activation is required for the development of Foxp3+ regulatory T cells. *J. Immunol. Baltim. Md 1950* **178,** 280–290 (2007).

158. Feng, Y. *et al.* Control of the inheritance of regulatory T cell identity by a cis element in the Foxp3 locus. *Cell* **158,** 749–763 (2014).

159. Li, X., Liang, Y., LeBlanc, M., Benner, C. & Zheng, Y. Function of a Foxp3 cis-element in protecting regulatory T cell identity. *Cell* **158,** 734–748 (2014).

160. Zhou, X. *et al.* Foxp3 instability leads to the generation of pathogenic memory T cells in vivo. *Nat. Immunol.* **10,** 1000–1007 (2009).

161. Rubtsov, Y. P. *et al.* Stability of the regulatory T cell lineage in vivo. *Science* **329,** 1667–1671 (2010).

162. Miyao, T. *et al.* Plasticity of Foxp3(+) T cells reflects promiscuous Foxp3 expression in conventional T cells but not reprogramming of regulatory T cells. *Immunity* **36,** 262–275 (2012).

163. Barnes, M. J. & Powrie, F. Hybrid Treg cells: steel frames and plastic exteriors. *Nat. Immunol.* **10,** 563–564 (2009).

164. Koch, M. A. *et al.* The transcription factor T-bet controls regulatory T cell homeostasis and function during type 1 inflammation. *Nat. Immunol.* **10,** 595–602 (2009).

165. Zheng, Y. *et al.* Regulatory T-cell suppressor program co-opts transcription factor IRF4 to control T(H)2 responses. *Nature* **458,** 351–356 (2009).

166. Wohlfert, E. A. *et al.* GATA3 controls Foxp3^{+} regulatory T cell fate during inflammation in mice. *J. Clin. Invest.* **121,** 4503–4515 (2011).

167. Chaudhry, A. *et al.* CD4+ regulatory T cells control TH17 responses in a Stat3-dependent manner. *Science* **326,** 986–991 (2009).

168. Zhou, L. *et al.* TGF-beta-induced Foxp3 inhibits T(H)17 cell differentiation by antagonizing RORgammat function. *Nature* **453,** 236–240 (2008).

169. Zhang, F., Meng, G. & Strober, W. Interactions among the transcription factors Runx1, RORgammat and Foxp3 regulate the differentiation of interleukin 17-producing T cells. *Nat. Immunol.* **9,** 1297–1306 (2008).

170. Massoud, A. H. *et al.* An asthma-associated IL4R variant exacerbates airway inflammation by promoting conversion of regulatory T cells to TH17-like cells. *Nat. Med.* (2016). doi:10.1038/nm.4147

171. Yang, B.-H. *et al.* Foxp3(+) T cells expressing RORγt represent a stable regulatory T-cell effector lineage with enhanced suppressive capacity during intestinal inflammation. *Mucosal Immunol.* **9,** 444–457 (2016).

172. Noval Rivas, M. *et al.* Regulatory T cell reprogramming toward a Th2-cell-like lineage impairs oral tolerance and promotes food allergy. *Immunity* **42,** 512–523 (2015).

173. Allan, S. E. *et al.* Activation-induced FOXP3 in human T effector cells does not suppress proliferation or cytokine production. *Int. Immunol.* **19,** 345–354 (2007).

174. Gavin, M. A. *et al.* Foxp3-dependent programme of regulatory T-cell differentiation. *Nature* **445,** 771–775 (2007).

175. Hill, J. A. *et al.* Foxp3 transcription-factor-dependent and -independent regulation of the regulatory T cell transcriptional signature. *Immunity* **27,** 786–800 (2007).

176. Ohkura, N., Kitagawa, Y. & Sakaguchi, S. Development and maintenance of regulatory T cells. *Immunity* **38,** 414–423 (2013).

177. Wilson, C. B., Rowell, E. & Sekimata, M. Epigenetic control of T-helper-cell differentiation. *Nat. Rev. Immunol.* **9,** 91–105 (2009).

178. Ansel, K. M., Lee, D. U. & Rao, A. An epigenetic view of helper T cell differentiation. *Nat. Immunol.* **4,** 616–623 (2003).

179. Schmidl, C. *et al.* Lineage-specific DNA methylation in T cells correlates with histone methylation and enhancer activity. *Genome Res.* **19,** 1165–1174 (2009).

180. Ohkura, N. *et al.* T cell receptor stimulation-induced epigenetic changes and Foxp3 expression are independent and complementary events required for Treg cell development. *Immunity* **37,** 785–799 (2012).

181. Polansky, J. K. *et al.* Methylation matters: binding of Ets-1 to the demethylated Foxp3 gene contributes to the stabilization of Foxp3 expression in regulatory T cells. *J. Mol. Med. Berl. Ger.* **88,** 1029–1040 (2010).

182. Lal, G. *et al.* Epigenetic regulation of Foxp3 expression in regulatory T cells by DNA methylation. *J. Immunol. Baltim. Md 1950* **182,** 259–273 (2009).

183. Yue, X. *et al.* Control of Foxp3 stability through modulation of TET activity. *J. Exp. Med.* **213,** 377–397 (2016).

184. Yang, R. *et al.* Hydrogen Sulfide Promotes Tet1- and Tet2-Mediated Foxp3 Demethylation to Drive Regulatory T Cell Differentiation and Maintain Immune Homeostasis. *Immunity* **43,** 251–263 (2015).

185. Wei, G. *et al.* Global mapping of H3K4me3 and H3K27me3 reveals specificity and plasticity in lineage fate determination of differentiating CD4+ T cells. *Immunity* **30,** 155–167 (2009).

186. DuPage, M. *et al.* The chromatin-modifying enzyme Ezh2 is critical for the maintenance of regulatory T cell identity after activation. *Immunity* **42,** 227–238 (2015).

187. Arvey, A. *et al.* Inflammation-induced repression of chromatin bound by the transcription factor Foxp3 in regulatory T cells. *Nat. Immunol.* **15,** 580–587 (2014).

188. Placek, K. *et al.* MLL4 prepares the enhancer landscape for Foxp3 induction via chromatin looping. *Nat. Immunol.* **18,** 1035–1045 (2017).

189. Hamamoto, R. *et al.* SMYD3 encodes a histone methyltransferase involved in the proliferation of cancer cells. *Nat. Cell Biol.* **6,** 731–740 (2004).

190. Nagata, D. E. de A. *et al.* Epigenetic control of Foxp3 by SMYD3 H3K4 histone methyltransferase controls iTreg development and regulates pathogenic T-cell responses during pulmonary viral infection. *Mucosal Immunol.* **8,** 1131–1143 (2015).

191. Van Aller, G. S. *et al.* Smyd3 regulates cancer cell phenotypes and catalyzes histone H4 lysine 5 methylation. *Epigenetics Off. J. DNA Methylation Soc.* **7,** 340–343 (2012).

192. Mazur, P. K. *et al.* SMYD3 links lysine methylation of MAP3K2 to Ras-driven cancer. *Nature* (2014). doi:10.1038/nature13320

193. Chen, L.-B., Xu, J.-Y., Yang, Z. & Wang, G.-B. Silencing SMYD3 in hepatoma demethylates RIZI promoter induces apoptosis and inhibits cell proliferation and migration. *World J. Gastroenterol.* **13,** 5718–5724 (2007).

194. Hamamoto, R. *et al.* Enhanced SMYD3 expression is essential for the growth of breast cancer cells. *Cancer Sci.* **97,** 113–118 (2006).

195. Shen, B. *et al.* Upregulated SMYD3 promotes bladder cancer progression by targeting BCLAF1 and activating autophagy. *Tumour Biol. J. Int. Soc. Oncodevelopmental Biol. Med.* **37,** 7371–7381 (2016).

196. Liu, H. *et al.* Elevated Levels of SET and MYND Domain-Containing Protein 3 Are Correlated with Overexpression of Transforming Growth Factor-β1 in Gastric Cancer. *J. Am. Coll. Surg.* **221,** 579–590 (2015).

197. Liu, Y. *et al.* SMYD3 overexpression was a risk factor in the biological behavior and prognosis of gastric carcinoma. *Tumour Biol. J. Int. Soc. Oncodevelopmental Biol. Med.* **36,** 2685–2694 (2015).

198. Sponziello, M. *et al.* Epigenetic-related gene expression profile in medullary thyroid cancer revealed the overexpression of the histone methyltransferases EZH2 and SMYD3 in aggressive tumours. *Mol. Cell. Endocrinol.* **392,** 8–13 (2014).

199. Giakountis, A., Moulos, P., Sarris, M. E., Hatzis, P. & Talianidis, I. Smyd3-associated regulatory pathways in cancer. *Semin. Cancer Biol.* (2016). doi:10.1016/j.semcancer.2016.08.008

200. Kim, H. *et al.* Requirement of histone methyltransferase SMYD3 for estrogen receptor-mediated transcription. *J. Biol. Chem.* **284,** 19867–19877 (2009).

201. de Almeida Nagata, D. E. *et al.* Epigenetic control of Foxp3 by SMYD3 H3K4 histone methyltransferase controls iTreg development and regulates pathogenic T-cell responses during pulmonary viral infection. *Mucosal Immunol.* (2015). doi:10.1038/mi.2015.4

202. Fujii, T., Tsunesumi, S., Yamaguchi, K., Watanabe, S. & Furukawa, Y. Smyd3 is required for the development of cardiac and skeletal muscle in zebrafish. *PloS One* **6,** e23491 (2011).

203. Proserpio, V., Fittipaldi, R., Ryall, J. G., Sartorelli, V. & Caretti, G. The methyltransferase SMYD3 mediates the recruitment of transcriptional cofactors at the myostatin and c-Met genes and regulates skeletal muscle atrophy. *Genes Dev.* **27,** 1299–1312 (2013).

204. Maillard, I. *et al.* Mastermind critically regulates Notch-mediated lymphoid cell fate decisions. *Blood* **104,** 1696–1702 (2004).

205. Sandy, A. R. *et al.* Notch Signaling Regulates T Cell Accumulation and Function in the Central Nervous System during Experimental Autoimmune Encephalomyelitis. *J. Immunol.* **191,** 1606–1613 (2013).

206. Miller, A. L., Bowlin, T. L. & Lukacs, N. W. Respiratory syncytial virus-induced chemokine production: linking viral replication to chemokine production in vitro and in vivo. *J. Infect. Dis.* **189,** 1419–1430 (2004).

207. Collison, L. W. & Vignali, D. A. A. In vitro Treg suppression assays. *Methods Mol. Biol. Clifton NJ* **707,** 21–37 (2011).

208. Wen, H., Dou, Y., Hogaboam, C. M. & Kunkel, S. L. Epigenetic regulation of dendritic cell-derived interleukin-12 facilitates immunosuppression after a severe innate immune response. *Blood* **111,** 1797–1804 (2008).

209. Mukherjee, S., Schaller, M. A., Neupane, R., Kunkel, S. L. & Lukacs, N. W. Regulation of T cell activation by Notch ligand, DLL4, promotes IL-17 production and Rorc activation. *J. Immunol. Baltim. Md 1950* **182,** 7381–7388 (2009).

210. Rudd, B. D. *et al.* MyD88-mediated instructive signals in dendritic cells regulate pulmonary immune responses during respiratory virus infection. *J. Immunol. Baltim. Md 1950* **178,** 5820–5827 (2007).

211. Lukacs, N. W. *et al.* Differential immune responses and pulmonary pathophysiology are induced by two different strains of respiratory syncytial virus. *Am. J. Pathol.* **169,** 977–986 (2006).

212. Plotnicky-Gilquin, H. *et al.* Gamma interferon-dependent protection of the mouse upper respiratory tract following parenteral immunization with a respiratory syncytial virus G protein fragment. *J. Virol.* **76,** 10203–10210 (2002).

213. Mukherjee, S. *et al.* IL-17-induced pulmonary pathogenesis during respiratory viral infection and exacerbation of allergic disease. *Am. J. Pathol.* **179,** 248–258 (2011).

214. Krishnamoorthy, N. *et al.* Early infection with respiratory syncytial virus impairs regulatory T cell function and increases susceptibility to allergic asthma. *Nat. Med.* **18,** 1525–1530 (2012).

215. Smigiel, K. S. *et al.* CCR7 provides localized access to IL-2 and defines homeostatically distinct regulatory T cell subsets. *J. Exp. Med.* **211,** 121–136 (2014).

216. Radtke, F., MacDonald, H. R. & Tacchini-Cottier, F. Regulation of innate and adaptive immunity by Notch. *Nat. Rev. Immunol.* **13,** 427–437 (2013).

217. Mota, C. *et al.* Delta-like 1-mediated Notch signaling enhances the in vitro conversion of human memory CD4 T cells into FOXP3-expressing regulatory T cells. *J. Immunol. Baltim. Md 1950* **193,** 5854–5862 (2014).

218. Workman, C. J., Szymczak-Workman, A. L., Collison, L. W., Pillai, M. R. & Vignali, D. A. A. The development and function of regulatory T cells. *Cell. Mol. Life Sci. CMLS* **66,** 2603–2622 (2009).

219. Haque, R. *et al.* Programming of regulatory T cells from pluripotent stem cells and prevention of autoimmunity. *J. Immunol. Baltim. Md 1950* **189,** 1228–1236 (2012).

220. Sakaguchi, S., Vignali, D. A. A., Rudensky, A. Y., Niec, R. E. & Waldmann, H. The plasticity and stability of regulatory T cells. *Nat. Rev. Immunol.* **13,** 461–467 (2013).

221. Mochizuki, K. *et al.* Delta-like ligand 4 identifies a previously uncharacterized population of inflammatory dendritic cells that plays important roles in eliciting allogeneic T cell responses in mice. *J. Immunol. Baltim. Md 1950* **190,** 3772–3782 (2013).

222. Reynolds, N. D., Lukacs, N. W., Long, N. & Karpus, W. J. Delta-like ligand 4 regulates central nervous system T cell accumulation during experimental autoimmune encephalomyelitis. *J. Immunol. Baltim. Md 1950* **187,** 2803–2813 (2011).

223. Curotto de Lafaille, M. A. & Lafaille, J. J. Natural and adaptive foxp3+ regulatory T cells: more of the same or a division of labor? *Immunity* **30,** 626–635 (2009).

224. Pierini, A. *et al.* Donor Requirements for Regulatory T Cell Suppression of Murine Graft-versus-Host Disease. *J. Immunol. Baltim. Md 1950* **195,** 347–355 (2015).

225. Hoffmann, P., Ermann, J., Edinger, M., Fathman, C. G. & Strober, S. Donor-type CD4(+)CD25(+) regulatory T cells suppress lethal acute graft-versus-host disease after allogeneic bone marrow transplantation. *J. Exp. Med.* **196,** 389–399 (2002).

226. Beres, A., Komorowski, R., Mihara, M. & Drobyski, W. R. Instability of Foxp3 expression limits the ability of induced regulatory T cells to mitigate graft versus host disease. *Clin. Cancer Res. Off. J. Am. Assoc. Cancer Res.* **17,** 3969–3983 (2011).

227. Feuerer, M. *et al.* Genomic definition of multiple ex vivo regulatory T cell subphenotypes. *Proc. Natl. Acad. Sci. U. S. A.* **107,** 5919–5924 (2010).

228. O'Donnell, D. R. & Openshaw, P. J. Anaphylactic sensitization to aeroantigen during respiratory virus infection. *Clin. Exp. Allergy J. Br. Soc. Allergy Clin. Immunol.* **28,** 1501–1508 (1998).

229. Wong, S. H. *et al.* Rorα is essential for nuocyte development. *Nat. Immunol.* **13,** 229–236 (2012).

230. Rigas, D. *et al.* Type 2 innate lymphoid cell suppression by regulatory T cells attenuates airway hyperreactivity and requires inducible T-cell costimulator-inducible T-cell costimulator ligand. *J. Allergy Clin. Immunol.* (2016). doi:10.1016/j.jaci.2016.08.034

231. Ermann, J. *et al.* Only the CD62L+ subpopulation of CD4+CD25+ regulatory T cells protects from lethal acute GVHD. *Blood* **105,** 2220–2226 (2005).

232. Kocks, J. R., Davalos-Misslitz, A. C. M., Hintzen, G., Ohl, L. & Förster, R. Regulatory T cells interfere with the development of bronchus-associated lymphoid tissue. *J. Exp. Med.* **204,** 723–734 (2007).

233. Loffredo-Verde, E. *et al.* Schistosome infection aggravates HCV-related liver disease and induces changes in the regulatory T-cell phenotype. *Parasite Immunol.* **37,** 97–104 (2015).

234. Curotto de Lafaille, M. A. *et al.* Adaptive Foxp3+ regulatory T cell-dependent and -independent control of allergic inflammation. *Immunity* **29,** 114–126 (2008).

235. Huang, H., Ma, Y., Dawicki, W., Zhang, X. & Gordon, J. R. Comparison of induced versus natural regulatory T cells of the same TCR specificity for induction of tolerance to an environmental antigen. *J. Immunol. Baltim. Md 1950* **191,** 1136–1143 (2013).

236. Tone, Y. *et al.* Smad3 and NFAT cooperate to induce Foxp3 expression through its enhancer. *Nat. Immunol.* **9,** 194–202 (2008).

237. Sandy, A. R. & Maillard, I. Notch signaling in the hematopoietic system. *Expert Opin. Biol. Ther.* **9,** 1383–1398 (2009).

238. Maillard, I., Adler, S. H. & Pear, W. S. Notch and the immune system. *Immunity* **19,** 781–791 (2003).

239. Radtke, F., Fasnacht, N. & Macdonald, H. R. Notch signaling in the immune system. *Immunity* **32,** 14–27 (2010).

240. Zhou, L., Chong, M. M. W. & Littman, D. R. Plasticity of CD4+ T cell lineage differentiation. *Immunity* **30,** 646–655 (2009).

241. Dillon, S. C., Zhang, X., Trievel, R. C. & Cheng, X. The SET-domain protein superfamily: protein lysine methyltransferases. *Genome Biol.* **6,** 227 (2005).

242. Castel, D. *et al.* Dynamic binding of RBPJ is determined by Notch signaling status. *Genes Dev.* **27,** 1059–1071 (2013).

243. van der Veeken, J. *et al.* Memory of Inflammation in Regulatory T Cells. *Cell* **166,** 977–990 (2016).

244. Huang, M.-T. *et al.* Notch Ligand DLL4 Alleviates Allergic Airway Inflammation via Induction of a Homeostatic Regulatory Pathway. *Sci. Rep.* **7,** 43535 (2017).

245. Mazur, P. K. *et al.* SMYD3 links lysine methylation of MAP3K2 to Ras-driven cancer. *Nature* **510,** 283–287 (2014).

246. Liu, C. *et al.* SMYD3 as an oncogenic driver in prostate cancer by stimulation of androgen receptor transcription. *J. Natl. Cancer Inst.* **105,** 1719–1728 (2013).

247. Koch, M. A. *et al.* The transcription factor T-bet controls regulatory T cell homeostasis and function during type 1 inflammation. *Nat. Immunol.* **10,** 595–602 (2009).

248. Jankovic, D. *et al.* In the absence of IL-12, CD4(+) T cell responses to intracellular pathogens fail to default to a Th2 pattern and are host protective in an IL-10(-/-) setting. *Immunity* **16,** 429–439 (2002).

249. Skokos, D. & Nussenzweig, M. C. CD8- DCs induce IL-12-independent Th1 differentiation through Delta 4 Notch-like ligand in response to bacterial LPS. *J. Exp. Med.* **204,** 1525–1531 (2007).

250. Kojima, S., Nara, K. & Rifkin, D. B. Requirement for transglutaminase in the activation of latent transforming growth factor-beta in bovine endothelial cells. *J. Cell Biol.* **121,** 439–448 (1993).

251. Wang, Z. & Griffin, M. TG2, a novel extracellular protein with multiple functions. *Amino Acids* **42,** 939–949 (2012).

252. Telci, D., Collighan, R. J., Basaga, H. & Griffin, M. Increased TG2 expression can result in induction of transforming growth factor beta1, causing increased synthesis and deposition of matrix proteins, which can be regulated by nitric oxide. *J. Biol. Chem.* **284,** 29547–29558 (2009).

253. Cao, L. *et al.* Tissue transglutaminase links TGF-β, epithelial to mesenchymal transition and a stem cell phenotype in ovarian cancer. *Oncogene* **31,** 2521–2534 (2012).

254. Shao, M. *et al.* Epithelial-to-mesenchymal transition and ovarian tumor progression induced by tissue transglutaminase. *Cancer Res.* **69,** 9192–9201 (2009).

255. Huang, C.-T. *et al.* Role of LAG-3 in regulatory T cells. *Immunity* **21,** 503–513 (2004).

256. Do, J.-S. *et al.* An IL-27/Lag3 axis enhances Foxp3+ regulatory T cell-suppressive function and therapeutic efficacy. *Mucosal Immunol.* **9,** 137–145 (2016).

257. Sega, E. I. *et al.* Role of lymphocyte activation gene-3 (Lag-3) in conventional and regulatory T cell function in allogeneic transplantation. *PloS One* **9,** e86551 (2014).

258. WHO | Estimates for 2000–2015. *WHO* Available at: http://www.who.int/healthinfo/global_burden_disease/estimates/en/. (Accessed: 27th January 2018)

259. Mizgerd, J. P. Lung infection--a public health priority. *PLoS Med.* **3,** e76 (2006).

260. Loebbermann, J., Durant, L., Thornton, H., Johansson, C. & Openshaw, P. J. Defective immunoregulation in RSV vaccine-augmented viral lung disease restored by selective chemoattraction of regulatory T cells. *Proc. Natl. Acad. Sci. U. S. A.* **110,** 2987–2992 (2013).

261. Zeng, R. *et al.* Interleukin-27 inhibits vaccine-enhanced pulmonary disease following respiratory syncytial virus infection by regulating cellular memory responses. *J. Virol.* **86,** 4505–4517 (2012).

262. González, P. A., Bueno, S. M., Carreño, L. J., Riedel, C. A. & Kalergis, A. M. Respiratory syncytial virus infection and immunity. *Rev. Med. Virol.* **22,** 230–244 (2012).

263. McNamara, P. S. & Smyth, R. L. The pathogenesis of respiratory syncytial virus disease in childhood. *Br. Med. Bull.* **61,** 13–28 (2002).

264. Graham, J. B., Da Costa, A. & Lund, J. M. Regulatory T cells shape the resident memory T cell response to virus infection in the tissues. *J. Immunol. Baltim. Md 1950* **192,** 683–690 (2014).

265. Brincks, E. L. *et al.* Antigen-specific memory regulatory CD4+Foxp3+ T cells control memory responses to influenza virus infection. *J. Immunol. Baltim. Md 1950* **190,** 3438–3446 (2013).

266. Chung, J. *et al.* Fibroblastic niches prime T cell alloimmunity through Delta-like Notch ligands. *J. Clin. Invest.* **127,** 1574–1588 (2017).

267. Grandbarbe, L. *et al.* Notch signaling modulates the activation of microglial cells. *Glia* **55,** 1519–1530 (2007).

268. Cao, Q. *et al.* Expression of Notch-1 receptor and its ligands Jagged-1 and Delta-1 in amoeboid microglia in postnatal rat brain and murine BV-2 cells. *Glia* **56,** 1224–1237 (2008).

269. Elyaman, W. *et al.* JAGGED1 and delta1 differentially regulate the outcome of experimental autoimmune encephalomyelitis. *J. Immunol. Baltim. Md 1950* **179,** 5990–5998 (2007).

270. Brückner, K., Perez, L., Clausen, H. & Cohen, S. Glycosyltransferase activity of Fringe modulates Notch-Delta interactions. *Nature* **406,** 411–415 (2000).

271. Yuan, J. S., Kousis, P. C., Suliman, S., Visan, I. & Guidos, C. J. Functions of notch signaling in the immune system: consensus and controversies. *Annu. Rev. Immunol.* **28,** 343–365 (2010).

272. Yuan, J. S. *et al.* Lunatic Fringe prolongs Delta/Notch-induced self-renewal of committed αβ T-cell progenitors. *Blood* **117,** 1184–1195 (2011).

273. Maeda, T. *et al.* Regulation of B versus T lymphoid lineage fate decision by the proto-oncogene LRF. *Science* **316,** 860–866 (2007).

274. Lee, S.-U. *et al.* LRF-mediated Dll4 repression in erythroblasts is necessary for hematopoietic stem cell maintenance. *Blood* **121,** 918–929 (2013).

275. Hsieh, C.-S. *et al.* Recognition of the peripheral self by naturally arising CD25+ CD4+ T cell receptors. *Immunity* **21,** 267–277 (2004).

276. Pacholczyk, R., Ignatowicz, H., Kraj, P. & Ignatowicz, L. Origin and T cell receptor diversity of Foxp3+CD4+CD25+ T cells. *Immunity* **25,** 249–259 (2006).

277. Wong, J. *et al.* Adaptation of TCR repertoires to self-peptides in regulatory and nonregulatory CD4+ T cells. *J. Immunol. Baltim. Md 1950* **178,** 7032–7041 (2007).

278. Chung, J. *et al.* Delta-like Ligands Expressed By Stromal Cells in Secondary Lymphoid Organs Deliver an Early Pulse of Notch Signaling and Drive T Cell Pathogenicity in Acute Graft-Versus-Host Disease. *Blood* **124,** 841–841 (2014).

279. Chadwick, N. *et al.* Identification of novel Notch target genes in T cell leukaemia. *Mol. Cancer* **8,** 35 (2009).

280. Wong, G. W., Knowles, G. C., Mak, T. W., Ferrando, A. A. & Zúñiga-Pflücker, J. C. HES1 opposes a PTEN-dependent check on survival, differentiation, and proliferation of TCRβ-selected mouse thymocytes. *Blood* **120,** 1439–1448 (2012).

281. Ciofani, M. *et al.* Obligatory role for cooperative signaling by pre-TCR and Notch during thymocyte differentiation. *J. Immunol. Baltim. Md 1950* **172,** 5230–5239 (2004).

282. Ciofani, M. & Zúñiga-Pflücker, J. C. Notch promotes survival of pre-T cells at the beta-selection checkpoint by regulating cellular metabolism. *Nat. Immunol.* **6,** 881–888 (2005).

283. Zhang, B., Chikuma, S., Hori, S., Fagarasan, S. & Honjo, T. Nonoverlapping roles of PD-1 and FoxP3 in maintaining immune tolerance in a novel autoimmune pancreatitis mouse model. *Proc. Natl. Acad. Sci. U. S. A.* **113,** 8490–8495 (2016).

284. Corse, E. & Allison, J. P. Cutting edge: CTLA-4 on effector T cells inhibits in trans. *J. Immunol. Baltim. Md 1950* **189,** 1123–1127 (2012).

285. Yao, Y. *et al.* Tr1 Cells, but Not Foxp3+ Regulatory T Cells, Suppress NLRP3 Inflammasome Activation via an IL-10-Dependent Mechanism. *J. Immunol. Baltim. Md 1950* **195,** 488–497 (2015).

286. Yao, S. *et al.* Control of pathogenic effector T-cell activities in situ by PD-L1 expression on respiratory inflammatory dendritic cells during respiratory syncytial virus infection. *Mucosal Immunol.* **8,** 746–759 (2015).

287. Han, J. *et al.* In Vivo Blockade of OX40 Ligand Prevents Respiratory Syncytial Virus (RSV)-Induced Airway Hyperresponsiveness (AHR) and Inflammation. *J. Allergy Clin. Immunol.* **125,** AB62 (2010).

288. Gagliani, N. *et al.* Coexpression of CD49b and LAG-3 identifies human and mouse T regulatory type 1 cells. *Nat. Med.* **19,** 739–746 (2013).

289. Bernier-Latmani, J. *et al.* DLL4 promotes continuous adult intestinal lacteal regeneration and dietary fat transport. *J. Clin. Invest.* **125,** 4572–4586 (2015).

290. Biancheri, P. *et al.* The role of transforming growth factor (TGF)-β in modulating the immune response and fibrogenesis in the gut. *Cytokine Growth Factor Rev.* **25,** 45–55 (2014).

291. Smythies, L. E. *et al.* Mucosal IL-8 and TGF-beta recruit blood monocytes: evidence for cross-talk between the lamina propria stroma and myeloid cells. *J. Leukoc. Biol.* **80,** 492–499 (2006).

292. Sun, C.-M. *et al.* Small intestine lamina propria dendritic cells promote de novo generation of Foxp3 T reg cells via retinoic acid. *J. Exp. Med.* **204,** 1775–1785 (2007).

293. Coombes, J. L. *et al.* A functionally specialized population of mucosal CD103+ DCs induces Foxp3+ regulatory T cells via a TGF-beta and retinoic acid-dependent mechanism. *J. Exp. Med.* **204,** 1757–1764 (2007).

294. Denning, T. L., Wang, Y., Patel, S. R., Williams, I. R. & Pulendran, B. Lamina propria macrophages and dendritic cells differentially induce regulatory and interleukin 17-producing T cell responses. *Nat. Immunol.* **8,** 1086–1094 (2007).

295. Sarris, M. E., Moulos, P., Haroniti, A., Giakountis, A. & Talianidis, I. Smyd3 Is a Transcriptional Potentiator of Multiple Cancer-Promoting Genes and Required for Liver and Colon Cancer Development. *Cancer Cell* **29,** 354–366 (2016).